

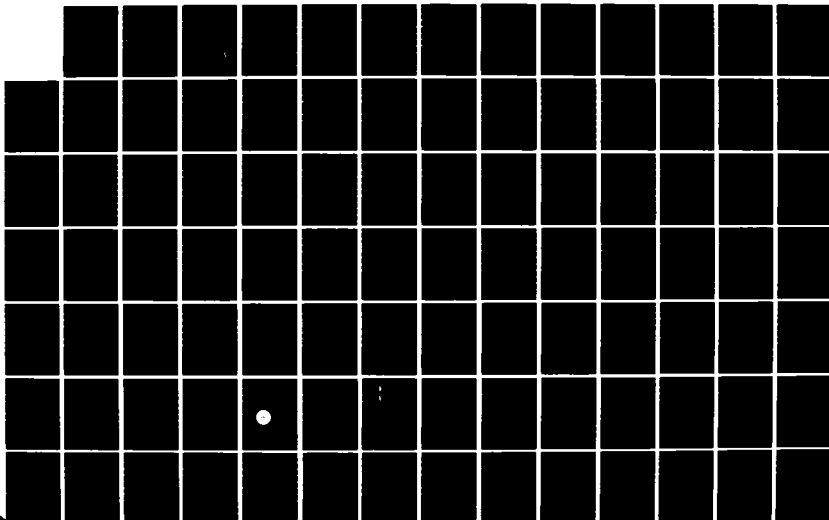
AD-A151 682

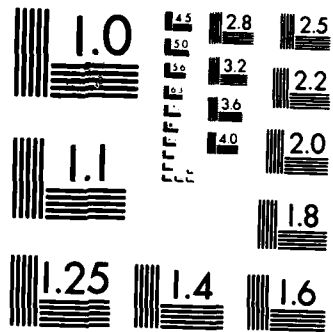
THE DEVELOPMENT AND IMPLEMENTATION OF AN OPTICAL
COMMUNICATIONS LABORATORY(U) AIR FORCE INST OF TECH
WRIGHT-PATTERSON AFB OH SCHOOL OF ENGINEERING W K RIU
DEC 84 AFIT/GE/EE/84D-12 F/G 17/2

1/2

UNCLASSIFIED

NL





MICROCOPY RESOLUTION TEST CHART
NATIONAL BUREAU OF STANDARDS-1963-A

DTIC

(D)

AD-A151 682



THE DEVELOPMENT AND IMPLEMENTATION
 OF AN OPTICAL COMMUNICATIONS LABORATORY

THESIS

William K. Aiu
 Captain, USAF

AFIT/GE/EE/84D-12

DTIC FILE COPY

DTIC
 E
 S MAR 28 1985
 D

DEPARTMENT OF THE AIR FORCE
 AIR UNIVERSITY
AIR FORCE INSTITUTE OF TECHNOLOGY

Wright-Patterson Air Force Base, Ohio

85 03 13 256

AFIT/GE/EE/84



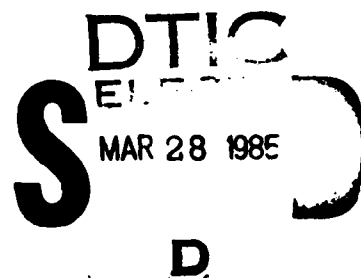
THE DEVELOPMENT AND IMPLEMENTATION
OF AN OPTICAL COMMUNICATIONS LABORATORY

THESIS

William K. Aiu
Captain, USAF

AFIT/GE/EE/84D-12

Accession For	
NTIS GRA&I	<input checked="" type="checkbox"/>
DTIC TAB	<input type="checkbox"/>
Unannounced	<input type="checkbox"/>
Justification	
By	
Distribution/	
Availability Codes	
Dist	Avail and/or Special
A-1	



Approved for public release; distribution unlimited

AFIT/GE/EE/84D-12

THE DEVELOPMENT AND IMPLEMENTATION OF AN
OPTICAL COMMUNICATIONS LABORATORY

THESIS

Presented to the Faculty of the School of Engineering
of the Air Force Institute of Technology
Air University

In Partial Fulfillment of the
Requirements for the Degree of
Master of Science in Electrical Engineering

William K. Aiu, B.S.E.E.

Captain, USAF

December 1984

Approved for public release; distribution unlimited

Preface

The purpose of this study was to develop some optical communication experiments to assist the student in learning and understanding of Electromagnetic wave theory propagation. The experiments were designed for a project-type laboratory; however, they may also be adapted for classroom demonstrations. Although only seven experiments were developed during this study effort, the potential for expansion is tremendous.

During the course of this thesis, the method used to expand and collimate the laser beam is described by adjusting the microscope objective such that the laser beam will focus to a point at some distance before the 25 μ pinhole spatial filter. Thus the light field emerging from the 25 μ pinhole spatial filter is the airy diffraction pattern of the pinhole.

Although the method just described is a valid one for obtaining a collimated wave field, the usable portion of this wave field (the central portion of the airy diffraction pattern) is very small (approximately 5 mm in diameter).

A preferred method for expanding and collimating the laser beam would be to adjust the microscope objective such that it focuses the laser beam to a point directly on the 25 μ pinhole. This creates a larger cross-sectional area

of a collimated beam to illuminate an object. This method was discovered during the final writing of this thesis.

I would like to give thanks to the moral support of my dear family whom without them this study would have only been a dream. I would also like to thank my roommate and close friend Paul DeRego for being like a brother to me during this long ordeal we shared together. I would also like to thank my advisor, Dr. Vic Syed, Dr. Mathew Kabrisky, and Maj Ken Castor for their many words of encouragement.

In addition, I would like to thank Mr. Stan Bashore, Mr. Ron Gabriel, Ms Judy Hughes, Mr. Curtis Atnipp and Mr. Karl Short for their support of equipment and laboratory supplies which I needed to conduct my study. A special thanks goes to Dr. Douglas Brown and Dr. Eddie Young for their technical advice and equipment support.

Furthermore, I would like to extend a big thanks to Mrs. Phyllis Reynolds for her outstanding work in typing my thesis. It was truly a joy working with her.

Finally, I'd like to give thanks to my dear Lord and Savior Jesus Christ. His guidance and care have been my true strength.

Table of Contents

	Page
Preface	ii
List of Figures	iv
Abstract	x
I. Introduction	1
Thesis Organization	3
II. Outline	5
III. Fraunhofer Diffraction in the Far Field	9
Assignment	9
Objectives of the Experiment	9
Equipment Needed	9
Theory/Background	10
Fraunhofer Diffraction Far Field	
Measurement Procedures	15
Special Problems	19
Results and Sample Questions	22
Bibliography	26
IV. Fraunhofer Diffraction Using Lenses	27
Assignment	27
Objectives of the Experiment	27
Equipment Needed	27
Theory/Background	28
Fraunhofer Diffraction with Lenses	
Measurement Procedures	38
Special Problems	42
Results	43
Bibliography	46
V. Imaging and Spatial Filtering	47
Assignment	47
Objectives of the Experiment	47
Equipment Needed	47

	Page
Theory/Background	49
Imaging and Spatial Filtering	
Measurement Procedures	57
Special Problems	64
Results	66
Bibliography	70
VI. Measuring the Bragg Angle with Acousto-Optic Cell	71
Assignment	71
Objectives of the Experiment	71
Equipment Needed	71
Theory/Background	72
Experimental Procedures	82
Bragg Angle Measurement Procedures	86
Special Problems	91
Results and Sample Questions	92
Bibliography	97
VII. Beam Deflection and Spectrum Analysis Using an Acousto-Optic Modulator (Bragg Cell).	98
Assignment	98
Objective	98
Equipment Needed	98
Theory/Background	100
Beam Deflection and Spectrum Analysis Measurement Procedures	108
Special Problems	115
Results	116
Bibliography	120
VIII. Laser Communications Using Acousto- Optic Cells	121
Assignment	121
Objectives	121
Equipment Needed	121
Theory/Background	123
Experimental Procedures	132
Laser Communications with Acousto- Optic Cell Procedures	135
Special Problems	140
Results	142
Bibliography	145

	Page
IX. Correlation Using Acousto-Optic Cells	146
Introduction	146
Theory Description	147
Experimental Procedures	151
Conclusion	154
Bibliography	156
X. Conclusion	157
Recommendations	157
Vita	162

List of Figures

Figure		Page
III-1.	Designation of Various Diffraction Regions	11
III-2.	Configuration for Fraunhofer Diffraction .	12
III-3.	Intensity Distribution of Slit Aperture . .	15
III-4.	Fraunhofer Diffraction (Far Field Experimental Setup)	17
III-5.	Rod/Platform Assembly with Diffraction Slide	21
IV-1.	The Thickness Function	30
IV-2.	Geometry for the Thickness Function	31
IV-3.	Fourier Transforming Configurations	33
IV-4.	Object Placed in Front of Lens	35
IV-5.	Fraunhofer Diffraction/Lenses Experimental Setup	40
V-1.	Geometry for Image Formation	50
V-2.	Two-Lens System in One Dimension	53
V-3.	Optical System Used to Investigate Coherent Image Formation	54
V-4.	Imaging and Spatial Filtering Experimental Setup	58
V-5.	Hexagonal Aperture with Fine Wire Mesh . .	62
V-6.	Photograph of the Unmodified Mesh and its Spectrum	62
V-7.	Mesh Filtered with Vertical Slit	64
V-8.	Three-Lens Imaging System	67

Figure	Page
VI-1. Optical Delay Line Refractive Index Product Phase Modulation	74
VI-2. Carrier (ω) and Sideband Spectrum of a Phase Modulated Wave	75
VI-3. Amplitude of Sideband Light versus Phase Excursion	76
VI-4. Sound Wave Propagating Upward will Generate Optical Phase Shifts which Cause Wavefront of First Order Sideband to Tilt. Carrier Wavefront (ω) Does Not Change . . .	78
VI-5. Acousto-Optic Interaction in the Raman-Nath Regime	80
VI-6. Acousto-Optic Interaction in the Bragg Regime	81
VI-7. Bragg Reflection--Upper and Lower Diffraction Order is Selected by Making Light Incident at the Appropriate Bragg Angle	83
VI-8. Bragg Angle Experimental Setup	87
VI-9. Photograph of Bragg Angle Experiment	88
VII-1. Optical Processing System	102
VII-2. Acousto-Optic Interaction in the Bragg Regime	104
VII-3. Bragg Diffraction Sound Cell Used as Spectrum Analyzer	105
VII-4. Beam Deflection and Spectrum Analysis Experimental Setup	109
VII-5. Photograph of the Optical System	110
VIII-1. Bragg Cell with Plane Wave Illumination . . .	124
VIII-2. Bragg Diffraction of an Acousto-Optic Cell .	127
VIII-3. Illustration of an Acousto-Optic Cell Tilted at the Bragg Angle	129

Figure	Page
VIII-4. Acousto-Optic System Converting Phase Modulation to Amplitude Modulation	131
VIII-5. Amplitude Modulated Laser Communications System Implemented with an Acousto-Optic Modulator (Bragg Cell) Experimental Setup .	133
VIII-6. $\text{Sin}^2(\theta)$ Curve	134
VIII-7. Frequency Modulated Laser Communication System Implemented with a Bragg Cell	143
IX-1. Time Integrating Correlator.	148
IX-2. Time Integrating Correlator Experimental Setup	152

Abstract

This report is an accumulation of seven optical laboratory experiments developed for the Optical Communications Program at the Air Force Institute of Technology. The projects include measurement of pertinent parameters of Fourier Optics (diffraction patterns and lenses) and Acousto-Optics (Bragg angle and beam deflection using an acousto-optic modulator), image construction and spatial filtering, laser communications with an acousto-optic modulator and a scheme for implementing a time integrating correlator using two full size acousto-optic modulators.

Each experiment is self-contained with subsections on project assignments, objectives, theory/background, special problems, and experimental results.

The results of this report recommend that the Optical Communications Program at AFIT further develop their experimental laboratory and acquire some state-of-the-art acousto-optic modulators for students to pursue research and future studies.

THE DEVELOPMENT AND IMPLEMENTATION OF AN
OPTICAL COMMUNICATIONS LABORATORY

I. Introduction

The Optical Communications/Signal Processing sequence at The Air Force Institute of Technology (AFIT) is relatively new and just starting to develop. The students in this sequence are not able to conduct Optical Communications/Signal Processing experiments because of inadequate laboratory facilities. With the growing need for faster and more reliable communications, and higher and higher signal processing rates, optical techniques are taking an ever more important role in the military environment. Therefore, the need for adequate laboratory facilities in this area is high.

The Optical Communications/Signal Processing laboratory, as envisioned by the AFIT Electrical Engineering Department, is to support research as well as teaching. The teaching support role of the lab will be in the form of demonstrations to complement the theoretical part of related courses.

The general problem with the Optical Communications Laboratory here at AFIT is that no written procedures have been developed for conducting optical experiments.

Students in the Optical Communications Sequence have been discouraged from working with the optical equipment due to the lack of well-developed procedures. Although lab procedures for some basic optical experiments (i.e., Fraunhofer Diffraction) have been developed, no procedures for Acousto-Optical Signal Processing have been developed. Hence, with this thesis effort, students pursuing the field of optical communications will be able to develop an understanding of, and further individual research efforts, with Acousto-Optic Modulators (Bragg Cells) in the area of Acousto-Optic Signal processing.

The objective of this thesis effort is to develop some basic optical and Acousto-Optic laboratory experiments which will enhance learning and understanding of wave propagation theory and provide the instructor with some useful tools for demonstrating the classroom-related theory with practical examples. This thesis effort consists of six experiments. The seventh experiment could not be completed due to the lack of proper optical equipment. These experiments will illustrate the concepts and theories presented in classes: EE 527 (Fourier Optics), EE 672 (Optical Communications), and EE 715 (Special Topics in Optical Processing and Communications). The experiments that have been developed are:

1. Fraunhofer Diffraction in the far field.
2. Fraunhofer Diffraction with lenses.

3. Imaging and Spatial Filtering.
4. Measurement of the Bragg Angle of an Acousto-Optic Modulator (Bragg Cell).
5. Beam Deflection and Spectrum Analysis using an Acousto-Optic Modulator (Bragg Cell).
6. Laser Communications using an Acousto-Optic Modulator (Bragg Cell).
7. Correlation with an Acousto-Optic Modulator (Bragg Cell).

Thesis Organization

This thesis begins with Chapter III which is Experiment 1. The experiments are self-contained presenting a different topic under each chapter. This will make referencing of each experiment much easier and will allow the user to have all the information of each experiment in one place. Chapter II describes the layout of each experiment, with the exception of Experiment 7 (Chapter IX).

Each experiment contains the following information:

1. Title
2. Project Assignment
3. Objectives of the Experiment
4. Equipment for the Experiment
5. Theory and Background
6. Experimental Procedures

7. Special Problems
8. Results and Sample Questions
9. References

Chapter IX starts with some theory and then goes into the discussion of some of the problems that were encountered in developing that particular experiment.

The last chapter (Chapter X) will propose some recommendations as to possible future developments for implementing a complete and suitable working laboratory for the Optical Communications sequence for the AFIT program.

II. Outline

The experiments developed in this thesis were designed to assist the student in grasping the basic fundamentals of both Optics and Communications. Therefore, each experiment should help the student strengthen his/her understanding of the principles of Optical Communications, particularly in the field of Acousto-Optics. The set of experiments presented in this thesis will enable the students to gain experience with handling, evaluating, and using optical equipment and associated communications equipment (i.e., photodetectors, Acousto-Optic Modulators (Bragg Cells), etc.). An underlying goal in developing these experiments was to provide some guidelines for the student in which he could perform some practical experiments with the existing equipment in the laboratories. The student should keep in mind that the equipment and setups used are by no means the only way to conduct the experiment. The student is strongly encouraged to use ingenuity and creativity when performing each of these experiments. With the addition of new equipment and supplies to the laboratory, simpler and more precise laboratory setups can be devised.

Each experiment presented in this thesis is self-contained in its own chapter. Each chapter, with the

exception of Chapters IX and X, contains the following outline:

Title--each experiment has a specific title indicating the particular project to be accomplished.

Project Assignment--gives the student a look-ahead view of what to expect from this experiment.

Objectives of the Experiment--what is to be accomplished in each experiment.

Equipment Needed--self-explanatory.

Theoretical Background--each experiment has a theoretical background which was developed from either EE 527, EE 672, or EE 715. This portion consists of a general description of wave theory propagation along with a little mathematical analysis. Calculations developed in this section are used to predict the Irradiance pattern (i.e., Intensity Distribution) in the detector plane.

Experimental Procedures--this section presents the procedures for implementing each experiment. A diagram of the optical equipment setup is given along with an explanation of the functional purpose of the equipment to be used.

Special Problems--this section describes the problems a student can run into while either setting up the experiment or conducting the experiment. Special attention should be given to this section since it will include many

common errors a student may encounter while performing the experiment.

Results and Sample Questions--this section contains the results collected from performing each of the various experiments. If the student performing the experiments does not end up with exactly the same results, DON'T PANIC!! Remember, much of the collected data was accumulated using some very crude measuring devices (i.e., meter sticks). Also keep in mind that this thesis effort, in developing the experiments for the purpose of enhancing a deeper understanding of classroom theory, is a first-pass effort. Therefore, there are bound to be some points which may have been overlooked. Although many long and tired hours were put forth to correct as many of the problems as possible, some small points may still have been missed. Therefore, it is recommended that if there is any discrepancy which is found, please bring it to the attention of the instructor so the problem may be clear for future students. The sample questions are designed to help the student get a deeper grasp of the concepts and practical problems encountered with each experiment. Some of the questions may also be found in the "experimental procedure" section. It is left up to the instructor to use the questions as an oral examination for the student.

References--this section contains a list of the bibliographies used during each experiment. The student is

encouraged to read the references presented at the end of each experiment to help gain a deeper understanding of the principles and concepts of the experimental project.

Chapter IX starts with an introduction to correlation techniques using an Acousto-Optic Cell. This chapter also presents a small section on the theory description and a recommended experimental setup. However, due to the lack of proper optical equipment needed to complete this experiment, the conclusion indicates possible future action needed to fully implement this experiment.

This thesis concludes with Chapter X and gives a list of recommendations for improving the existing conditions of the Optical Communications laboratory.

III. Fraunhofer Diffraction in the Far Field

Assignment

The student will predict the Fraunhofer Diffraction pattern in the far field and then verify this pattern using a collimated beam of light. The locations of the minimas will be calculated and measured to see how well theory agrees with practice.

Objectives of the Experiment

1. To acquaint the student with laser light and its characteristics.
2. To relate classroom theory of Fraunhofer Diffraction with practical application.
3. To give the student some experience with simple apertures and laser light.

Equipment Needed

Laser Source: Spectra Physics Helium-Neon Class IIIb
4 mw (Model 102-1) and Spectra Physics
Laser Exciter (Model 212-1).

Newport Laser Mount (Model 810), 1 each
Newport Support Post (Model VPH-4), 1 each
Newport Post Holder (Model SP-4), 1 each

Jordan Spatial
Filter:

- a. Microscope Objective 10X
 - b. 25 micron Pinhole Spatial Filter
 - c. Spherical Collimating lens
- Newport Support Post (Model VPH-4), 1 each
Newport Post Holder (Model SP-4), 1 each

Diffraction Grating Slides (1 set)

Three Finger Holder with stand or equivalent

Newport Rod and Platform Assembly (Model 300)

Metrologic Maggie "U" mount; Part No. 30180, 2 each

Magnetic Tape 1" x 28" (Metrologic Part No. 00068)

Measuring Ruler (Meter Stick)

White Cardboard Screen, 2 ft. x 2 ft.

Theory/Background

The diffraction of light as it passes through an aperture has been explained elsewhere in great detail (1; 3; 5; 6; 7). In this section, a brief description and background of the propagation nature of light will be given.

As a plane wave propagates through an aperture, it spreads out more than can be accounted for by geometrical construction (6; 7). The wave will have a tendency to spread to the regions which are not directly exposed to the oncoming light. This phenomenon is known as diffraction.

Diffraction can be explained by using the Huygens principle and the principle of interference (6; 7). There are two general classes of diffraction. The first class

is that in which the light source and the observation screen are effectively at an infinite distance from the aperture. The second is where the light source and the observation screen are a finite distance from the aperture. These classes of observation are known as the Fraunhofer and Fresnel diffraction regions respectively (see Figure III-1). Both these classes have been covered extensively in the literature. For the purpose of this experiment, we will ignore the Fresnel Region and work only with the Fraunhofer Region.

The Fraunhofer Region can be considered that region beyond the aperture where the distance from the aperture to the observation screen is much greater than the maximum radial extent of the aperture (3:375). We will use this fact to develop some equations for the intensity distribution in the observation (Fraunhofer) region.

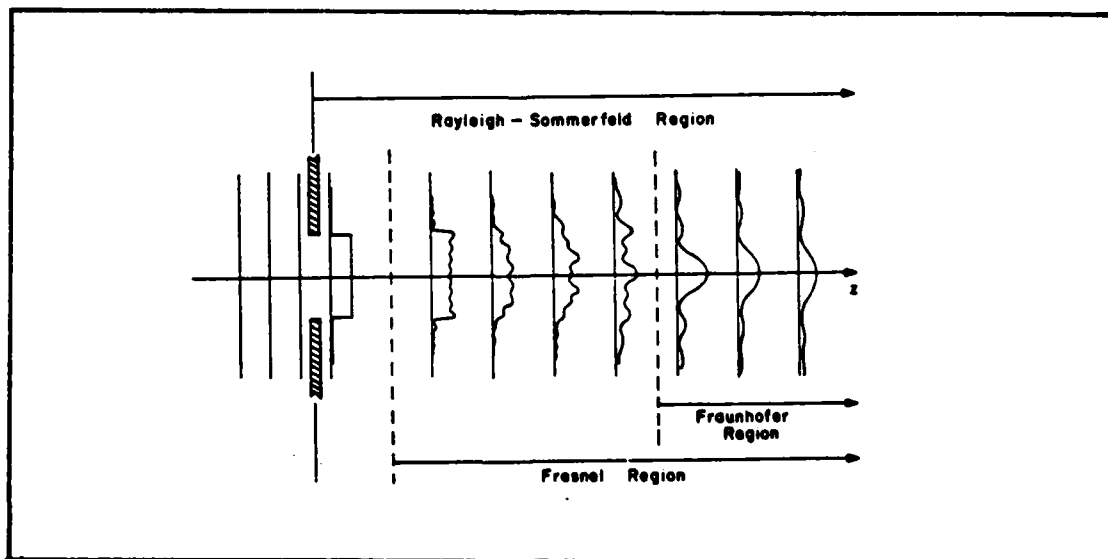


Fig. III-1. Designation of Various Diffraction Regions (3:361)

From the text by Gaskill and Goodman (3; 4), the Rayleigh-Sommerfield formula is used to describe the disturbance of light behind the aperture (see Figure III-1). From Figure III-2, we can use the Huygens-Fresnel principle (4:58) to determine the field amplitude response in the $Z = Z_2$ plane.

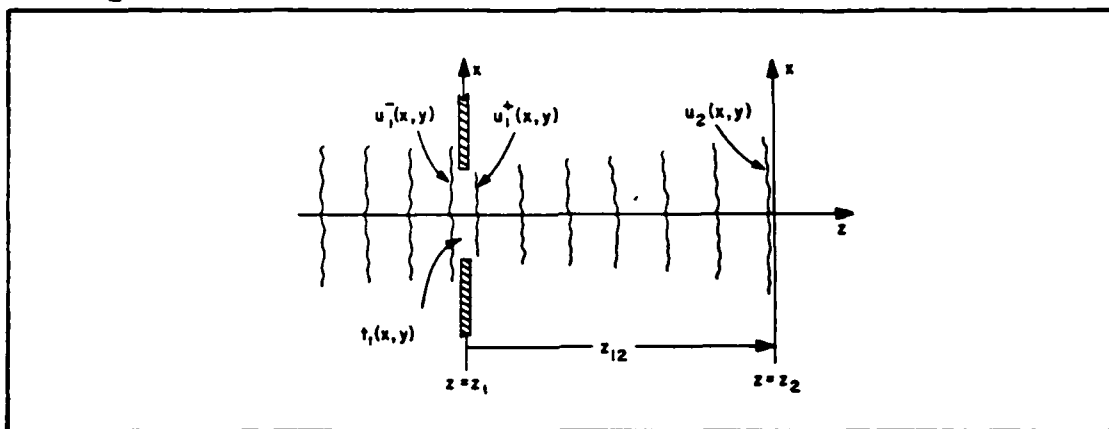


Fig. III-2. Configuration for Fraunhofer Diffraction (3:377)

Let $U_1[x, y]$ be the input signal to this system. From (2) the response of the system $U_2[x, y]$ in the Z_2 plane is given by

$$U_2(x, y) = \frac{\exp(jkz) \exp[j \frac{k}{2z}(x_2^2 + y_2^2)]}{j\lambda z} \iint_{-\infty}^{\infty} U_1(x, y) \exp[-j \frac{2\pi}{\lambda z}(x_2 x_1 + y_2 y_1)] dx_1 dy_1 \quad (1)$$

where

$$k = \frac{2\pi}{\lambda} ,$$

$z = z_{12}$ distance from z_1 to z_2 , and

λ = optical wavelength.

The impulse response of this system is given by Goodman (4:59) which is

$$h(x_2, y_2; x_1, y_1) = \frac{\exp(jkz)}{j\lambda z} \exp\left[j\frac{k}{2z} [(x_2 - x_1)^2 + (y_2 - y_1)^2]\right] \quad (2)$$

Taking a close look at Eq (1), we see that the response of the system of Figure III-2 is just the Fourier Transform of the input signal and given by Eq (3),

$$U_2(x, y) = A \cdot F\{U_1(x, y)\} \quad \left| \begin{array}{l} f_x = \frac{x_2}{\lambda z} \\ f_y = \frac{y_2}{\lambda z} \end{array} \right. \quad (3)$$

where

$F\{\dots\}$ = Fourier transform, and

$$A = \frac{\exp(jkz) \exp\left[j\frac{k}{2z}(x_2^2 + y_2^2)\right]}{j\lambda z} .$$

The input signal $U_1[x, y]$ is just the transmittance function of the aperture ($T_1[x, y]$), in the Z_1 plane, times the unit amplitude, uniform monochromatic wave impinging on the aperture at normal incidence. Since the field to the left of the aperture is uniform with unit amplitude, the input signal is just the transmittance function (i.e., $U_1[x, y] = T_1[x, y]$) given by

$$U_1(x,y) = \begin{cases} 1 & x,y = \text{inside the aperture} \\ 0 & \text{otherwise} \end{cases} \quad (4)$$

From Eq (3) the response of the system in the Z_2 plane is

$$U_2(x,y) = A \ell_x \ell_y \text{sinc} \ell_x f_x \text{sinc} \ell_y f_y \quad (5)$$

where

ℓ_x = maximum radial extent of the object (aperture) in the Z_1 plane in the x-direction, and
 ℓ_y = maximum radial extent of the object in the y direction.

The intensity distribution $I[x,y]$ in the z_2 plane is just the square of the field in this plane given by

$$\begin{aligned} I(x,y) &= |U_2(x,y)|^2 \\ &= \ell_x^2 \ell_y^2 \text{sinc}^2 \ell_x f_x \text{sinc}^2 \ell_y f_y \end{aligned} \quad (6)$$

The phase terms will go away since we are squaring the magnitude of the function. From Eq (6) we can now predict the intensity pattern in the Z_2 plane for the given input signal $U_1[x,y]$. Notice that from Eq (6), the intensity distribution is a sinc function. The null points (minimas) of the function can be found by setting the argument of the sinc function equal to an integer (see Figure III-3).

Thus, the intensity $I[x,y] = 0$ when

$$\begin{aligned} \ell_x f_x &= 1, 2, 3 \dots & \text{where } f_x &= \frac{x_2}{\lambda z} \\ \ell_y f_y &= 1, 2, 3 \dots & f_y &= \frac{y_2}{\lambda z} \end{aligned} \quad (7)$$

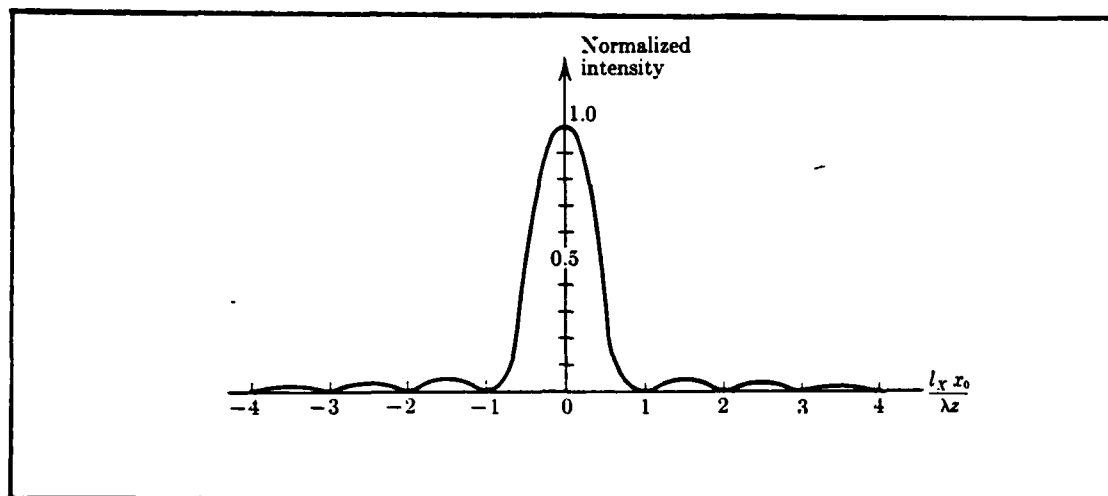


Fig. III-3. Intensity Distribution of Slit Aperture (4:63)

The evaluation of Eq (7) will be important when determining the minimas of the intensity pattern. Notice that the intensity distribution in the Z_2 plane is for the given input signal $U_1[x,y]$. This particular input signal will be used to demonstrate the intensity distribution in the Fraunhofer region for this experiment.

Fraunhofer Diffraction Far Field Measurement Procedures

Before starting this experiment, some simple calculations need to be performed. In this experiment, the student will predict the null points (minimas) of the Fraunhofer diffraction pattern for two different diffraction slit widths and two different observation distances. The positions of the first minimas of the Fraunhofer diffraction pattern can be predicted by using Eq (7) and the given data below:

1. Screen distance from aperture 1 meter
2. Light wavelength 633 nm
3. Diffraction slit width 0.04 mm

Note that the diffraction slit width is only given in one dimension. The reason for this is that the diffraction slits used (borrowed from the AFIT Physics Department) were only one-dimensional slits. Therefore, the determination of the minimas need only be determined in one direction either "x" or "y," depending on the orientation of the slit. Next, predict the position of the minimas for a screen distance of two meters away from the aperture.

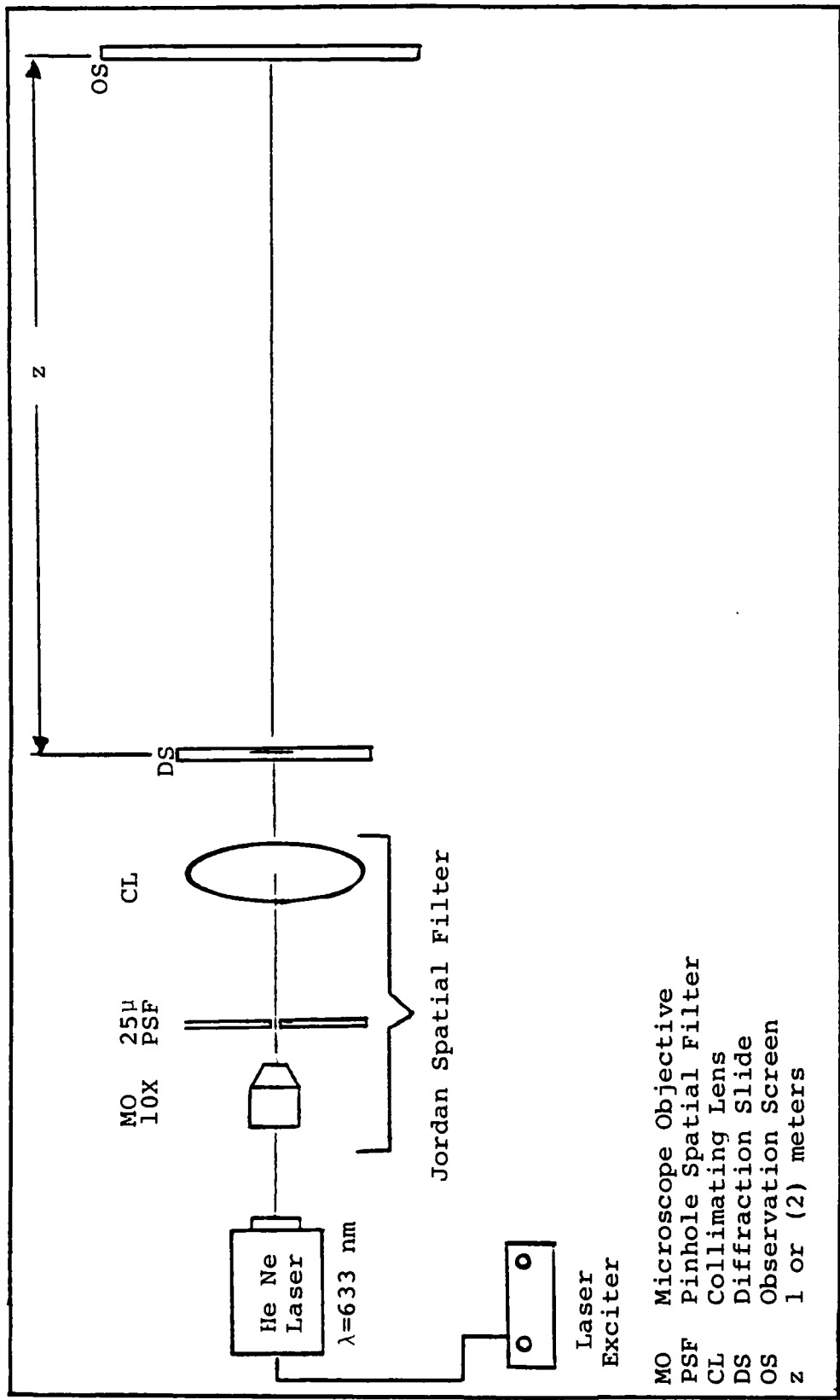
Repeat the prediction of the minimas for a diffraction slit width of 0.08 mm for a screen distance of one and two meters away from the aperture.

Figure III-4 illustrates the optical equipment setup used for this experiment. It is recommended that the following procedural steps be used to assist the student in performing the measured values of the Fraunhofer diffraction pattern.

STEPS

INSTRUCTIONS

1. Assembling the Laser Source--assemble Spectra Physics laser into laser mount and attach to a support post and post holder. Fasten the post holder to the optical table. Connect the He-Ne laser to the laser exciter.



- MO Microscope Objective
- PSF Pinhole Spatial Filter
- CL Collimating Lens
- DS Diffraction Slide
- OS Observation Screen
- z 1 or (2) meters

Fig. III-4. Fraunhofer Diffraction (Far Field) Experimental Setup

2. Jordan Spatial Filter (JSF)--fasten a post holder, approximately four inches in front of the laser post holder, to the optical table. Attach a support post to the JSF and secure it in the post holder.
3. Collimating the laser beam--turn on the laser exciter and allow a few minutes for the laser to laze. Remove the spherical collimating lens from the JSF. Adjust both the laser mount and the 25 micron pinhole filter for a good airy disk pattern out of the pinhole. (The airy disk pattern can be observed on a screen placed approximately one meter away from the JSF.) Refer to either (3:382) or (4:66) for a picture of an airy disk pattern.
Note: This step may take a few moments to align properly. Next, replace the spherical collimating lens back on the JSF and adjust until a good collimated beam is observed. A good collimated beam is one which will propagate over a long distance (30 m) and maintain the same shape and size of its pattern.
4. Put a diffraction grating slide (the slide marked with a single slit aperture), in the three-finger holder and place it approximately two inches in front of the JSF. Position the slide such that the central portion of the airy disk pattern completely lights the object (diffraction slit) of

interest (i.e., if the predictions calculated earlier were with a .04 mm slit, then illuminate the .04 mm slit on the slide).

5. Place a white screen approximately one meter away from the diffraction slide. At this distance, the Fraunhofer conditions will be satisfied. Observe the diffraction pattern in the white screen. Does the pattern in the observation screen agree with the predicted (calculated) intensity pattern? The room lights may have to be turned down if the intensity pattern is not very visible.
6. Use a small school ruler and measure the distance between the first two minimas. Does this figure agree with the calculated value? Why or why not?
7. Move the screen back two meters away from the diffracting aperture and repeat step 6.
8. Readjust the diffracting slide to fully illuminate the 0.08 mm slit and repeat steps 5-7.

The Fraunhofer diffraction pattern can be realized for other types of diffracting objects (i.e., circular shapes). This setup can also be used to determine the Fourier Transform of an object as seen from Eq (3).

Special Problems

In setting up this experiment, a very critical step is the proper collimation of the laser light. If the light

beam is not collimated properly, the far field pattern will be distorted and slightly larger than predicted. The student should pay close attention to the 25 micron spatial filter and the microscope objective on the Jordan Spatial Filter. When aligning the laser beam with the microscope objective, ensure that the laser beam is centered on the microscope objective. If the beam is not centered, it will strike the side of the microscope objective, bounce around and exit at some angle away from the optic axis. With this condition, alignment of the 25 micron pinhole spatial filter will be near to impossible. When the microscope objective and the pinhole filter are aligned properly with the laser beam, the student should see an airy disk (Fraunhofer diffraction pattern of a circular aperture (3:382)) pattern on the screen. Some slight adjustments may need to be made to obtain the best airy disk pattern out. After adjusting for the best airy pattern, screw the collimating lens back on the JSF and adjust the lens until a good collimated beam is achieved. Use a small 3" x 5" card and mark the size of the central portion of the airy pattern. Then move back approximately 20 to 30 meters and measure the central portion of the airy pattern again. The beam will be very nearly collimated if the size (radius) of the airy pattern is the same.

During the setup phase of this experiment, the use of the three-finger holder was quite awkward and difficult

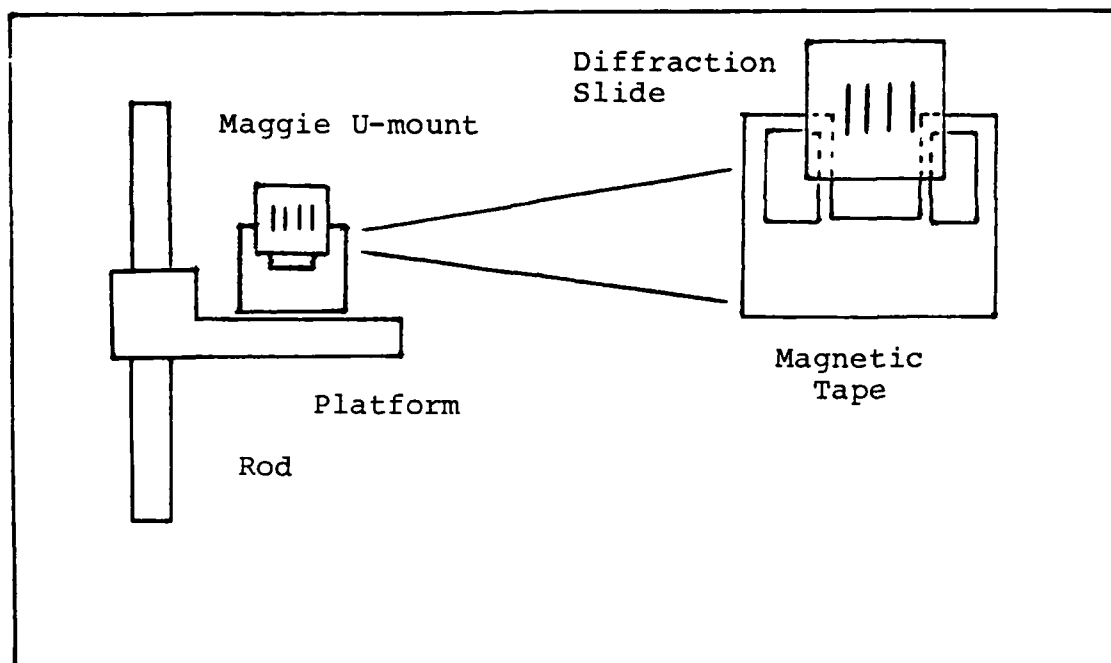


Fig. III-5. Rod/Platform Assembly with Diffraction Slide

to adjust for aligning the diffraction aperture slits up with the central beam of the laser. An easier way discovered was to use some "U-shape" brackets with magnetic stickers attached to them (see Figure III-5). A rod and platform assembly were attached to the table approximately two inches in front of the JSF. The platform was adjusted so the laser would shine between the U-shape brackets. The diffraction slides have metal strips already attached so the magnetic stickers on the brackets held the slide in place. This made setting up the diffraction slit apertures much easier.

When illuminating the diffraction slits, the student should ensure that the slit is completely illuminated

by the central portion of the airy pattern. This will enable as much of the light energy to light up the diffracting object and ensure a brighter Fraunhofer diffraction pattern.

A meter stick was laid down on the table and used as a marker to indicate where the proper distances were for the object plane and the observation screen.

Results and Sample Questions

The author's calculations and predicted patterns agreed closely with the patterns observed. Comparing the results of the predicted (theoretical) calculations to the measured values, the results are as follows:

Theoretical Predictions.

Diffraction slit: 0.04 millimeters (mm)

Screen distance: 1 meter (m)

Light wavelength: 633 nanometers (nm)

First minima: 15.8 mm; distance to the first null (minima) measured from the center of the sinc function

Diffraction slit: 0.04 mm

Screen distance: 2 m

Light wavelength: 633 nm

First minima: 31.7 mm; distance to the first null (minima) measured from the center of the sinc function

Diffraction slit: 0.08 mm
Screen distance: 1 m
Light wavelength: 633 nm
First minima: 7.9 mm; distance to the first null
(minima) measured from the center of the sinc function

Diffraction slit: 0.08 mm
Screen distance: 2 m
Light wavelength: 633 nm
First minima: 15.8 mm; distance to the first null
(minima) measured from the center of the sinc function

Measured Values.

Diffraction slit: 0.04 mm
Screen distance: 1 m
First minima: 31 mm; distance measured between
first two minimas

Diffraction slit: 0.04 mm
Screen distance: 2 m
First minima: 63 mm; distance measured between
first two minimas

Diffraction slit: 0.08 mm
Screen distance: 1 m
First minima: 15 mm; distance measured between
first two minimas

Diffraction slit: 0.08 mm

Screen distance: 2 m

First minima: 30 mm; distance measured between first two minimas

As seen from these results the measured values agreed very closely with the predicted values. Notice that the predicted values are measured from the center ($x=0$) of the sinc function. Thus, simple arithmetic will indicate that both the measured and predicted values are very comparable. The reason for any discrepancies in the answers is due to:

1. The alignment setup. Because of the precise nature of an optical beam, meticulous alignment of the equipment is critical. The type of equipment at hand only allowed for rough measurements; thus, some of the error is due to this problem.

2. When measuring the spacing between the first two minimas, it is very difficult to make markings right on when the type of measuring equipment used is large and inaccurate compared to the physical size of the intensity distribution. Thus, human error is always a factor with any experiment.

Sample Questions.

1. Could Eq (6) be used for observation distances less than 0.5 meters?

Ans: In arriving at Eq (6), the assumption was made that the observation distance be very large (4:61) compared to the maximum radial extent of the diffracting object. Therefore, Eq (6) may indeed be used for observation distances less than 0.5 meters if and only if the maximum radial extent of the object satisfies the Fraunhofer condition.

2. Could incoherent light be used to perform this experiment?

Ans: As mentioned earlier in the theory portion, the light field was assumed to be highly monochromatic and coherent. This assumption allowed us to use the Huygen's construction along with the principles of interference (called the Huygen's-Fresnel principle) to obtain the diffraction effects of the object (1). Therefore, incoherent light is not a comparable source for performing this experiment due to the non-uniform phase nature of light.

Bibliography

1. Born, Max and Emil Wolf. Principles of Optics (Electromagnetic Theory of Propagation, Interference and Diffraction of Light) [Sixth (Corrected) Edition]. Elmsford NY: Pergamon Press, 1983.
2. Class Lectures or Lecture Materials. Syed, Vagar lecture notes distributed in EE 527 "Introduction to Fourier Optics," School of Engineering, Air Force Institute of Technology (AU), Wright-Patterson AFB OH, October 1983.
3. Gaskill, Jack D. Linear Systems, Fourier Transforms and Optics. New York: John Wiley and Sons, Inc., 1978.
4. Goodman, Joseph W. Introduction to Fourier Optics. New York: McGraw Hill Book Co., 1968.
5. Jenkins, Francis A. and Harvey E. White. Fundamentals of Optics (Fourth Edition). New York: McGraw Hill Book Co., 1976.
6. Meyer-Arendt, Jurgen R. Introduction to Classical and Modern Optics. Englewood Cliffs NJ: Prentice Hall, Inc., 1972.
7. Young, Hugh D. Fundamentals of Waves, Optics, and Modern Physics (Second Edition). New York: McGraw Hill Book Co., 1976.

IV. Fraunhofer Diffraction Using Lenses

Assignment

The student will observe the Fraunhofer Diffraction in the near field using a lens. The student will predict the intensity pattern in the focal plane of the lens and plot a graph of it. The student will then compare results with the previous far field experiments.

Objectives of the Experiment

1. To acquaint the student with the use of lenses.
2. To relate classroom theory of Fraunhofer Diffraction with practical application.
3. To give the student some experience with simple apertures, lenses, and laser light.

Equipment Needed

Laser Source: Spectra Physics Helium-Neon Class IIIb
4 mw (Model 102-1) and Spectra Physics
Laser Exciter (Model 212-1).

Newport Laser Mount (Model 810), 1 each

Newport Support Post (Model VPH-4), 1 each

Newport Post Holder (Model SP-4), 1 each

Jordan Spatial
Filter:

- a. Microscope Objective 10X
- b. 25 micron Pinhole Spatial Filter
- c. Spherical Collimating lens

Newport Support Post (Model VPH-4), 1 each

Newport Post Holder (Model SP-4), 1 each

Focusing
Lens:

- a. Spherical Convex Lens with Holder
(150 mm) or equivalent

- b. Translational Stage Newport Model 430

Newport Support Post (Model VPH-4), 1 each

Newport Post Holder (Model SP-4), 1 each

Diffraction Grating Slides (1 set)

Three Finger Holder with stand or equivalent

White Cardboard Screen, 2 ft. x 2 ft.

Theory/Background

From Chapter III, the Fraunhofer Diffraction Theory was derived and implemented for students to get an understanding and some intuitive feeling for the optics involved. The observation screen was placed in the far field of the aperture so the Huygens principle would be seen to agree with mathematical analysis. The results proved to be quite favorable and extremely close to calculated values. An important component of an optical system is a lens. The properties of a lens and its geometrical ray diagrams can be found in references (1; 5; 6; 7; 8). For the purpose of

discussion, the approach to lenses we will discuss in this chapter will be like that presented in Goodman (4).

A lens is made of some optically dense material (glass, plastic) in which the propagation velocity of the light through the lens is slower than the velocity of light in air. A thin lens is defined to be that in which a ray of light entering at coordinates (x,y) will emerge at the opposite end of the lens at the same coordinates (x,y) (i.e., the ray translation in the lens is extremely small). Therefore, a lens can be thought of as an optical delay which delays an incident wavefront by some amount proportional to the thickness at some particular coordinate. Since much of the derivations and theory of deriving a transmittance function for a lens is treated in Goodman and covered in (2) (Introduction to Fourier Optics), we will just briefly touch on the highlights of using a lens as a phase transformer.

Referring to Figure IV-1, let the maximum thickness of the lens be Δ_0 and the thickness at coordinates (x,y) be $\Delta(x,y)$. Then the total phase delay suffered by the wave at (x,y) in propagating through the lens is

$$\phi(x,y) = kn\Delta(x,y) + k[\Delta_0 - \Delta(x,y)] \quad (1)$$

where

n = index of refraction for the lens material;

$k\Delta(x,y)$ = phase delay introduced by the lens; and

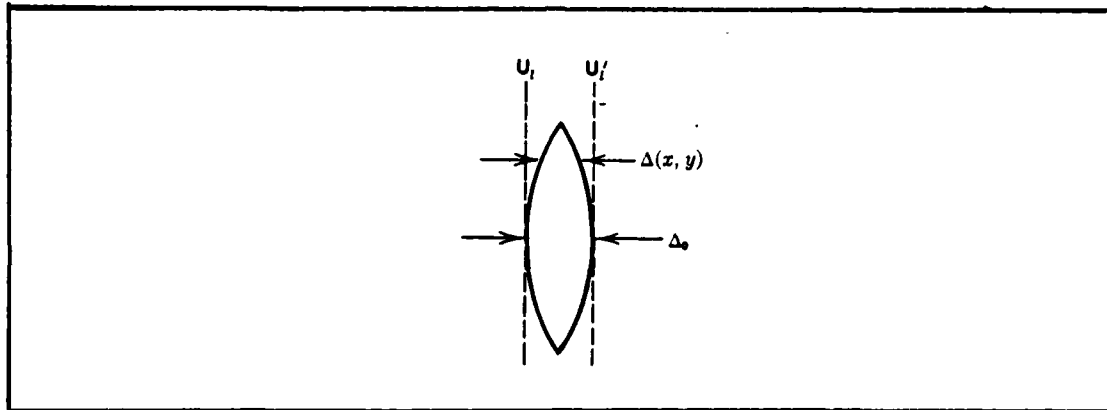


Fig. IV-1. The Thickness Function (4:78)

$k[\Delta_0 - \Delta(x, y)]$ = phase delay introduced by the remaining free space region between the two planes.

Adopting the sign convention of light rays traveling through a lens as outlined in Goodman (4:78), the thickness function can be derived by separating the lens into two halves as outlined in Figure IV-2. Referring to the geometry as shown in the figure, the thickness function can be written, with the help of some paraxial approximations, as

$$\Delta(x, y) = \Delta_0 - \frac{x^2 + y^2}{2} \left[\frac{1}{R_1} - \frac{1}{R_2} \right] \quad (2)$$

It should be noted that many of the steps in arriving at this function should be covered in (2).

The lens can be thought of as a multiplicative transmittance function where the transmittance function can

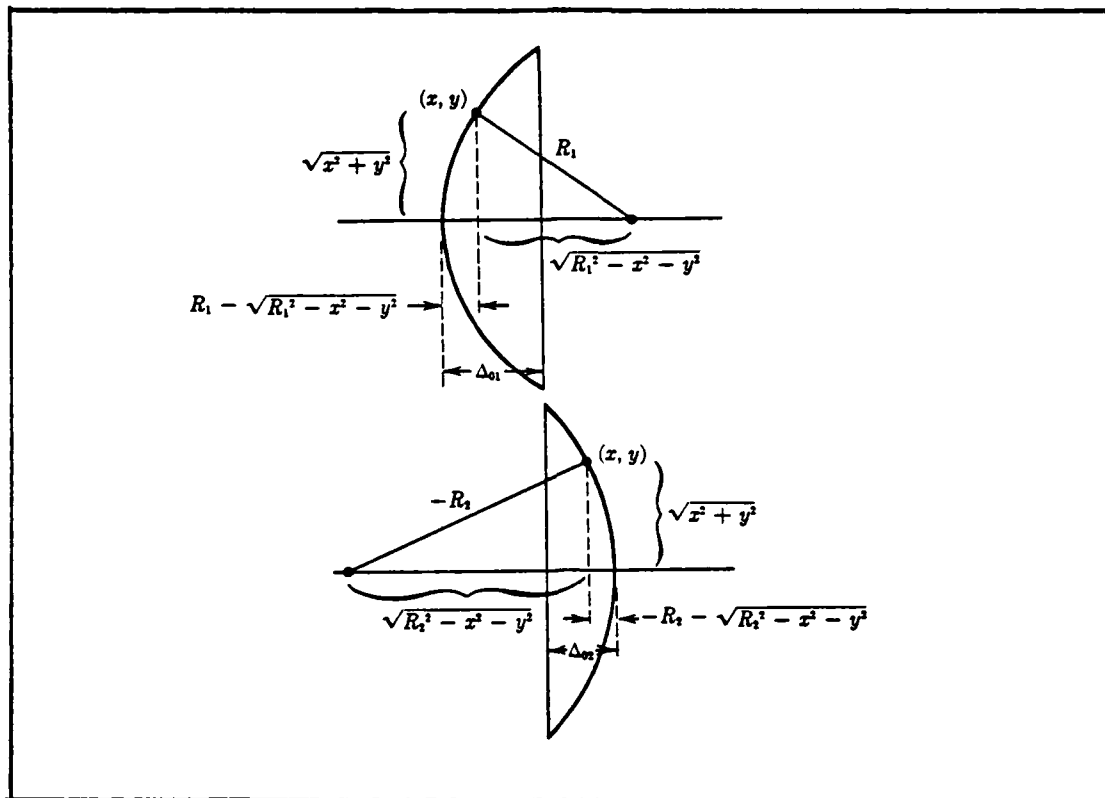


Fig. IV-2. Geometry for the Thickness Function (4:79)

be written as

$$t_0(x,y) = \exp j[\phi(x,y)] \quad (3)$$

From Figure IV-1, the complex field $U_\ell'(x,y)$ across a plane immediately behind the lens is related to the complex field U_ℓ immediately across a plane in front of the lens by

$$U_\ell'(x,y) = t_0(x,y)U_\ell(x,y) \quad (4)$$

Substitution of Eq (2) into Eq (1) and then substituting Eq (1) into Eq (3), the transmittance function of the lens becomes, with a little rearranging,

$$t_0(x,y) = \exp[j\Delta_0 kn] \exp[-jk(n-1) \frac{x^2+y^2}{2} (\frac{1}{R_1} - \frac{1}{R_2})] \quad (5)$$

The physical properties of a lens (that is n , R_1 , R_2) can be combined into a single number f called the focal length (4:80) which is defined by

$$\frac{1}{f} \triangleq (n-1) (\frac{1}{R_1} - \frac{1}{R_2}) \quad (6)$$

Substitution of Eq (6) into Eq (5), the phase transformation of the lens, becomes

$$t_0(x,y) = \exp[jkn\Delta_0] \exp[-j\frac{k}{2f}(x^2 + y^2)] \quad (7)$$

This equation will be used to represent the effects of a lens on some incidence disturbance. Note that although this equation was derived with a particular geometry for a lens, this equation may be used to represent other types of lenses (4:81) as long as the proper sign is used for the focal length.

Fourier Transforming Properties of Lenses. A very useful property of a converging lens is its ability to perform two-dimensional Fourier transforms. In Goodman, three separate configurations are used to perform the transform operation (see Figure IV-3). In case (a) the object to be transformed is placed directly in front of the lens; in case (b) the object is placed a distance d_0 in front of

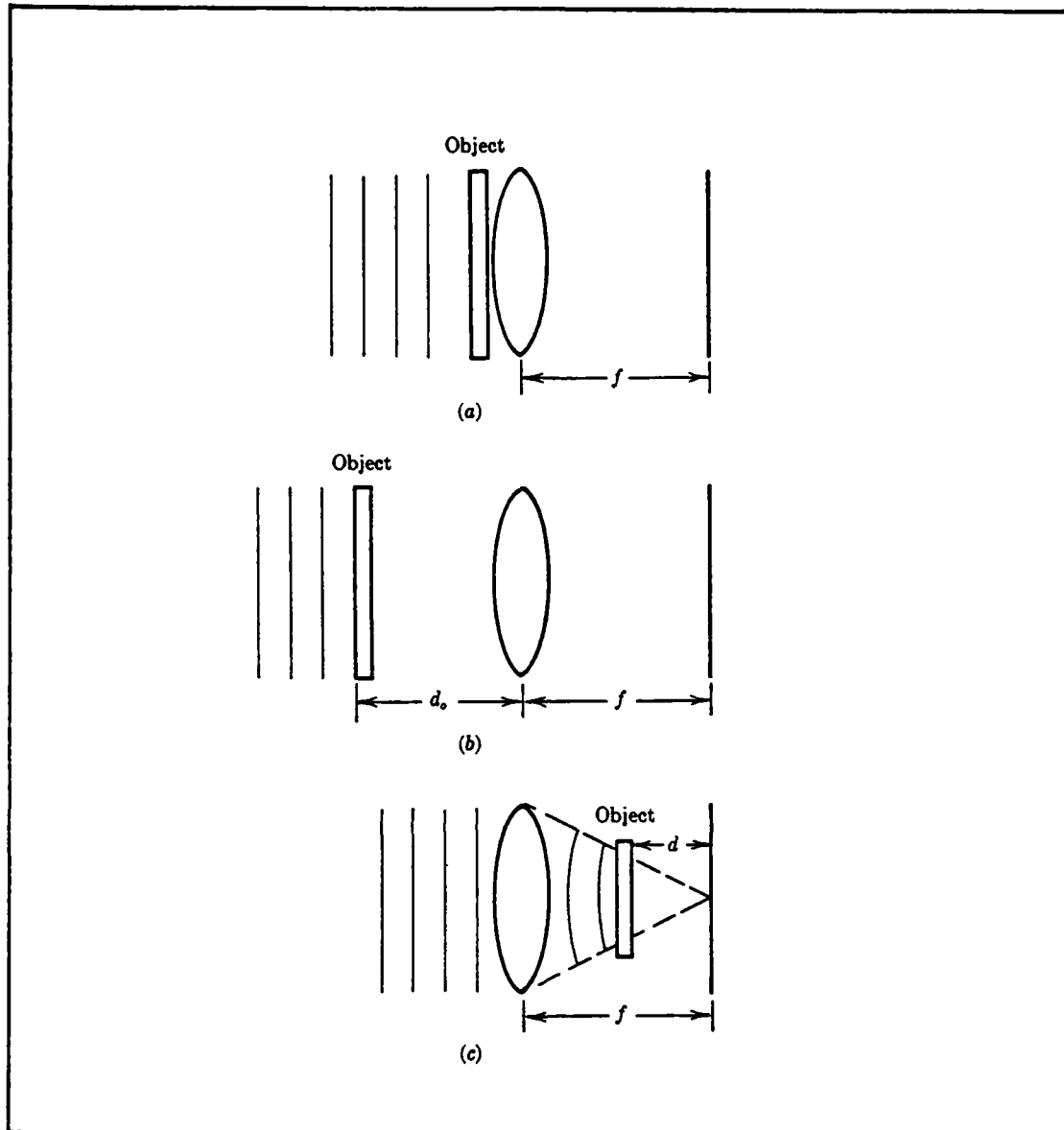


Figure IV-3. Fourier Transforming Configurations (4:84)

- (a) Object Against Lens
- (b) Object in Front of Lens
- (c) Object in Back of Lens

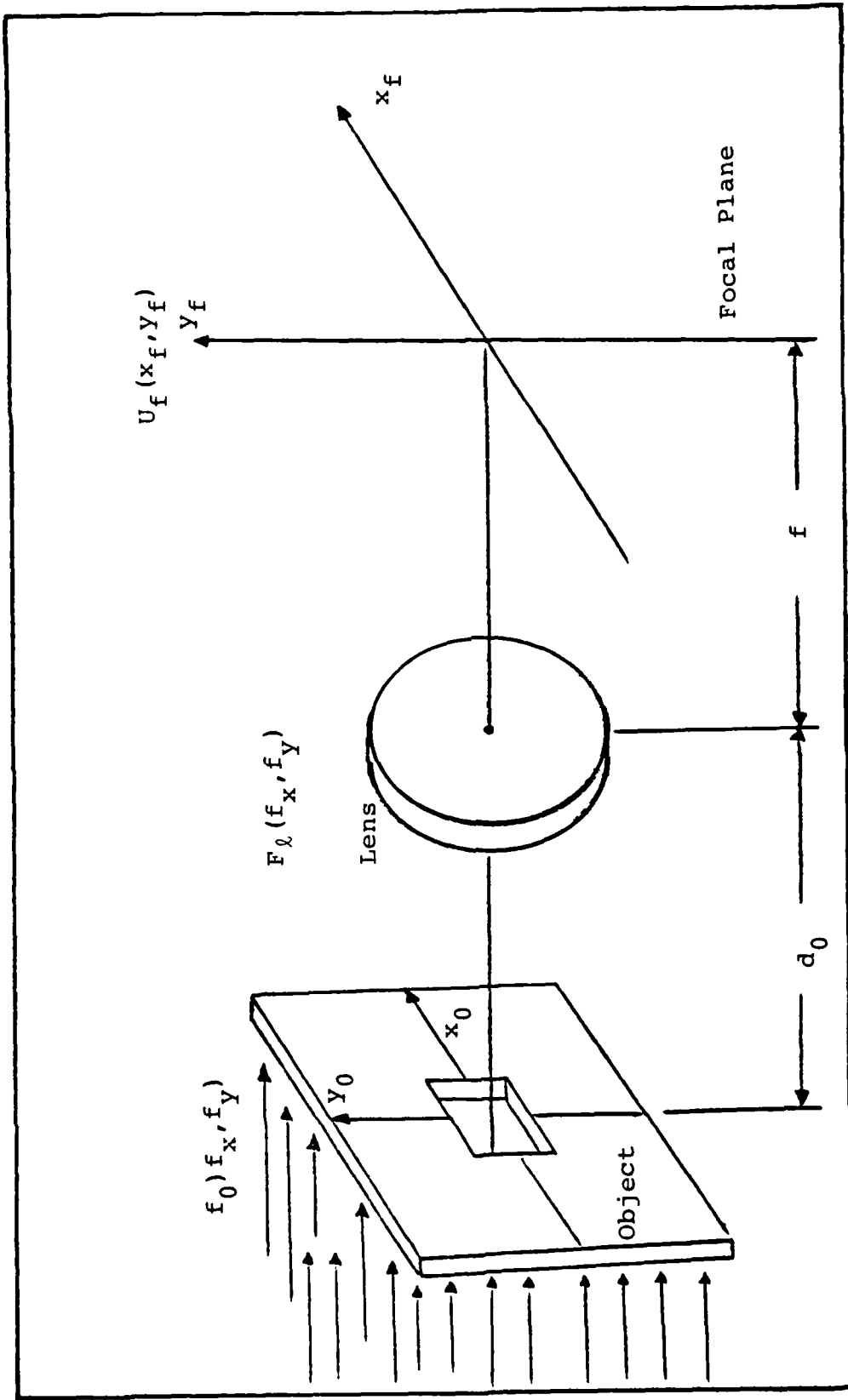


Fig. IV-4. Object Placed in Front of Lens

where

the constant phase factor $\exp(jkz)$ has been dropped
and d_0 is the object's distance (z) to the lens.

The amplitude distribution $U_f(x,y)$ in the focal plane
(Fourier plane) of the lens is given by

$$U_f(x_f, y_f) = - \frac{A \exp\left[j \frac{k}{2f} \left(1 - \frac{d_0}{f}\right) (x_f^2 + y_f^2)\right]}{j \lambda f} \iint_{-\infty}^{\infty} t_0(x_0, y_0) \exp\left[-j \frac{2\pi}{\lambda f} (x_0 x_f + y_0 y_f)\right] dx_0 dy_0 \quad (12)$$

where

the aperture effects of the lens have been
neglected (i.e., the pupil function of the lens
= 1).

The amplitude and phase of the light at coordinates (x_f, y_f)
are related to the amplitude and phase of the object
spectrum at spatial frequencies ($f_x = x_f/\lambda \cdot f$, $f_y = y_f/\lambda \cdot f$).
From Eq (12) we see that a phase factor precedes the
transform integral; however, at the special distance $d_0=f$
this phase factor vanishes and the field in the back focal
plane of the lens is an exact Fourier transform of the
object's transmittance function. With $d_0=f$ the field in the
back focal plane becomes:

$$\begin{aligned}
U_f(x_f, y_f) &= \frac{A}{j\lambda f} \iint_{-\infty}^{\infty} t_0(x_0, y_0) \exp[-j \frac{2\pi}{\lambda f} (x_0 x_f + y_0 y_f)] dx_0 dy_0 \\
&+ \frac{A}{j\lambda f} F[t_0(x_0, y_0)] \Big|_{\substack{f_x = \frac{x_f}{\lambda f} \\ f_y = \frac{y_f}{\lambda f}}}
\end{aligned} \tag{13}$$

The intensity pattern in the back focal plane is

$$I_f(x_f, y_f) = |U_f(x_f, y_f)|^2 = \frac{A^2}{\lambda^2 f^2} |F[t_0(x_0, y_0)]|^2 \tag{14}$$

From these results it is realized that the intensity pattern $I_f(x_f, y_f)$ is the same as the intensity pattern for the Fraunhofer diffraction from Chapter III and the advantage of a lens is that the pattern appears in a plane much closer to the object.

One of our earlier assumptions was that the pupil function of the lens can be neglected. This assumption is valid as long as the object is much smaller than the lens aperture. Taking the effects of the lens aperture into account, the use of geometrical optic approximations is needed. These approximations are valid if the distance d_0 is sufficiently small such that the object is well within the Fresnel diffraction region of the lens. This limitation of the effective object by the finite lens aperture is called

"vignetting." Two ways to reduce the vignetting effect are: (1) move the object closer to the lens, or (2) use a larger lens aperture.

In practice, it is best to place the object well against the front surface of the lens to minimize the vignetting effect; however, for analysis, it is preferred to place the object in the front focal plane of the lens to obtain an exact Fourier Transform relationship.

These results show that the Fraunhofer Diffraction pattern in the far field can be realized in the near field by using a convex lens. This experiment will use the results of these calculations and the student should be able to observe, in the back focal plane of a lens, the Fraunhofer Diffraction pattern (Fourier Transform) of an object placed one focal length in front of the lens.

Fraunhofer Diffraction with Lenses Measurement Procedures

Preliminary Calculations. Before performing the experiment, some calculations need to be performed. Referring to Figure IV-4, let the object transmittance function be the diffraction slit (0.04 mm or 0.08 mm) used in the far field experiment. With the distance d_0 equal to f (focal length of the lens), determine the intensity distribution $(I(x,y) = |U_f(x_p, y_p)|^2)$ for the screen in the back focal plane of the lens and calculate the

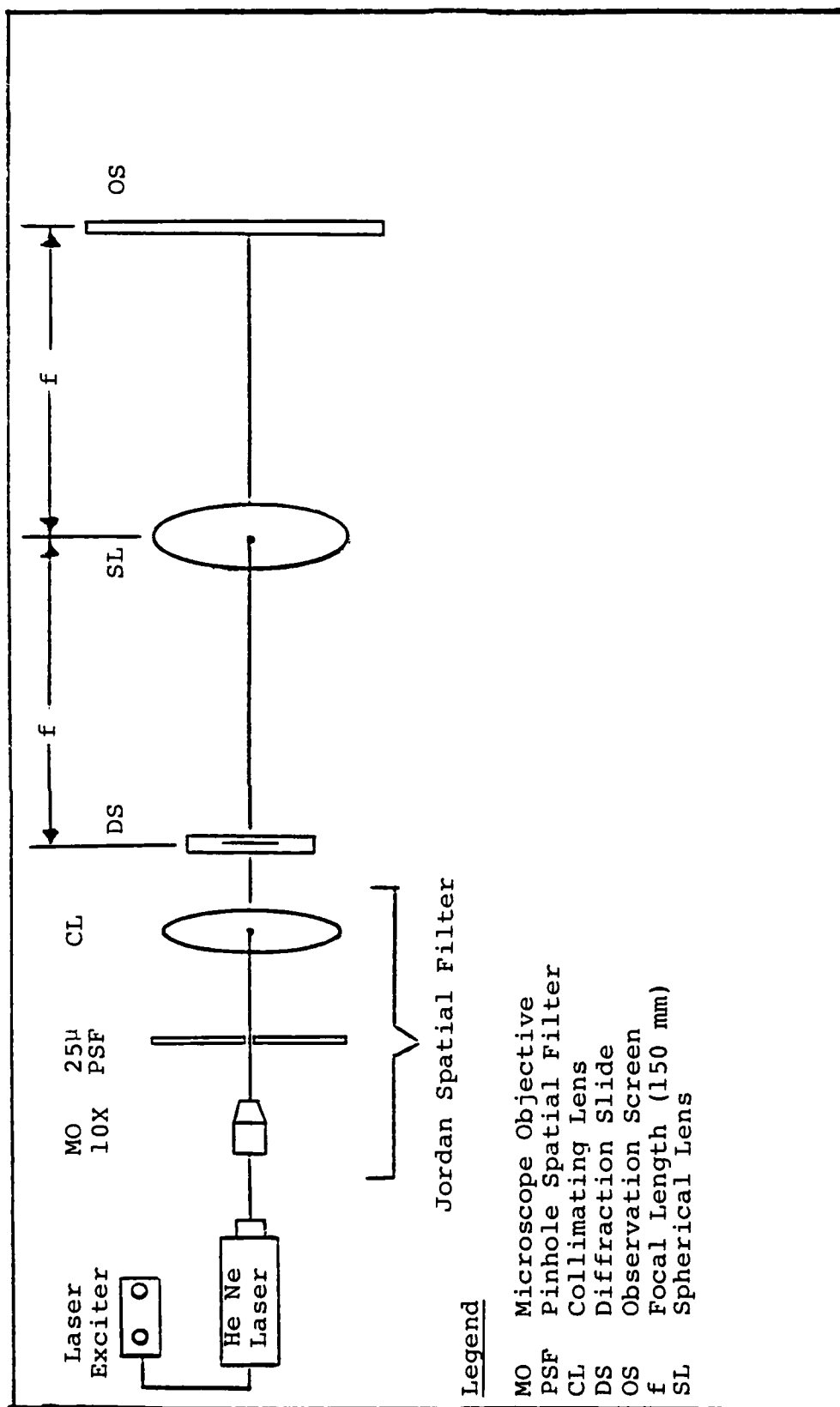
positions for the minimas (nulls) of the intensity pattern. Plot a graph of the intensity distribution.

The experimental setup used is identical to that of Fraunhofer Diffraction in the far field, except here a lens is placed one focal length in front of the object and a screen one focal length behind the lens (see Figure IV-5). Conducting this experiment is relatively simple and straightforward. The following steps will help to properly implement this experiment.

STEPS

INSTRUCTIONS

1. Assembling the Laser Source--assemble Spectra Physics laser into laser mount and attach to a support post holder. Fasten the post holder to the optical table. Connect the He-Ne laser to the laser exciter.
2. Jordan Spatial Filter (JSF)--fasten a post holder, approximately four inches in front of the laser post holder, to the optical table. Attach a support post to the JSF and secure it in the post holder.
3. Collimating the laser beam--turn on the laser exciter and allow a few minutes for the laser to lase. Remove the spherical collimating lens from the JSF. Adjust both the laser mount and the 25 micron pinhole filter for a good airy disk pattern



Legend

- MO Microscope Objective
- PSF Pinhole Spatial Filter
- CL Collimating Lens
- DS Diffraction Slide
- OS Observation Screen
- f Focal Length (150 mm)
- SL Spherical Lens

Fig. IV-5. Fraunhofer Diffraction/Lenses Experimental Setup

out of the pinhole. (The airy disk pattern can be observed on a screen placed approximately one meter away from the JSF.) Note: This step may take a few moments to align properly. Next, replace the spherical collimating lens back on the JSF and adjust until a good collimated beam is observed.

4. Focusing Lens--fasten a support post to a translation stage and secure the post in a post holder placed in front (200 mm) of the JSF. The stage should move in a parallel line with the laser beam. Next, fasten a spherical lens with holder to the translation stage and adjust the height of the support post so the laser beam strikes the center portion of the lens.
5. Put a diffraction grating slide (the slide marked with single slit apertures), in the three-finger holder and place it one focal length (150 mm) in front of the lens. Position the slide such that the central portion of the airy disk pattern completely lights the object (diffraction slit) of interest (i.e., if the predictions calculated earlier were with a .04 mm slit, then illuminate the .04 mm slit on the slide).
6. Place a white screen in the back focal plane (Fourier Transform plane) of the lens and observe the pattern. Is this the same pattern observed

for the far field experiments? What differences, if any, are there? How well does the pattern compare to the one predicted earlier?

Steps 5 and 6 can be repeated for different diffraction slits. The student should perform at least two different diffraction slits to develop a good understanding of the irradiance pattern.

Special Problems

The student is reminded here that collimating the laser beam is a very important step. From Chapter III, the problems of collimating a beam were explained and the student should review these findings so as not to repeat the same errors.

In setting this experiment up, it is important that the screen be located exactly one focal length behind the lens. If this distance is not precise, the irradiance pattern observed on the screen may not be a true Fourier Transform Spectrum.

During the setup phase of this experiment, the use of the three finger holder was quite awkward and difficult to adjust for aligning the diffraction aperture slits up with the central beam of the laser. An easier way discovered was to use some "U-shape" brackets with magnetic stickers attached to them (see Figure III-5). A rod and platform assembly were attached to the table approximately

one focal length in front of the lens. The platform was adjusted so the laser would shine between the U-shape brackets. The diffraction slides have metal strips already attached so the magnetic stickers on the brackets held the slide in place. This made setting up the diffraction slit apertures much easier.

A meter stick was laid down on the table and used as a marker to indicate where the proper distances were for the object plane and the observation screen.

Results

The author's calculations and predicted patterns agreed closely with the patterns observed. In comparing the results of this chapter to Chapter III, the results showed negligible differences. The theoretical calculations are as follows:

Theoretical Predictions.

Diffraction slit: 0.04 millimeters (mm)

Screen distance: 150 mm

Light wavelength: 633 nanometers (nm)

First minima: 2.37 mm; distance to the first null (minima) measured from the center of the sinc function

Diffraction slit: 0.08 mm

Screen distance: 150 mm

Light wavelength: 633 nm

First minima: 1.18; distance to the first null (minima) measured from the center of the sinc function

Measured Values.

Diffraction slit: 0.04 mm

Screen distance: 150 mm

First minima: 5 mm (approximate measurement); distance measured between first two minimas

As seen from these results, the measured values agreed very closely with the predicted values. The measurement for the second diffraction slide was not taken due to the physical size of the pattern and the crude measuring device used.

The observation was made that the Intensity Pattern behind the lens was a lot smaller than the Intensity Pattern for the far field pattern. The reason for the difference is, the size of the pattern in the focal plane is due to the phase transformation of the convex lens Eq (14) where the size of the far field pattern is due to the diffraction spreading of the laser light itself (see Chapter III, Eq (6)). The difference in size was predicted in the theoretical calculations above; thus, the fact that the size of the near field pattern was much smaller than the far field pattern should have been expected. A graph of the intensity function agreed with

the intensity function of Chapter III (Figure III-3);
therefore, it was not repeated here.

Bibliography

1. Born, Max and Emil Wolf. Principles of Optics (Electromagnetic Theory of Propagation, Interference and Diffraction of Light) [Sixth (Corrected) Edition]. Elmsford NY: Pergamon Press, 1983.
2. Class Lectures or Lecture Materials. Syed, Vagar lecture notes distributed in EE 527 "Introduction to Fourier Optics," School of Engineering, Air Force Institute of Technology (AU), Wright-Patterson AFB OH, October 1983.
3. Gaskill, J. D. Linear Systems, Fourier Transforms and Optics. New York: John Wiley and Sons, 1978.
4. Goodman, Joseph W. Introduction to Fourier Optics. New York: McGraw Hill Book Co., 1968.
5. Jenkins, Francis A. and Harvey E. White. Fundamentals of Optics (Fourth Edition). New York: McGraw Hill Book Co., 1976.
6. Klein, Miles V. Optics. New York: John Wiley and Sons, Inc., 1970.
7. Meyer-Arendt, Jurgen R. Introduction to Classical and Modern Optics. Englewood Cliffs NJ: Prentice Hall, Inc., 1972.
8. Young, Hugh D. Fundamental of Waves, Optics, and Modern Physics (Second Edition). New York: McGraw Hill Book Co., 1976.

V. Imaging and Spatial Filtering

Assignment

The student will apply the knowledge learned from Chapter IV and extend this to Imaging of an object using a two-lens system. The student will also observe the Fraunhofer Diffraction in the near field using a lens and perform some simple linear Spatial Filtering using an aperture stop.

Objectives of the Experiment

1. To acquaint the student with the use of a two-lens system.
2. To relate classroom theory of Fourier Transformation and Convolution to Fraunhofer Diffraction and spatial filtering.
3. To observe the various intensity distributions for different types of diffraction grating apertures.

Equipment Needed

Laser Source: Spectra Physics Helium-Neon Class IIIb
4 mw (Model 102-1) and Spectra Physics
Laser Exciter (Model 212-1).

Newport Laser Mount (Model 810), 1 each

Newport Support Post (Model VPH-4), 1 each

Newport Post Holder (Model SP-4), 1 each

Jordan Spatial
Filter:

a. Microscope Objective 10X

b. 25 micron Pinhole Spatial Filter

c. Spherical Collimating lens

Newport Support Post (Model VPH-4), 1 each

Newport Post Holder (Model SP-4), 1 each

Focusing
Lens:

a. Spherical Convex Lens with Holder

(150 mm) or equivalent, 3 each

b. Translational Stage Newport (Model 430),
3 each

Newport Support Post (Model VPH-4), 3 each

Newport Post Holder (Model SP-4), 3 each

Diffraction Grating Slides (1 set)

Three Finger Holder with stand or equivalent

Newport Rod and Platform Assembly (Model 300), 2 each

Metrologic Maggie "U" mount, Part No. 30180, 4 each

Magnetic Tape 1" x 28" (Metrologic Part No. 00068)

1/8" size Architecture lettering or equivalent

White Cardboard Screen, 2 ft. x 2 ft.

Theory/Background

In this chapter we will use the concepts of linear shift-invariant systems and our understanding of diffraction to analyze various images for coherent illumination. We will start by analyzing some imaging effects of a one-lens system and then go to a two-lens system for further analysis. For the lenses, objects and collimated light that will be used in this chapter, we shall assume that the lenses are free of aberrations, the object is fully illuminated by the laser, and the object is well within the pupil function of the lens. This will help to simplify analyzing the developments of the optical systems.

The most familiar property of a single lens is the ability to form images. If an object is placed in front of a lens and illuminated, then under certain conditions (1), there will appear across a second plane behind the lens, an intensity distribution which closely resembles that of the object. This distribution is known as the image of the object.

Referring to Figure V-1, let an object be illuminated a distance d_0 in front of a convex lens, with monochromatic light. The complex field immediately behind the object is represented by $U_0(x_0, y_0)$. The field $U_i(x_i, y_i)$ can be represented by the superposition integral

$$U_i(x_i, y_i) = \iint_{-\infty}^{\infty} h(x_i, y_i; x_0, y_0) U_0(x_0, y_0) dx_0 dy_0 \quad (1)$$

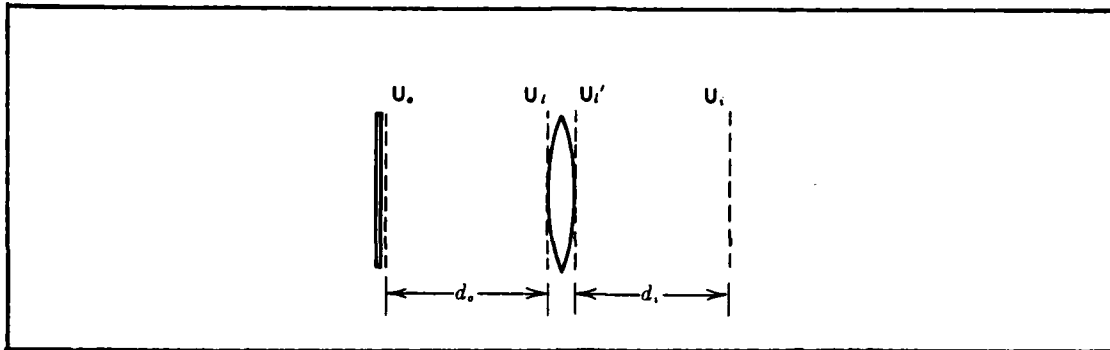


Fig. V-1. Geometry for Image Formation (3:90)

where the impulse response $h(x_i, y_i; x_0, y_0)$ is the field amplitude produced at coordinates (x_i, y_i) by a unit amplitude point source applied at the object coordinates (x_0, y_0) . This impulse response is simplified if the condition

$$\frac{1}{d_0} + \frac{1}{d_i} = \frac{1}{f} \quad (2)$$

where

d_i = observation distance behind the lens, and
 f = focal length of lens,

is satisfied. Therefore, satisfying Eq (3) the impulse response h becomes

$$h(x_i, y_i; x_0, y_0) = \frac{1}{\lambda^2 d_0 d_i} \iint P(x, y) \exp[-j \frac{2\pi}{\lambda d_i} [(x_i + Mx_0)x + (y_i + My_0)y]] dx dy \quad (3)$$

where

$P(x, y)$ = pupil function of the lens, and

$M = \frac{d_i}{d_0}$ (magnification of the system).

Notice that the impulse response h is just the Fraunhofer Diffraction pattern of the pupil function of the lens centered on image coordinates $(x_i = -Mx_0, y_i = -My_0)$.

By using our previous assumption of neglecting the pupil function ($P(x,y)=1$) and allowing the wavelength λ to approach zero, in which case diffraction effects become negligible, the impulse response can be reduced to

$$h(x_i, y_i; x_0, y_0) = \frac{1}{M} \delta\left(\frac{x_i}{M} + x_0; \frac{y_i}{M} + y_0\right) \quad (4)$$

Substituting Eq (4) into Eq (1) the relationship between $U_0(x_0, y_0)$ and $U_i(x_i, y_i)$ becomes

$$U(x_i, y_i) = \frac{1}{M} U_0\left(-\frac{x_i}{M}, -\frac{y_i}{M}\right) \quad (5)$$

Thus in conclusion, the image predicted on the basis of geometric optics is an exact replica of the object except magnified and inverted in the image plane (3:95).

Now note that diffraction effects have not been included in the exact geometrical optics prediction. For a more complete understanding of the relationship between an object and its image, diffraction effects must be included. Therefore, to include the diffraction effects, a revised impulse response is necessary to give the relationship between the object and its image more validity. Thus,

$$U_i(x_i, y_i) = h_r(x_i, y_i) * U_g(x_i, y_i) \quad (6)$$

where

$$\begin{aligned}
 U_g(x_i, y_i) &= \text{the image predicted on the basis of} \\
 &\quad \text{geometrical optics Eq (5), and} \\
 h_r(x_i, y_i) &= \text{revised impulse response} \\
 &= M \iint_{-\infty}^{\infty} P(\lambda d_i \hat{x}, \lambda d_i \hat{y}) \exp[-j2\pi(x_i \hat{x} + y_i \hat{y})] \\
 &\quad \hat{d}x \hat{d}y. \quad (7)
 \end{aligned}$$

Thus, as we can see that when the diffraction effects of the pupil are included, the image is no longer an exact replica but a smoothed version of the object which is a consequence of the nonzero width of the impulse response h (3:96).

Now let us further our analysis to a two-lens system. Since there are so many different two-lens system configurations, we will only consider one special case in our analysis. The configuration of Figure V-2 is the simplest of all the two-lens systems (2:474). Reference Figure V-3. Let's define some terms that will be used.

$$z_{ij} = z_j - z_i \quad (8)$$

with plane wave illumination

$$z_{ij} = \infty \quad j = 2, 3, 4, 5, 6$$

U_k^- = plane immediately in front of the k th component or object (i.e., U_3^- = plane directly in front of the lens at $z = z_3$)

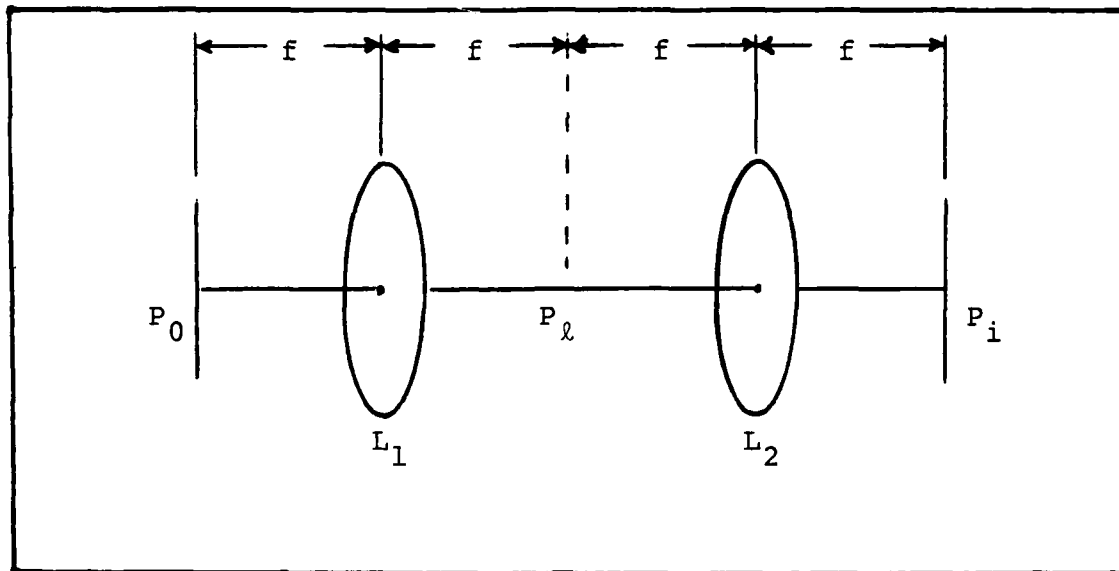


Fig. V-2. Two-Lens System in One Dimension

U_k^+ = plane immediately behind the kth component or object

Let the distance $z_{23} = z_{34} = z_{45} = z_{56} = f$. Then from Chapter IV the field amplitude distribution at $z = z_4$ is given by

$$U_4^-(x, y) = A \frac{e^{j2kf}}{j\lambda f} T_2\left(\frac{x}{\lambda f}, \frac{y}{\lambda f}\right) \quad (9)$$

where

A = amplitude of incident light, and

$$T_2(f_x, f_y) = \text{FT}[t_2(\hat{x}, \hat{y})] \Big|_{f_x = \frac{x}{\lambda f}, f_y = \frac{y}{\lambda f}}$$

= Fourier Transform of the object's transmittance function.

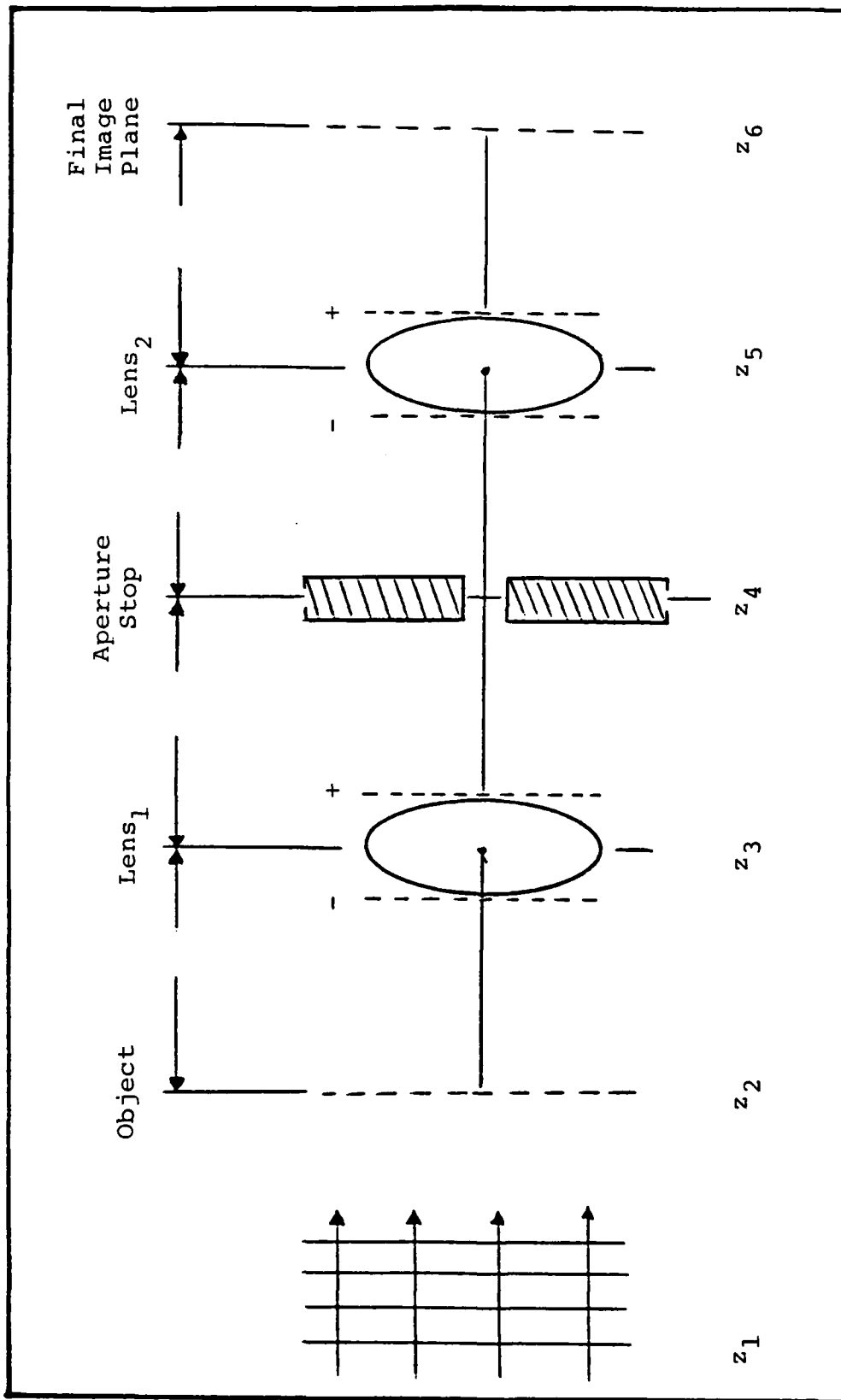


Fig. V-3. Optical System Used to Investigate Coherent Image Formation

The aperture stop has a pupil function $P_4(x,y)$; thus, the field behind the stop becomes

$$U_4^+(x,y) = U_4^-(x,y) \cdot P_4(x,y) \quad (10)$$

Now let's define

$$v_4(x,y) = \frac{e^{j2kf}}{j\lambda f} T_2\left(\frac{x}{\lambda f}, \frac{y}{\lambda f}\right) P_4(x,y) \quad (11)$$

Thus we obtain

$$U_4^+(x,y) = A v_4(x,y) \quad (12)$$

From (2:451-452) the field in plane $z = z_6$ becomes

$$U_6(x,y) = A \frac{e^{j2kf}}{j\lambda f} v_4\left(\frac{x}{\lambda f}, \frac{y}{\lambda f}\right) \quad (13)$$

and with

$$v_4(a,b) = \frac{e^{j2kf}}{j\lambda f} (\lambda f)^2 t_2(-\lambda f a, -\lambda f b) ** P_4(a,b) \quad (14)$$

we can write

$$\begin{aligned} U_6(x,y) &= -A \frac{e^{j4kf}}{(\lambda f)^2} [t_2(-x, -y) ** P_4\left(\frac{x}{\lambda f}, \frac{y}{\lambda f}\right)] \\ &= -A e^{j4kf} [t_2(-x, -y) ** \frac{1}{(\lambda f)^2} P_4\left(\frac{x}{\lambda f}, \frac{y}{\lambda f}\right)] \end{aligned} \quad (15)$$

As we can see from the conclusion, the image amplitude is given by the convolution of the geometrical image of

$t_2(-x, -y)$ and the Fraunhofer Diffraction pattern of the exit pupil. In this case, the exit pupil is the aperture stop in the plane $z = z_4$. The expression of Eq (15) is valid as long as the following conditions are met:

1. The aperture stop must be the limiting element of the system and must be located in the frequency plane.

2. The Fresnel conditions must be satisfied for each segment of the system.

The convolution of Eq (15) suggests that the image might be regarded as the output of a linear shift invariant system. With this in mind, let's use the frequency domain approach developed from linear systems (2:208-212).

The object can be related to the output by:

$$U_6(f_x, f_y) = U_2(f_x, f_y) H_{26}(f_x, f_y) \quad (16)$$

where

$$\begin{aligned} H_{26}(f_x, f_y) &= F^{-1} \left[\frac{1}{(\lambda f)^2} P_4 \left(\frac{x}{\lambda f}, \frac{y}{\lambda f} \right) \right] \\ &= p_4(-\lambda f f_x, -\lambda f f_y) \end{aligned} \quad (17)$$

Note: The subscript 26 means the transfer function from the plane $z = z_2$ to the plane $z = z_6$. Thus we see that the transfer function is simply a scaled version of the exit pupil. The effects of placing the aperture stop in the frequency plane is to cause the spectrum of the input to be multiplied by an appropriate scaled version of the

aperture stop transmittance function. Thus we have made use of the multiplicative nature of the transfer function. From this we can see that if the stop is in any other plane except the frequency plane, the system will not multiply the frequency spectrum of the input with the transfer function and thus the system will lose its shift invariant properties.

Thus the image spectrum can be determined by

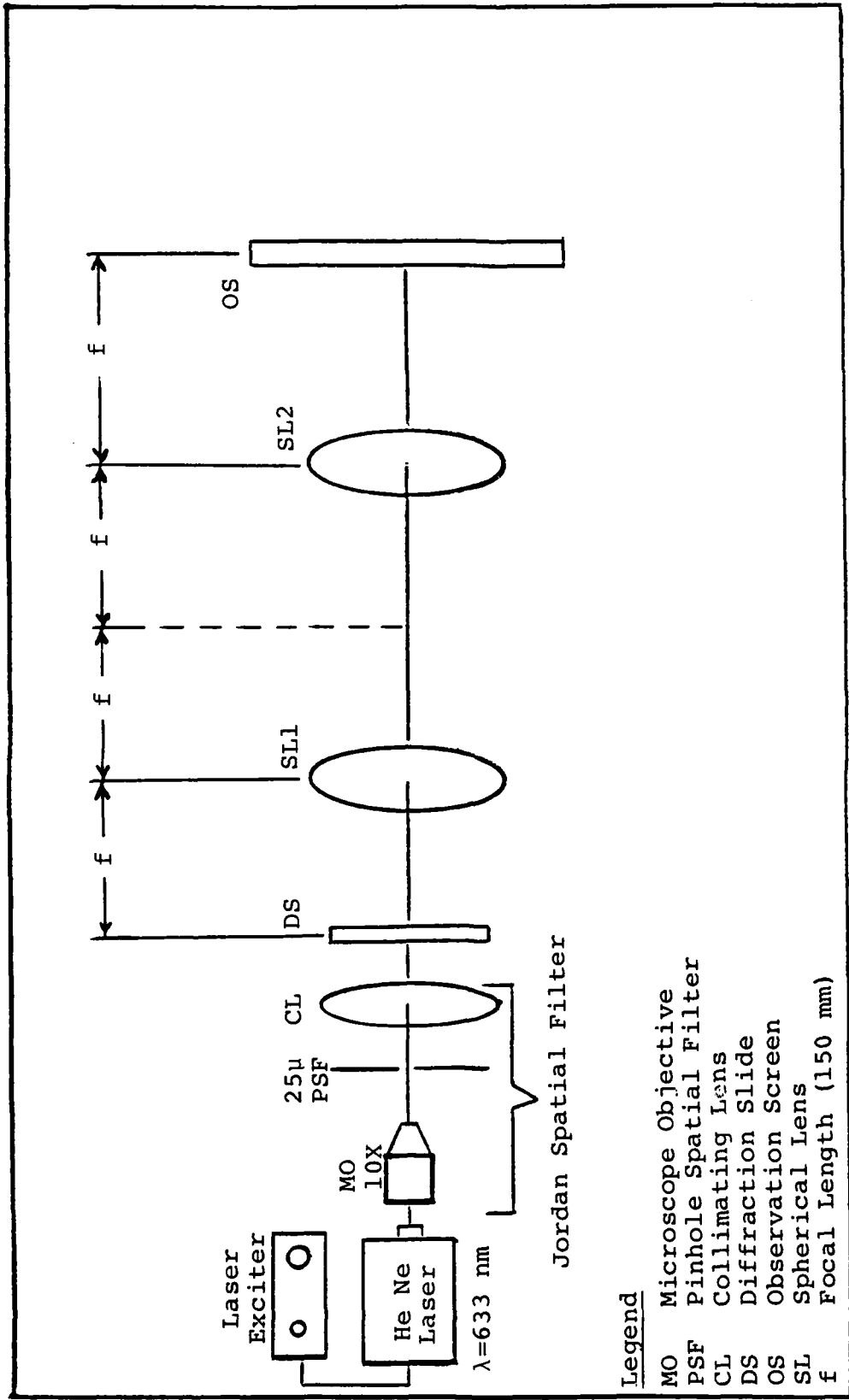
$$u_6(x,y) = AF^{-1}[T_2(f_x, f_y) \cdot P_4(-\lambda ff_x, -\lambda ff_y)] \quad (18)$$

Note: Because we have assumed all distances to be equal to the focal lengths and the two lenses have the same focal length, all magnification factors are reduced to 1. Thus, the image size should be the same as that of the object.

In this experiment, the student will be able to look at the Fourier Transform of an object and observe the inverted image spectrum. Some simple spatial filtering will be performed and the effects of a finite aperture stop will be demonstrated as a multiplicative transfer function.

Imaging and Spatial Filtering Measurement Procedures

In this experiment, the equipment setup will be that given in Figure V-4. The setup is very similar to that of Chapter IV with the addition of another lens. Thus



- Legend**
- MO Microscope Objective
 - PSF Pinhole Spatial Filter
 - CL Collimating Lens
 - DS Diffraction Screen
 - OS Observation Screen
 - SL Spherical Lens
 - f Focal Length (150 mm)

Fig. V-4. Imaging and Spatial Filtering Experimental Setup

the equipment setup procedure given in Chapter IV may be used with the addition of another lens. By now the student should be able to perform the equipment setup without too much difficulty. If difficulty persists, then use the procedural steps outlined below; otherwise, skip down to step 8.

STEPS

INSTRUCTIONS

1. Assembling the Laser Source--assemble Spectra Physics laser into laser mount and attach to support post and post holder. Fasten the post holder to the optical table. Connect the He-Ne laser to the laser exciter.
2. Jordan Spatial Filter (JSF)--fasten a post holder, approximately four inches in front of the laser post holder, to the optical table. Attach a support post to the JSF and secure it in the post holder.
3. Collimating the laser beam--turn on the laser exciter and allow a few minutes for the laser to lase. Remove the spherical collimating lens from the JSF. Adjust both the laser mount and the 25 micron pinhole filter for a good airy disk pattern out of the pinhole. (The airy disk pattern can be observed on a screen placed approximately one meter away from the JSF.) Note: This step may take

a few moments to align properly. Next, replace the spherical collimating lens back on the JSF and adjust until a good collimated beam is observed.

4. Spherical Lens I--fasten a support post to a translation stage and secure the post in a post holder placed in front (250 mm) of the JSF. The stage should move in a parallel line with the laser beam. Next, fasten a spherical lens with holder to the translation stage and adjust the height of the support post so the laser beam strikes the center portion of the lens.
5. Spherical Lens II--assemble a second support post to another translation stage and secure the post in a post holder placed a distance two focal lengths in front of spherical lens I. Attach a spherical lens with holder to the translation stage and adjust the height of the support post so the laser beam strikes the center portion of the lens. Note: Depending on the positioning of spherical lens I, the translational stage may need adjusting to acquire a distance of two focal lengths between the lenses.
6. Platform I--position a rod/platform assembly between the JSF and spherical lens I located approximately one focal length (i.e., 150 mm) from spherical lens I.

Platform II--position a second rod/platform assembly at equidistance between the two spherical lenses.

7. Place a white screen in the back focal plane (Fourier Transform plane) of the spherical lens II.
8. The equipment setup should look like that of Figure V-4. Now for this experiment the student will use different types of diffracting objects to observe the Fraunhofer Diffraction pattern (Fourier Transform) and the inverted image (second Fourier Transform) of the object. The student will also perform some spatial filtering and observe the effects of this action.
9. Find the diffraction grating slide with the hexagonal aperture and the fine wire mesh (Figure V-5). Set up the slide on a maggie U-mount with some magnetic tape and position the mount on platform I with the slide a distance one focal length from Spherical Lens I. Adjust the slide so the central portion of the laser beam illuminates the hexagonal aperture. Take a 3" x 5" card and hold it in the Fourier plane of spherical lens I (i.e., over Platform II). Observe the intensity pattern on the card. Compare the pattern to that of Figure V-6. What, if any, are the differences between the patterns and why are they different?

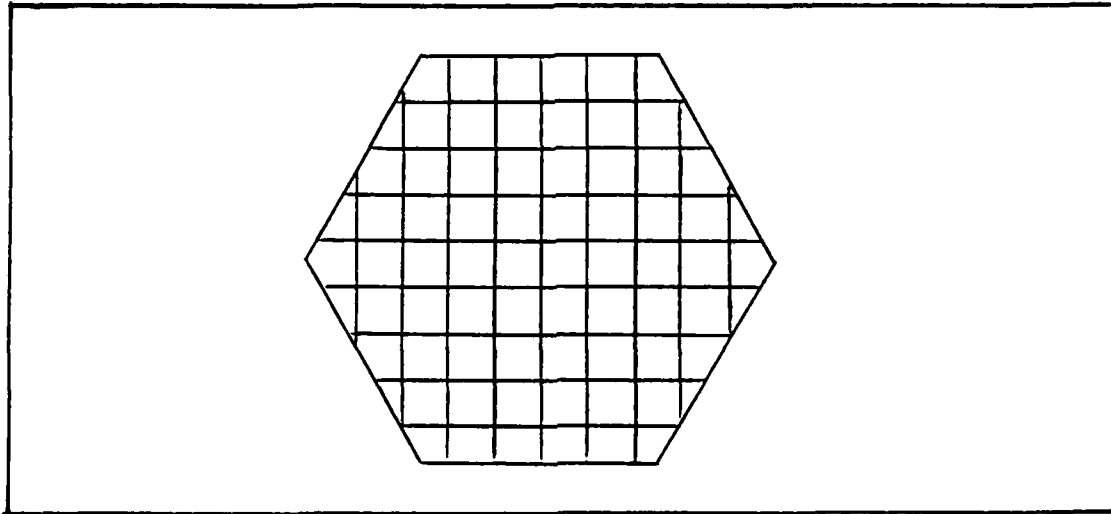


Fig. V-5. Hexagonal Aperture with Fine Wire Mesh

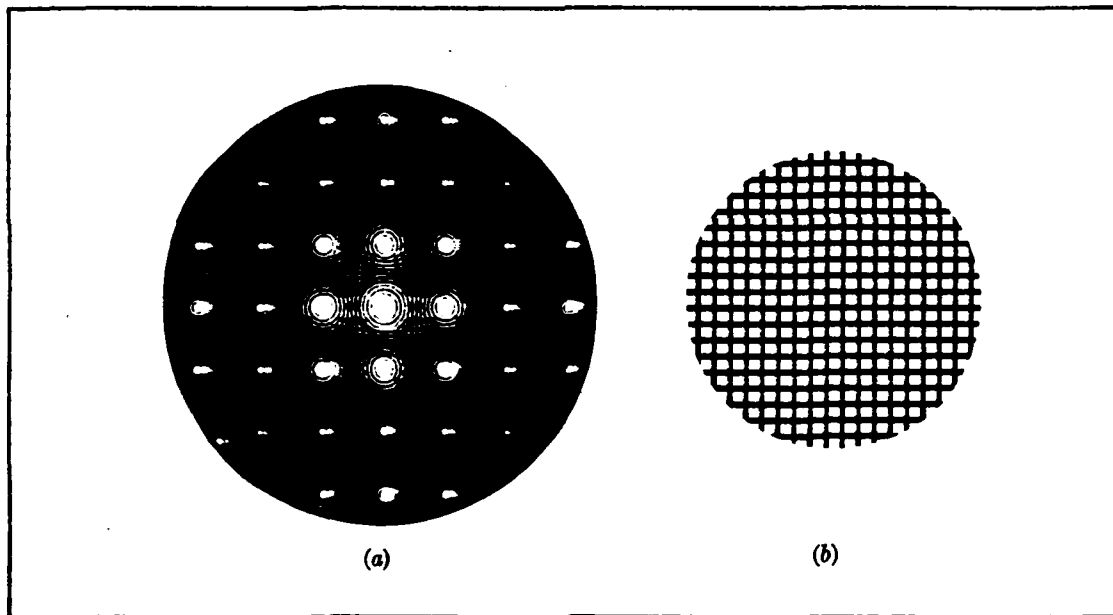


Fig. V-6. Photograph of the Unmodified Mesh and its Spectrum. (a) Spectrum; (b) Image

10. Remove the 3" x 5" card from the optical system and observe the pattern in the screen. It should be the image of the diffracting object. Notice that due to the symmetrical shape of the hexagonal aperture, the inverted image is not noticed.
11. Spatial Filtering--find the diffracting slide with the single slit apertures (i.e., the aperture slide used in Chapters III and IV). Take a maggie U-mount and secure the slide to the mount with some magnetic tape. Place the slide and mount on platform II and position it so only one line of the Fraunhofer diffraction pattern is passed through one of the slits as in Figure V-7 (i.e., use the .05 mm slit). Observe the pattern on the screen. What is the difference between the images before and after filtering? What is the reason for the blurred image during filtering? How could you sharpen the image (i.e., make it less blurry)?
12. Move the diffraction slide over so the square aperture with the fine wire mesh is illuminated. Repeat steps 9-11. Note: It should be easier to filter the components of the square aperture since the geometry is much simpler.

In order to observe the inverted nature of the two-lens system, take the architecture lettering template and illuminate one of the letters (i.e., a nonsymmetrical

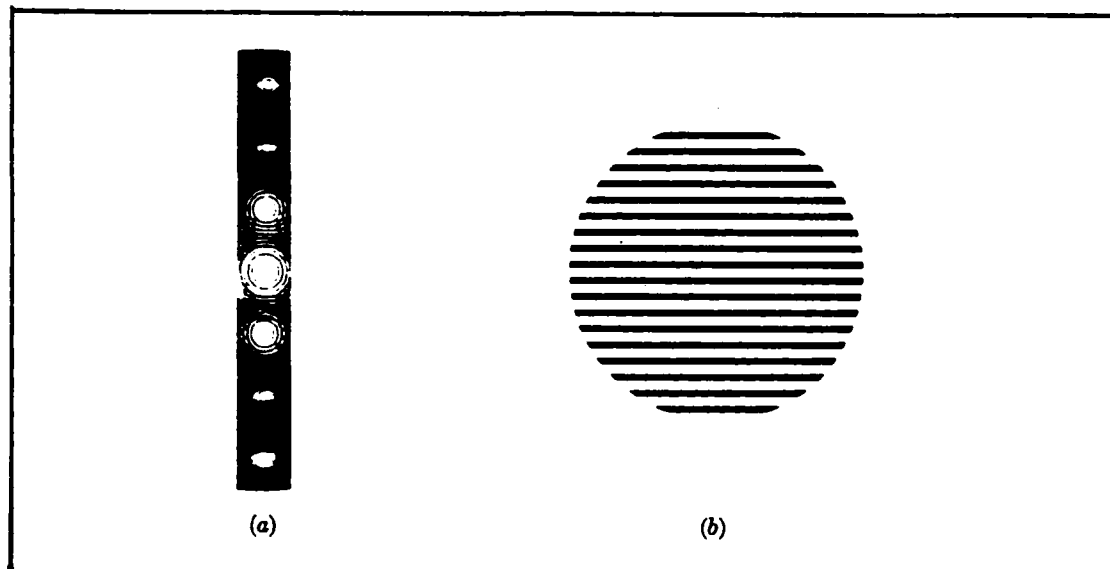


Fig. V-7. Mesh Filtered with Vertical Slit.
(a) Spectrum; (b) Image (3:144)

letter like the letter "W") and observe the image on the screen. Notice now that the image is an inverted image of the object. With this two-lens system, the student can observe various diffracting objects and look at both the Fourier Transform Spectrum and the image of the object. It is left up to the student to use any one of a number of diffracting objects and analyze both the Fourier Spectrum and the image of the object.

Special Problems

The student is reminded here that collimating the laser beam is a very important step. From Chapter III, the problems of collimating a beam were explained and the student should review these findings so as not to repeat the same errors.

Again (reference Chapter IV, Special Problems), in setting this experiment up, it is important that the screen be located exactly one focal length behind the lens. If this distance is not precise, the irradiance pattern observed on the screen may not be a true Fourier Transform Spectrum or image pattern.

During the setup phase of this experiment, the use of the three finger holder was quite awkward and difficult to adjust for aligning the diffraction aperture slits up with the central beam of the laser. Therefore, this method was not used in the setup procedures of this experiment. The procedure implemented was to use some "U-shape" brackets with magnetic stickers attached to them (see Figure III-5). A rod and platform assembly were attached to the table approximately one focal length in front of the lens (reference Step 6). The platform was adjusted so the laser would shine between the U-shape brackets. The diffraction slide has metal strips already attached so the magnetic stickers on the brackets held the slide in place. This made setting up the diffraction slit apertures much easier.

A meter stick was laid down on the table and used as a marker to indicate where the proper distances were for the object plane (Platform I), Spherical Lens I, the Fourier Transform plane (Platform II), Spherical Lens II and the Image plane (observation screen).

While performing this experiment, a very crucial problem was the physical size of the diffracting object, the Fourier Spectrum pattern, and the image pattern. A student performing the mathematical analysis of the patterns may have no idea of just how small the objects he/she is working with. Consequently, although the analysis indicates where the particular patterns are spatially, the patterns were so small it was difficult to observe all the resolution of the patterns. Therefore, in order to observe the diffracting patterns, the screen was moved back a distance of five meters to allow the magnification of the system to operate on the patterns. At this screen distance, the pattern observed on the screen was not the image of the object but the Fourier Spectrum of the diffracting object. Why? In order to observe the image of the object, a third lens was used and placed a distance of two focal lengths from the second spherical lens (Figure V-8). Thus, by inserting a third lens into the system, a magnified image of the object could be observed quite readily.

Results

In setting up this experiment, the critical factor is the proper distances between the optical components. The student should ensure all distances are as accurate as possible so as to eliminate any misfocusing problems or multiplicative transmittance function anomalies. This

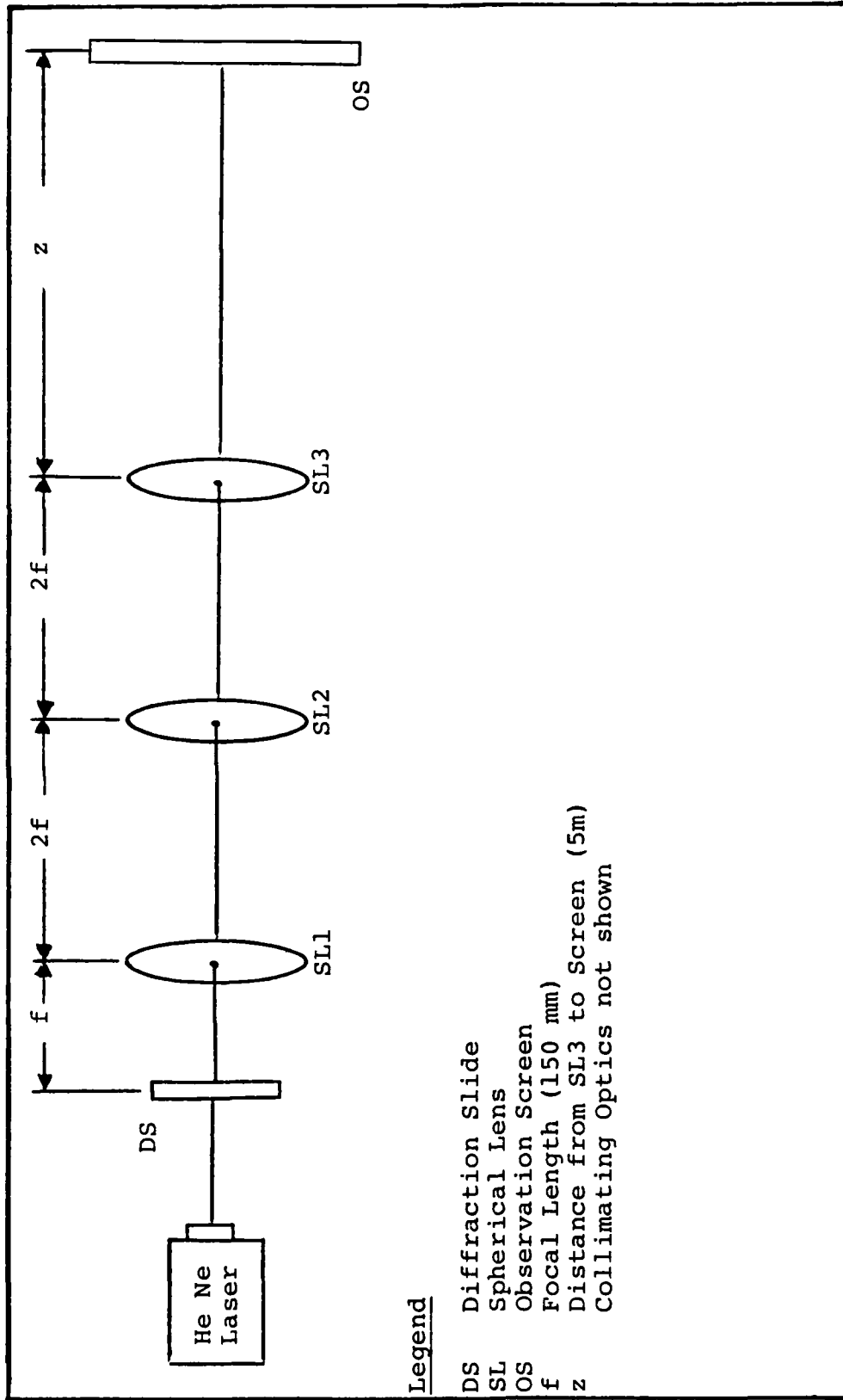


Fig. V-8. Three-Lens Imaging System

experiment proved to be quite informative in that it demonstrated the effects of convolving an aperture transmittance function and showed the effects of this action. It also demonstrated the inverted image pattern of performing the Fourier Transform twice on a two-dimensional diffracting object. Answers to various questions posed above are as follows:

Reference Step 9. The differences between the pattern observed on the 3" x 5" card and Figure V-6 were that the pattern observed on the card did not exhibit a symmetrical nature like that of Figure V-6. The reason for this is the diffracting object itself. The hexagonal perimeter of the diffracting object on the slide was not a perfect circle. This caused the pattern on the 3" x 5" card to exhibit a slight difference from that of Figure V-6. The pattern of Figure V-6 came from (3:143).

Reference Step 11. The difference between the images before and after filtering was that before filtering, the image portrayed the fine wire mesh in both the vertical and horizontal direction. After filtering, the image only portrayed the fine wire mesh in one direction (3:143-144). The reason the image is blurred is due to the low-pass filtering of the aperture transmittance function (2:481). In order to sharpen the image, the aperture transmittance function must be widened to allow the higher spatial frequency components to pass through (2:481).

Reference Special Problems. As the screen distance was moved back to five meters, the pattern observed on the screen became the Fourier Transform Spectrum of the diffracting object rather than an enlarged image. This is due to the Optical System that is being used. A two-lens system for which the distance between the two lenses is the exact sum of their focal lengths is referred to as an "afocal system." This type of system has no finite focal points. This simply means that light rays entering the system which are parallel to the optic axis also exit parallel to the axis. Therefore, this type of system has the interesting characteristic where light entering the system as a collimated (parallel) beam also leaves the system as a collimated beam. Thus by moving the distance of the screen back five meters, the diffracting pattern on the screen is the Fraunhofer Diffraction pattern, of the diffracting object, in the far field. Placing the third lens a distance of two focal lengths away from spherical lens II, the system is now an imaging system with the orientation of the image rightside up and magnified by the appropriate scale factor.

Bibliography

1. Class Lectures or Lecture Materials. Syed, Vagar lecture notes distributed in EE 527 "Introduction to Fourier Optics," School of Engineering, Air Force Institute of Technology (AU), Wright-Patterson AFB OH, October 1983.
2. Gaskill, J. D. Linear Systems, Fourier Transforms and Optics. New York: John Wiley and Sons, 1978.
3. Goodman, Joseph W. Introduction to Fourier Optics. New York: McGraw Hill Book Co., 1968.

VI. Measuring the Bragg Angle with
Acousto-Optic Cell

Assignment

The student will measure the Bragg Angle using an Acousto-Optic Cell.

Objective of the Experiment

1. To acquaint the student with Acousto-Optic Cells.
2. To relate classroom theory of Bragg Diffraction with practical application.
3. To give the student some experience with Bragg Angle alignment and Acousto-Optic cells.

Equipment Needed

Laser Source: Spectra Physics Helium-Neon Class IIIb
4 mw (Model 102-1) and Spectra Physics
Laser Exciter (Model 212-1)

Newport Laser Mount (Model 810), 1 each

Newport Support Post (Model VPH-4), 1 each

Newport Post Holder (Model SP-4), 1 each

Jordan Spatial
Filter:

- a. Microscope Objective 10X
- b. 25 micron Pinhole Spatial Filter

c. Spherical Collimating lens

Newport Support Post (Model VPH-4), 1 each

Newport Post Holder (Model SP-4), 1 each

Iris

Diaphragm:

Newport Model ID-15

Newport Support Post (Model VPH-4), 1 each

Newport Post Holder (Model SP-4), 1 each

Focusing
Lens:

a. Spherical Convex Lens with Holder

(150 mm) or equivalent

b. Translational Stage Newport Model 430

Newport Support Post (Model VPH-4), 1 each

Newport Post Holder (Model SP-4), 1 each

Bragg Cell
and Mount:

a. Newport EOS Acousto-Optic

Modulator Model N230

b. Newport Translational Stage

Model 430, 3 each

c. Newport 90 degree Angle Mount

RF Driver: Newport Modulator Driver Model N210 DS

White Cardboard Screen, 2 ft. x 2 ft.

Theory/Background

Acousto-Optic deals with the interaction of sound and light. Diffraction of light by high frequency sound waves, often called Brillouin scattering after the man who first predicted it, was first observed in 1932 (1). A

great deal of experimental and theoretical work was done in the following years. With the development of the laser in the 1960s, and the many advances made with high frequency techniques, a wide range of light and sound interaction experiments was developed. Coherent light permits the observation of acoustic waves in a solid up to frequencies in the microwave region.

In the following discussion, we will look at the interaction of sound and light in the Raman-Nath region sometimes called the Debye-Sears effect (3:594). The primary instrument we will be concerned with is called an Acousto-Optic modulator or Bragg Cell. This discussion will be qualitative and will lean mostly on electrical engineering concepts. Much of the terminology used will be that of Communications engineering in that we will be up shifting and down shifting frequencies. It is recommended that you refer to a good introduction text on PM or FM modulation techniques for quick reference (6). Later we will go into sound and light interaction in the Bragg regime and discuss how to maximize the diffraction pattern coming out of the Bragg Cell (4).

Let's assume we have a plane wave of light with angular frequency " ω " and vacuum wavelength " λ_0 " traveling from left to right in a slab of length "d" (Figure VI-1) with index of "n" (1). The velocity of light in the slab

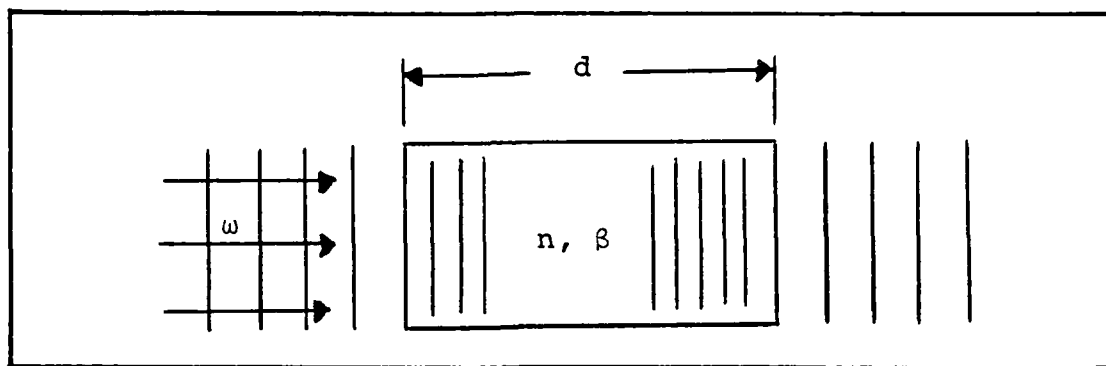


Fig. VI-1. Optical Delay Line
Refractive Index Produce Phase Modulation

reduces from its vacuum speed c to c/n . The wavelength of light in the slab becomes

$$\lambda = 2\pi c/n\omega \quad (1)$$

and the propagation constant β (the number of waves per 2 unit length) is

$$\beta = \omega n/c \quad (2)$$

The slab can be considered an optical delay line with time delay $\tau = dn/c$ and phase shift $\phi = d\beta$ radians.

If we can vary the index of refraction by some small amount, say some Δn , then in doing so, we can vary the time delay and also vary the phase excursion. Thus the resulting phase excursion at the output of the slab is

$$\begin{aligned} \Delta\phi &= d\Delta\beta \\ &= d\beta\Delta n/n \\ &= d2\pi\Delta n/\lambda \end{aligned} \quad (3)$$

If we allow Δn to vary sinusoidally at the modulation frequency ω_m , the output light, emerging from the right end of the slab, will now be phase modulated (1; 7). According to reference (6:237), a phase modulated signal is composed of a carrier and sidebands with amplitudes that are a function of the maximum phase deviation, known as the modulation index. Figure VI-2 shows the carrier and its sidebands and Figure VI-3 is a graph of the amplitudes of the carrier and its sidebands versus phase deviation. Up to $\Delta\phi = 0.5$ radians, only the first pair of sidebands has significant amplitude. As you increase phase deviation, more and more sidebands grow (6:237) until you reach a phase deviation where $\Delta\phi = 2.4$ radians and the carrier will drop out (Figure VI-3). With this phase deviation, the light emerging out of the right side of the slab will have amplitudes in the sideband frequencies $\omega \pm \omega_m$, $\omega \pm 2\omega_m$, etc., in accordance with the graph of Figure VI-3.

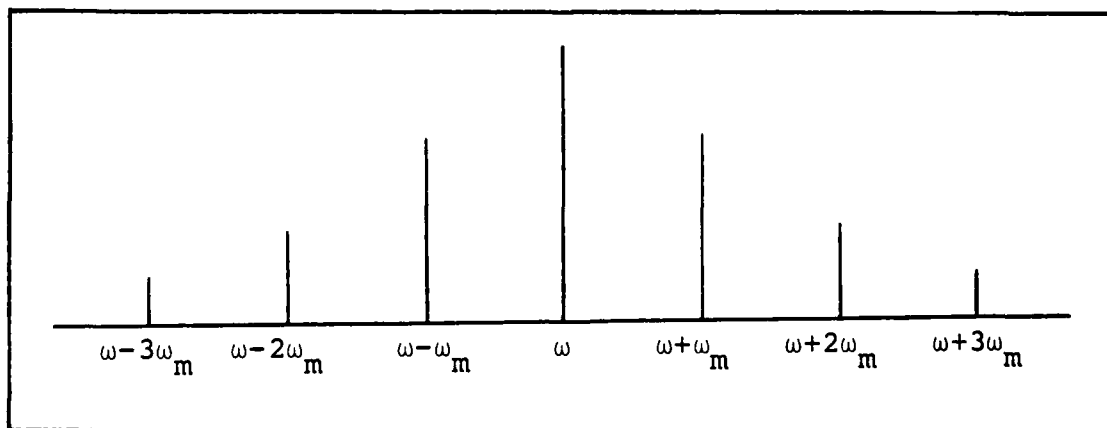


Fig. VI-2. Carrier (ω) and Sideband Spectrum of a Phase Modulated Wave

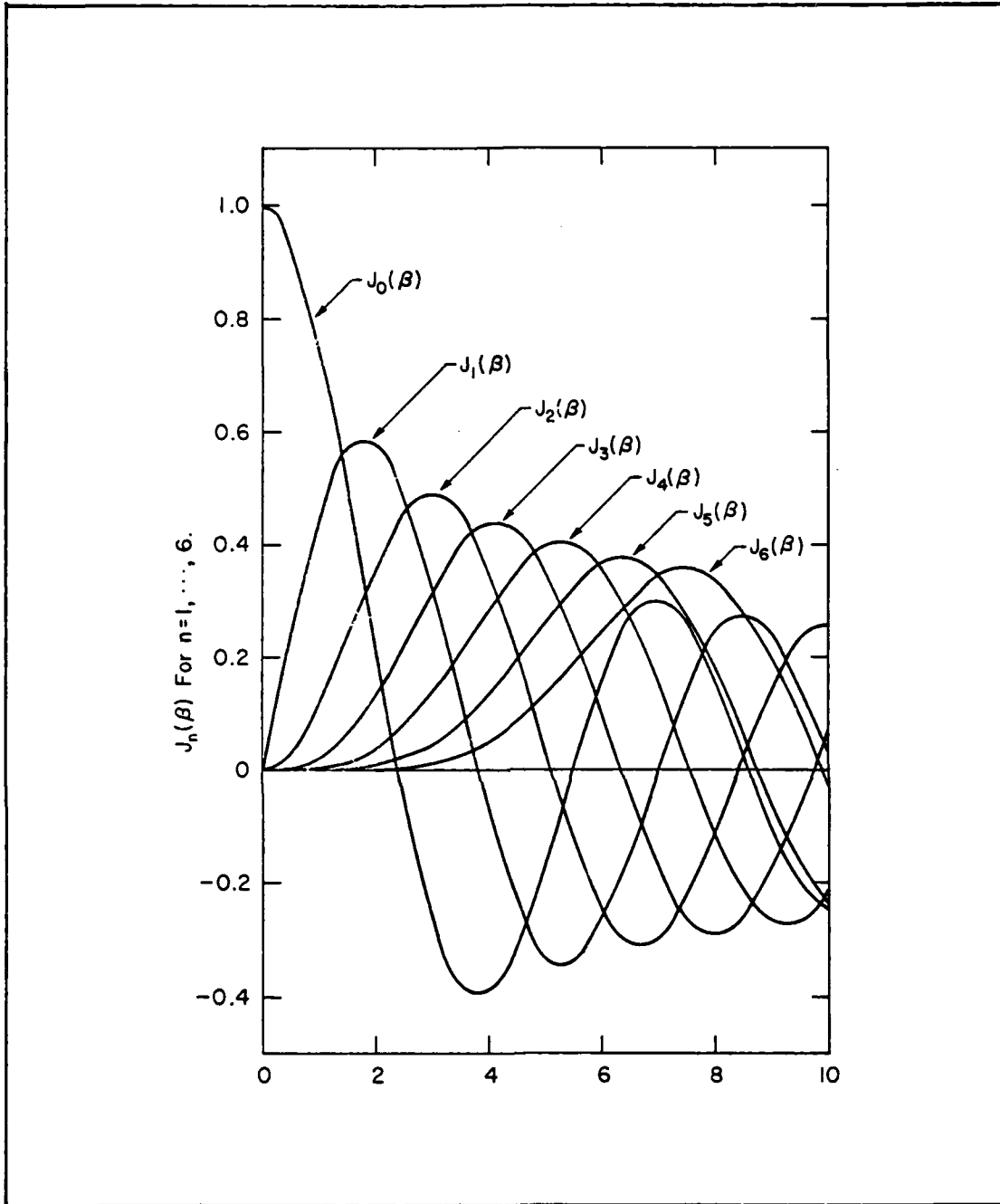


Fig. VI-3. Amplitude of Sideband Light
 versus Phase Excursion
 Note: This is the Bessel Function (6:227)

In order to illustrate the principles of a Bragg cell, we will look at a bunch of slabs (like those in Figure VI-1) and stack them on top one another (Figure VI-4). Now suppose we send a compressional wave with frequency ω_m traveling upward. As the sound wave propagates up the column, each slab will encompass some incremental portion (i.e., phase) of the acoustic wave. This incremental phase change, from the acoustic wave, will cause compressions and dilations (refractions) in the index of refraction along the entire length of the column [e.g., Figure VI-4 illustrated six sections of an acoustic transmission line (i.e., one slab is one section of the acoustic line) each having a quarter of an acoustic wavelength phase variation]. If slab four is dilated (i.e., the index of refraction for that slab is $n - \Delta n$) then one-half cycle later it will be compressed (i.e., index of refraction is $n + \Delta n$, like slab six). Thus we see that the index of refraction along the entire length of the column is constantly varying where the variation from slab to slab is linear.

Let a plane wave of light of angular frequency " ω " impinge on the column and travel from left to right at normal incidence (Figure VI-4). Each slab will phase modulate the optical wave as discussed earlier and produce at the output (i.e., right side of the column) a carrier and some sideband frequencies. Since the carrier wave has

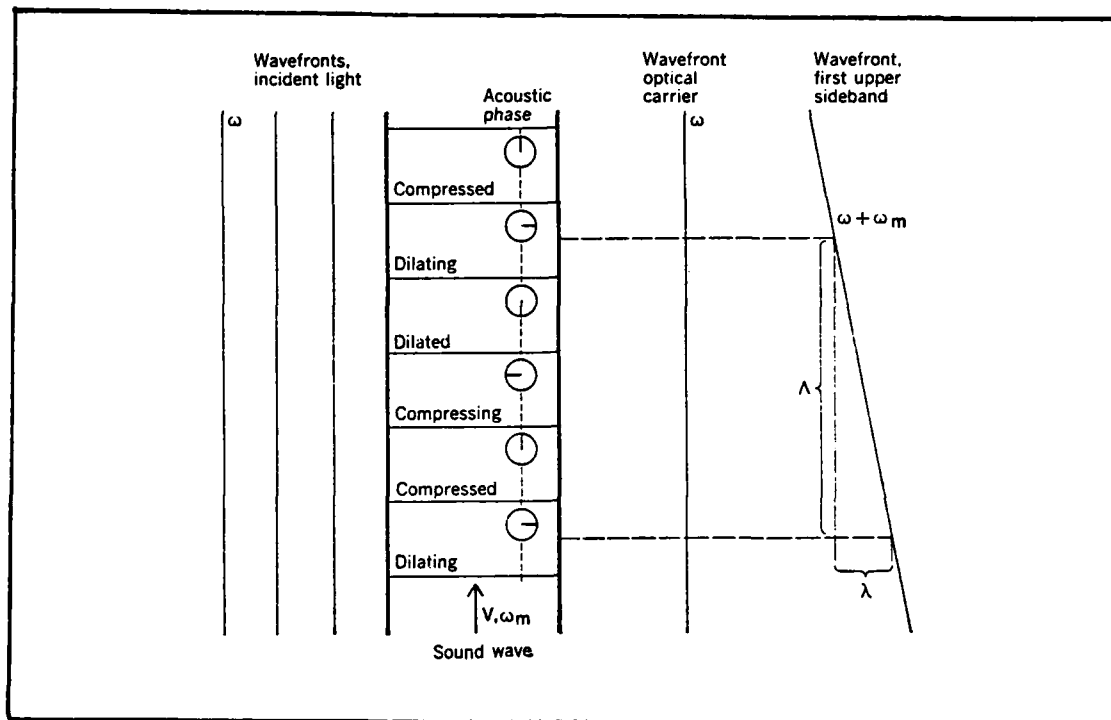


Fig. VI-4. Sound Wave Propagating Upward will Generate Optical Phase Shifts which Cause Wavefront of First Order Sideband to Tilt. Carrier Wavefront (ω) Does Not Change (1:44)

the same phase for all slabs hence, light at the incident frequency will propagate in the original direction (i.e., in the horizontal direction if the column is vertical). The sideband frequencies, however, do not propagate in the direction of the carrier. To determine the direction of propagation of the sideband light, we construct a wavefront by connecting points of equal phase together (7). By doing so we find that the direction of propagation-- which in isotropic substances must be perpendicular to the wavefront--is deflected up for upper sidebands at an angle

$$\alpha = N\lambda/\Lambda \quad (4)$$

and down for lower sidebands at the same angle where Λ is the acoustic wavelength and N is an integer (N is the higher order sideband number; i.e., $N = 3$ indicates the third order sideband). In Acousto-Optics these sidebands are the diffraction orders (5).

Due to the diffraction characteristics of the light wave, special cases of diffraction can be characterized (2) by the parameter

$$Q = k^2 d / \beta \quad (5)$$

where K is the propagation constant ω_m/V of the sound and $\beta =$ propagation constant $n\omega/c$ of the light within the acoustic medium and V is the acoustic velocity. If Q is much less than one, then the experiments for which this condition holds are said to be within the Raman-Nath regime (Figure VI-5). If Q is greater than one, then the experiments for this condition are said to be in the Bragg regime. For a given incoming light of angular frequency " ω ," the two parameters which govern the diffraction pattern at the output are: (1) the interaction length " d " (Figure VI-1) and (2) the acoustic frequency (1).

Given the Bragg Cell in Figure VI-6, suppose a monochromatic plane wave of light illuminates it at normal incidence. The diffraction pattern at the output will have the zeroth and two first order diffraction components. To achieve maximum diffraction efficiency, the Bragg cell

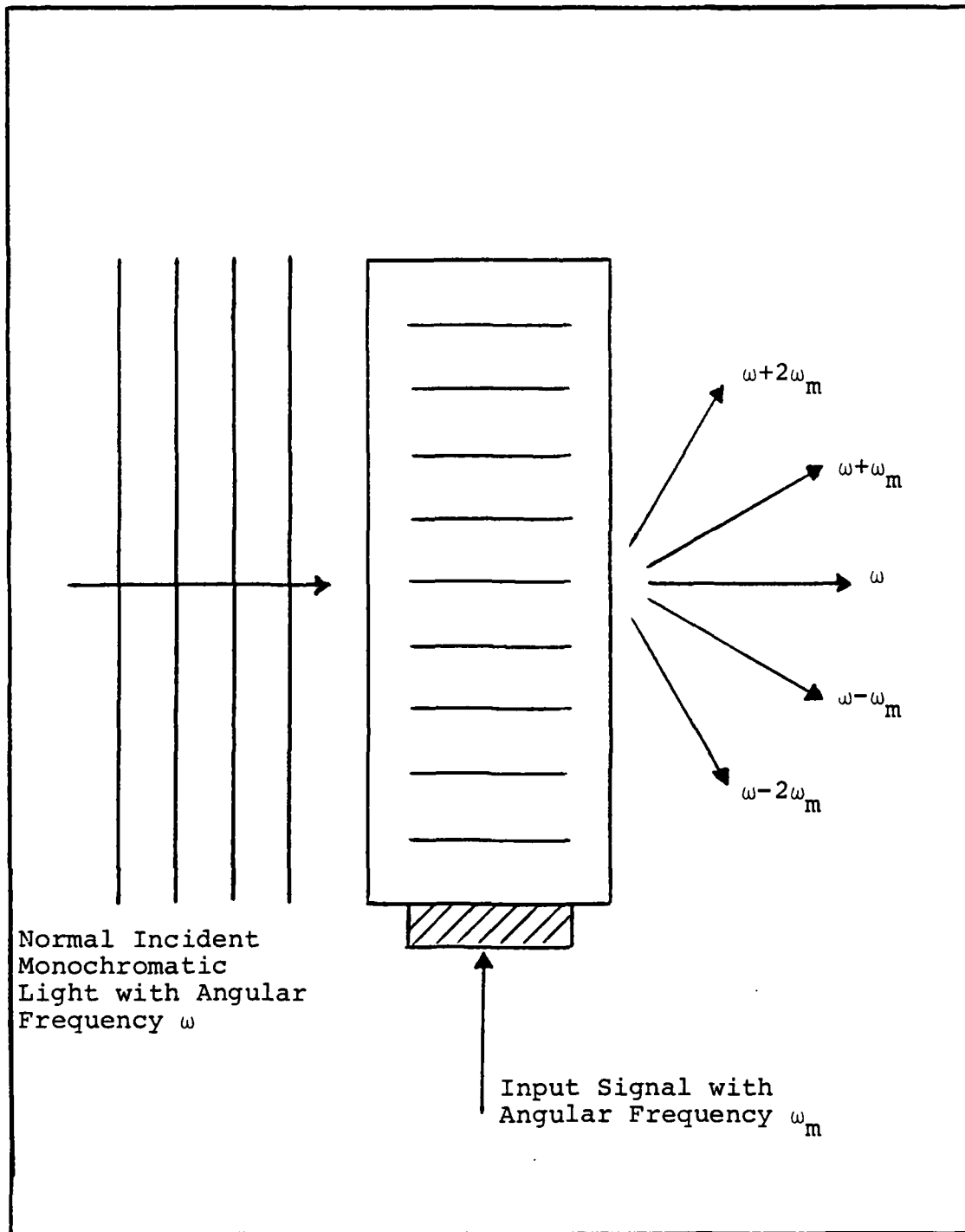


Fig. VI-5. Acousto-Optic Interaction in the Raman-Nath Regime

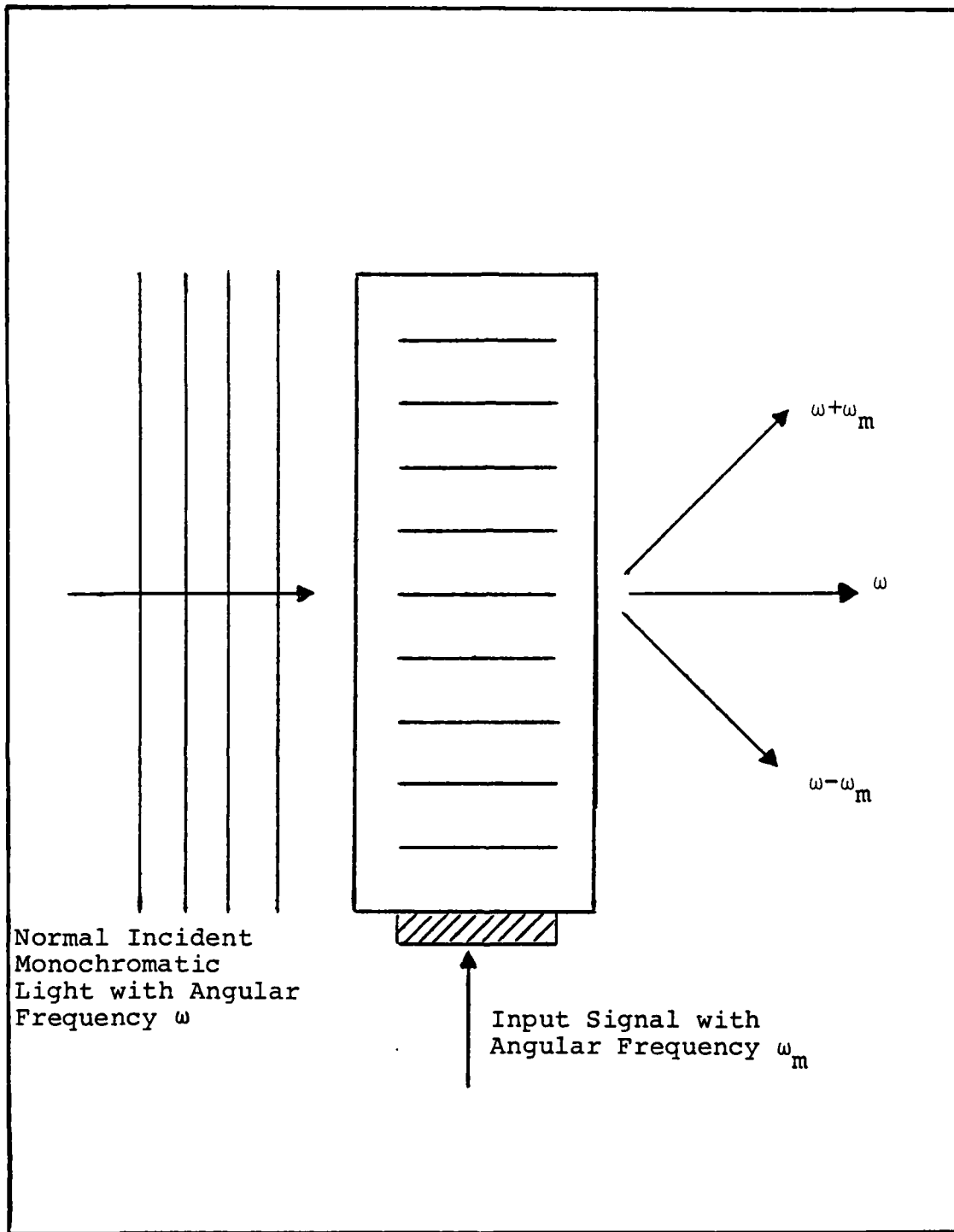


Fig. VI-6. Acousto-Optic Interaction in the Bragg Regime

must be tilted at an angle with respect to the incoming light (4). This angle θ_B is known as the Bragg Angle and is given by:

$$\theta_B = \sin^{-1} \lambda/2\Lambda \quad (6)$$

Figure VI-7 illustrates the effect of tilting the incoming light to the Bragg angle. Notice that only one of the first order diffraction components, along with the zeroth order component, will emerge from the output of the Bragg Cell. For this experiment, the student will measure the Bragg Angle and look at the diffraction efficiency of the cell as light impinges on it at normal incidence.

Experimental Procedures

Introduction. Acousto-Optic devices can be used to alter the amplitude, position, or frequency of a laser beam. As discussed earlier, an RF signal is applied to a piezoelectric transducer to set up a pressure wave that propagates through an acoustic wave supporting material (in the Newport AOM, a Tellurium Dioxide crystal is the acoustic wave medium). This pressure wave causes a periodic change in density of the crystal material and therefore its index of refraction varies. In this experiment the student will align a laser beam at a specific angle (θ_B) known as the Bragg Angle to obtain an efficient diffraction of the laser intensity in the first order output beam.

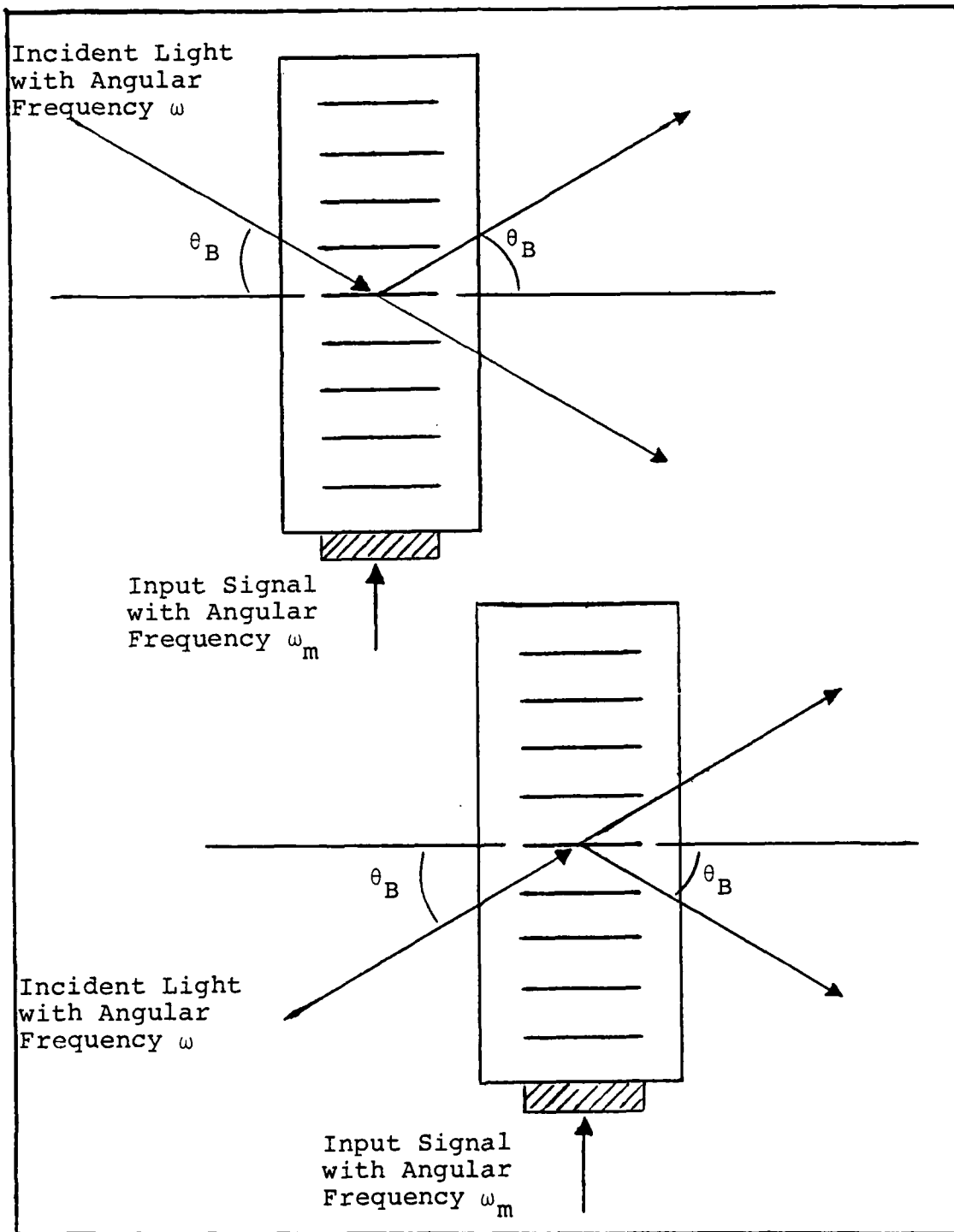


Fig. VI-7. Bragg Reflection--Upper and Lower Diffraction Order is Selected by Making Light Incident at the Appropriate Bragg Angle

In this experiment we will see the deflected beam being shifted in frequency by the value of the RF frequency due to constructing wavefronts of equal phases (7) and determine the direction of propagation (Doppler effect) (5).

Some characteristics of an AOM (Bragg Cell) are:

- a. Diffraction Efficiency
- b. RF Drive Power
- c. Rise Time

Diffraction efficiency (η) is the ratio of the diffracted beam intensity to the intensity of the incident optical beam. It is related to the RF drive power (PRF) by the expression

$$(\eta) = \sin^2 \left[\frac{\pi}{2} \sqrt{\frac{2}{\lambda_0} \frac{M \cdot d}{h} (\text{PRF})} \right] \quad (7)$$

where

λ_0 = free space optical wavelength;

h = beam height (beam diameter);

d = optical path length in the Acoustic Material; and

M = figure of merit related to acoustic material.

Another form of the diffraction efficiency is given by:

$$(\eta) = \sin^2 \left(\frac{\xi}{2} \right) \quad (8)$$

where

$$\zeta = \frac{2\pi}{\lambda} \frac{\Delta n \cdot d}{\cos \theta_B} ;$$

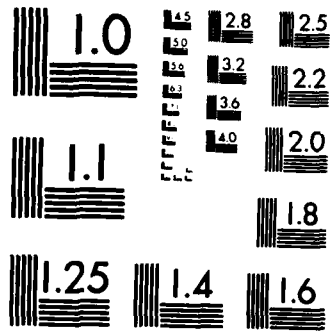
Δn = change in refractive index; and

(θ_B) = Bragg angle.

The Newport acousto-optic modulator (N230) used in this experiment uses a tellurium dioxide crystal, with a lithium niobate transducer because of its large refractive index ($n = 2.2$), its low optical absorption and its resistance to optical damage. The RF modulator driver (N210-DS) is a digital driver. It takes a TTL input for the modulating signal and drives the Bragg Cell (AOM) at an RF frequency of 80 MHz.

An important characteristic of the digital modulation system is the rise time of the output laser pulses. This is determined by the transit time of the acoustic wave across the optical beam path. The rise time can be thought of as the time it takes the leading edge of the moving grating to completely cross the laser beam. So for a fast rise time, a lens will be used to focus the laser to a smaller waist size in the Bragg Cell.

There are practical limits to the amount one can improve the rise time by focusing the laser beam. Focusing the laser beam too tight may cause optical damage to the crystal, depending on the input power of the laser. Be



MICROCOPY RESOLUTION TEST CHART
NATIONAL BUREAU OF STANDARDS-1963-A

sure to check the energy constraints (i.e., the maximum laser power the AOM can withstand) of the Bragg Cell before focusing the laser beam into the Bragg Cell.

Precheck Procedures. Before starting, check the RF output power level of the Newport (N210-DS) EOS Modulator Driver. Use either an appropriate power measuring device (i.e., Hewlett Package 432B) or a Spectrum Analyzer (i.e., Hewlett Packard 141T). The Bragg Cell (AOM N230) will operate at an 85 percent Diffraction efficiency at 750 milliwatts of input RF power.

```
*****
*                                     *
*                               CAUTION *
*                                     *
* Too much RF power will cause severe damage *
* to the lithium niobate transducer. Ensure *
* that the output power of the RF driver does *
* not exceed 1 watt of continuous output power.*
*****
```

Bragg Angle Measurement Procedures

The experimental setup used is shown in Figure VI-8. The picture of the optical system (Figure VI-9) should help to illustrate the equipment setup.

STEPS

INSTRUCTIONS

1. Assembling the Laser Source--assemble Spectra Physics laser into laser mount and attach to

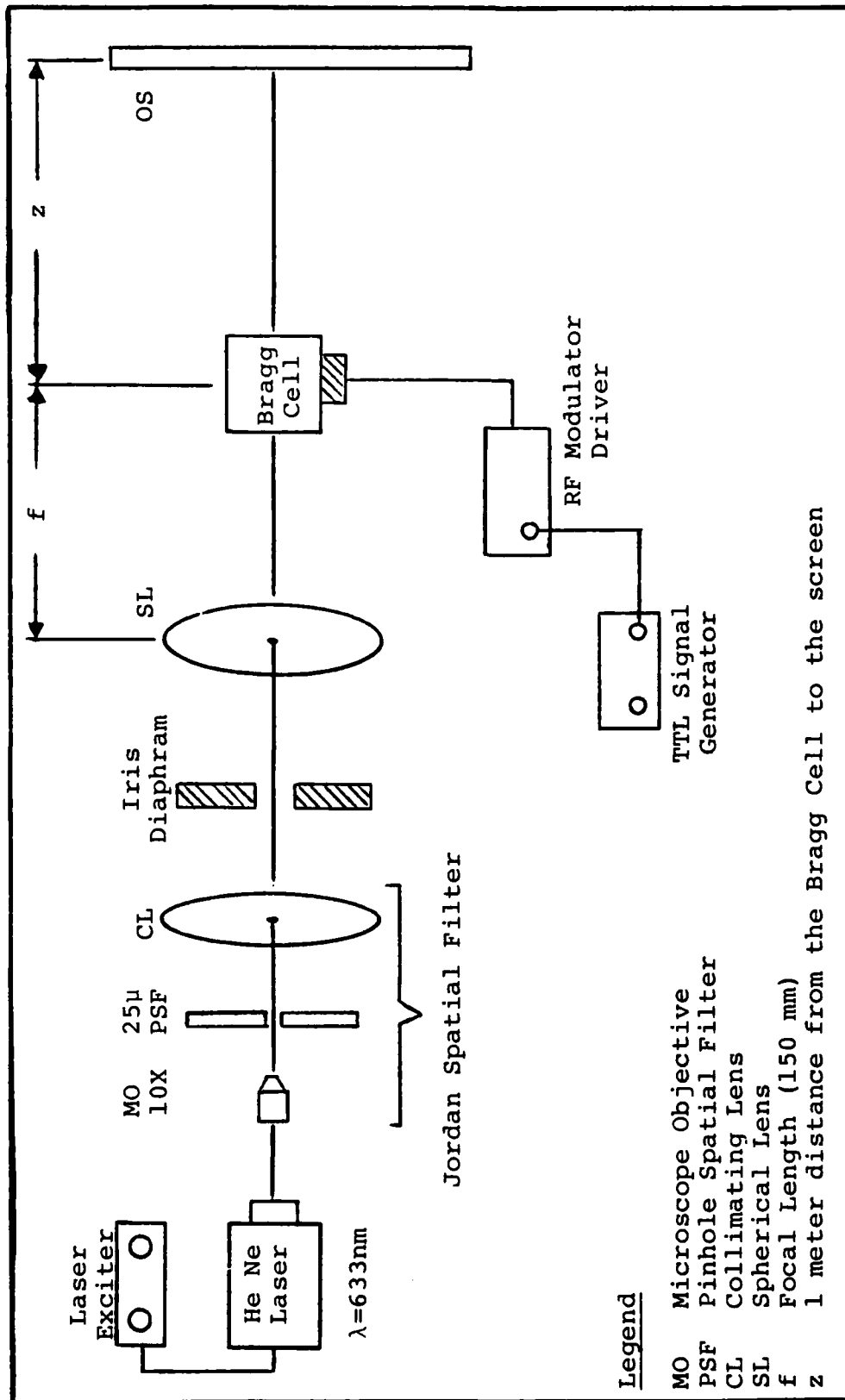


Fig. VI-8. Bragg Angle Experimental Setup

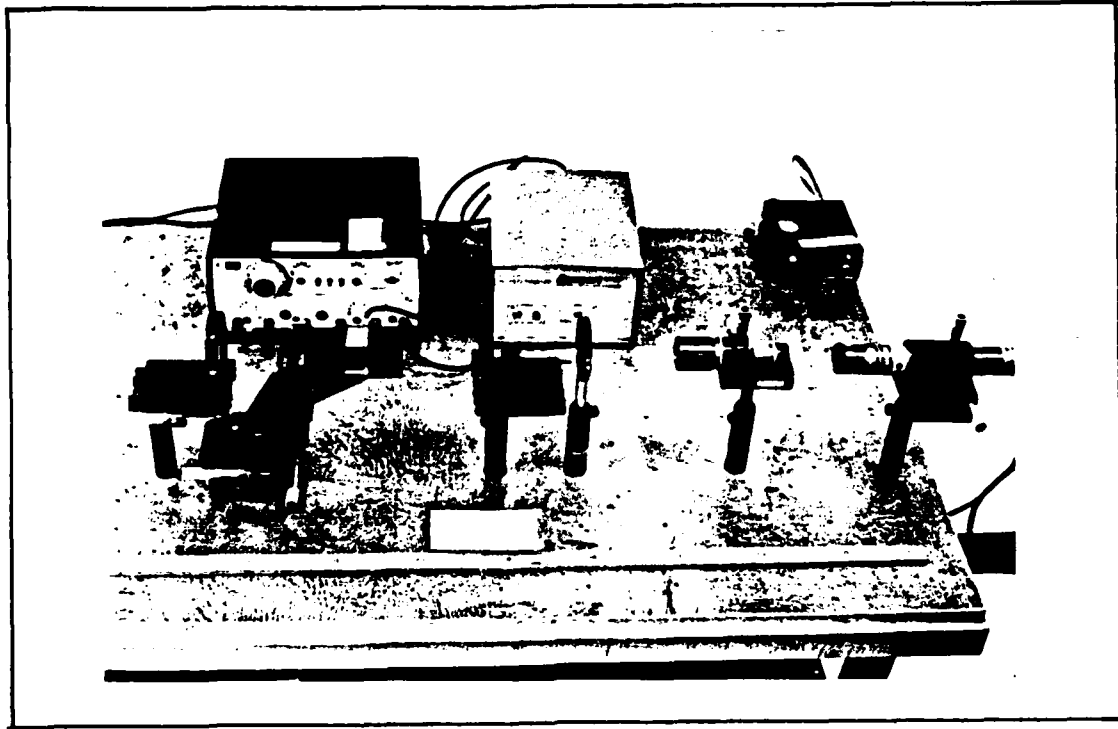


Fig. VI-9. Photograph of
Bragg Angle Experiment

- support post and post holder. Fasten the post holder to the optical table. Connect the He-Ne laser to the laser exciter.
2. Jordan Spatial Filter (JSF)--fasten a post holder, approximately four inches in front of the last post holder, to the optical table. Attach a support post to the JSF and secure it in the post holder.
 3. Collimating the laser beam--turn on the laser exciter and allow a few minutes for the laser to lase. Remove the spherical collimating lens from the JSF. Adjust both the laser mount and the 25

micron pinhole filter for a good airy disk pattern out of the pinhole. (The airy disk pattern can be observed on a screen placed approximately one meter away from the JSF.) Note: This step may take a few moments to align properly. Next, replace the spherical collimating lens back on the JSF and adjust until a good collimated beam is observed.

4. Connect an Iris diaphragm to a support post and secure it in a post holder. Fasten the post holder approximately two inches in front of the JSF. Next, close the diaphragm down until the laser beam diameter is approximately three to four mm in diameter. Note: This should allow only the central portion of the airy disk through and block all the other rings.
5. Focusing Lens--fasten a support post to a translation stage and secure the post in a post holder placed in front (one to two inches) of the iris diaphragm. The stage should move in a parallel line with the laser beam. Next, fasten a spherical lens with holder to the translation stage and adjust the height of the support post so the laser beam strikes the center portion of the lens.
6. Bragg Cell and Mount--build an X-Y-Z translational stage using three translational stages and two 90-degree angle mounts. See Figure VI-9. Fasten the

component is visible on the screen. To ensure that the diffraction pattern observed is the zeroth and first diffracted orders, switch the MODE switch to "Normal" and observe that the first diffracted order will disappear.

11. Switch the MODE switch back to "Continuous" and ensure that only one of the first order diffraction components is strongly illuminated (i.e., adjust for the Bragg angle).
12. Measure the distance from the Bragg Cell to the screen and record it. Next, measure the distance from center to center of the zeroth and first order diffraction components. The Bragg angle can be computed by the formula:

$$(\theta_B) = \sin^{-1}[\text{CCD}/2*Z] \quad (9)$$

where

CCD = the center-center distance between the zeroth and first order component, and
Z = distance from the Bragg Cell to the screen.

Special Problems

The alignment of the laser beam and the Bragg Cell is a very crucial step. With a laser beam waist size of .51 mm, any small movement will cause a misalignment and

the diffraction pattern will be lost. A common problem encountered is the angle the laser beam makes with the Bragg Cell. The laser should impinge on the Bragg Cell aperture at normal incidence. The student may have to adjust the alignment on the laser to ensure the proper incident angle.

Another common problem is the position of the laser beam on the crystal in the Bragg Cell. The TeO_2 crystal does not fill the entire aperture. The effective aperture of the crystal in the Bragg Cell is 1.5 mm in height. The Bragg window is 2.5 mm in diameter. When directing a 0.5 mm beam into the crystal, ensure that the beam pattern on the observation screen, with the MODE switch on the Modulator driver in the "Normal" position, is a circle. Ensure that the laser beam is actually passing through the crystal.

As a protection to the equipment, ensure that the RF power out to the Bragg Cell is below one watt. Remember, too much RF power could cause severe damage to the crystal.

Results and Sample Questions

During the course of this experiment, there were many practical mistakes discovered which any new student could encounter while performing this exercise. Listed are a few of the problems which were encountered during previous implementation of this experiment.

The first attempt at measuring the Bragg angle entailed the equipment setup in Figure VI-8. After successfully collimating the laser beam, the iris diaphragm and spherical lens were set up to reduce the beam diameter to .5 mm. The RF driver to the Bragg Cell was turned off and the optical pattern was observed on the screen. The pattern on the screen was predicted to be a circular pattern; however, no such pattern existed. Thus an attempt was made to adjust the X-Y-Z translational stage until a circular pattern appeared on the screen. The problem with the first pattern detected, was that it did not propagate through the TeO_2 crystal. To ensure the laser propagated through the crystal, the casing on the Bragg Cell was removed so the crystal was exposed. The X-Y-Z translational stage was then adjusted so the laser would properly propagate through the crystal.

Once this step was established, the RF driver was turned on and the MODE switch was switched to "Continuous," the pattern observed on the screen did not have a first order component. The angle the Bragg Cell made with the laser light was adjusted until the first order diffracted component was visible on the screen. To ensure that the observation pattern was the first order diffracted component, the MODE switch was flipped to "Normal" and the first order component disappeared.

A TTL wave generator was used to modulate the RF carrier out of the Modulator Driver. The modulating signal was a slow 10 Hz signal and on the observation screen the first diffracted order was blinking at a rate of the modulating signal (10 Hz). The modulating signal was increased to 1 KHz and the first diffracted order component was observed to blink at the 1 KHz rate. The measurements that were collected are:

Bragg Cell--Screen distance = 1000 mm

Center-Center distance of
zero and first orders = 12.7 mm

Bragg Angle measured = 6.35 milliradians

The specified Bragg Angle for this particular Acousto-Optic Cell is 5.9 milliradians. The error is due to inaccurate measuring equipment and subjective interpretation. Another problem encountered was the illumination of the optical pattern on the screen. The existing setup (Figure VI-8) filtered much of the laser energy before it propagated to the screen. Most of the energy was being blocked by the JSF. Therefore, in order to have a brighter illumination, the JSF was removed and the experiment conducted as written. The effects of this change in the equipment setup resulted in a brighter illumination and ease of viewing.

Sample Questions.

1. Does the amplitude of the acoustic wave in the Bragg Cell have any effect on the diffraction efficiency?

Ans: As seen from Eq (7) the diffraction efficiency is affected by the power of the RF signal. Thus by increasing or decreasing the amplitude of the RF signal in the Bragg Cell, the amount of light diffracted will increase/decrease accordingly. However, there is a practical limitation to the amount one can increase the amplitude of the RF signal in the Bragg Cell (see Precheck Procedures).

2. We know from previous discussions that the deflection angle of the first diffracted order has a definite relationship to the Acoustic wavelength in the Bragg Cell. Given the acoustic velocity (4.26×10^3 m/s), and light wavelength (633 nm), calculate the Bragg angle (θ_B) for an input RF frequency of 90 MHz. What would it be if the input RF frequency was 70 MHz?

Ans: The first thing to determine is the acoustic wavelength. From any general physics book, the frequency is related to wavelength by the velocity of the medium.

Thus,

$$f = \frac{V}{\Lambda}$$

$$\Lambda = \frac{V}{f}$$

$$= \frac{4.26 \times 10^3 \text{ m/s}}{90 \text{ MHz}}$$

$$= 4.733 \times 10^{-5} \text{ m}$$

where,

f = RF frequency;

V = acoustic velocity; and

Λ = acoustic wavelength.

Bragg Angle

$$\theta_B(90 \text{ MHz}) = \sin^{-1}\left(\frac{\lambda}{2\Lambda}\right)$$

$$\sim \frac{\lambda}{2\Lambda}$$

$$\sim \frac{633 \times 10^{-9} \text{ m}}{2 \cdot 4.733 \times 10^{-5} \text{ m}}$$

$$\theta_B(90 \text{ MHz}) \cong 6.68 \text{ milliradians}$$

Similarly,

$$\theta_B(70 \text{ MHz}) \cong 5.20 \text{ milliradians}$$

Bibliography

1. Alder, Robert. "Interaction Between Light and Sound," IEEE Spectrum, 4: 42-53 (May 1967).
2. Berg, Norman J. and John H. Lee. Acousto-Optic Signal Processing (Theory and Implementation). New York: Marcel Dekker, Inc., 1983.
3. Born, Max and Emil Wolf. Principles of Optics (Electromagnetic Theory of Propagation, Interference and Diffraction of Light) [Sixth (Corrected) Edition]. Elmsford NY: Pergamon Press, 1983.
4. Class Lectures or Lecture Materials. Syed, Vagar lecture notes distributed in EE 672 "Optical Communications," School of Engineering, Air Force Institute of Technology (AU), Wright-Patterson AFB OH, January 1984.
5. Korpel, Adrianus. "Acousto-Optics--A Review of Fundamentals," Proceedings of the IEEE, 69(1): 48-53 (January 1981).
6. Peebles, Peyton Z., Jr. Communication System Principles. Reading MA: Addison-Wesley Publishing Co., 1976.
7. Wilson, J. and J. F. B. Hawkes. Optoelectronics: An Introduction. Englewood Cliffs NJ: Prentice Hall Book Co., 1983.

VII. Beam Deflection and Spectrum Analysis
Using an Acousto-Optic Modulator (Bragg Cell)

Assignment

To use the Bragg Cell as a spectrum analyzer, the student will perform some calculations of spatial positions for various input RF frequencies. The student will then measure the Bragg angle for these various RF frequency inputs and compare it to calculated results. Finally, the student will input two different RF frequencies and observe the resolution quality of the Bragg Cells Time-Bandwidth product.

Objective

1. To acquaint the student with using the Bragg Cell as a Beam Deflector and relate its use as a Spectrum Analyzer.
2. To relate classroom theory of Bragg Diffraction with practical application.
3. To observe the resolution quality of the Bragg Cells Time-Bandwidth Product.

Equipment Needed

Laser Source: Spectra Physics Helium-Neon Class IIIb
4 mw (Model 102-1)

Newport Laser Mount (Model 806), 1 each
Newport Support Post (Model VPH-4), 1 each
Newport Post Holder (Model SP-4), 1 each

Jordan Spatial
Filter:

- a. Microscope Objective 10X
- b. 25 micron Pinhole Spatial Filter
- c. Spherical Collimating lens

Newport Support Post (Model VPH-4), 1 each
Newport Post Holder (Model SP-4), 1 each

Iris
Diaphragm:

Newport Model ID-15
Newport Support Post (Model VPH-4), 1 each
Newport Post Holder (Model SP-4), 1 each

Focusing
Lens:

- a. Spherical Convex Lens with Holder
(150 mm) or equivalent
- b. Translational Stage Newport Model 430
Newport Support Post (Model VPH-4), 1 each
Newport Post Holder (Model SP-4), 1 each

Bragg Cell
and Mount:

- a. Newport EOS Acousto-Optic Modulator
Model N230
- b. Newport Translational Stage Model 430,
3 each
- c. Newport 90-degree Angle Mount, 2 each

RF Driver:

Hewlett Packard 8640B Signal Generator,
2 each, or equivalent

White Cardboard Screen, 2 ft. x 2 ft.

Theory/Background

Spectrum analysis is one of the most useful techniques in modern science. Virtually every area of science (Astronomy, Geology, Medicine, etc.) make use of it in one form or another (7).

Quite often an important requirement in spectrum analysis is the Real-Time operation. Real time spectrum analysis below 2 MHz bandwidth is predominately performed in special-purpose digital equipment. Above 10 MHz bandwidth, electronic analog, and optical techniques dominate the field.

In communications, the spectrum of a signal is used to analyze the effects of a signal as the signal is changed in frequency, amplitude or phase (5). In Acousto-Optics, primarily using Bragg cells as the medium for light diffraction, a change in frequency of a signal corresponds to a spatial frequency change of the light beam. An amplitude change of a signal corresponds to an intensity change in the light beam.

Optical spectrum analyzers can be divided into two major classes based on the variable of integration for the Fourier Transform operation. The "Space integrating

Architecture" performs a Fourier Transform with respect to a spatial variable. The "Time integrating Architecture" performs the Fourier Transform with respect to a temporal variable "t." One- and two-dimensional transforms exist for both types of optical spectrum analyzers. Some techniques and practical examples of both time and space integrating architectures are presented in (7).

An optical processor (Figure VII-1) must have a means of converting information (usually in the form of an electrical signal) into an optical format for transmission by some light source. The receiving end of the processor must also have a means for converting the optical format back to an electrical signal for further processing. The most practical highly developed and real-time input device for an optical system is the Bragg cell (1; 8). A brief discussion and operating characteristics of the Bragg cell are given in (7; 8). At the receiving end of the processor (Figure VII-1), is the optical sensors. One-dimensional photosensitive arrays are currently available in sizes from 64 to more than 1700 elements. The one-dimensional photosensor arrays are the most prevalent output device in optical processing (2).

From the Bragg angle experiment (Chapter VI), a relationship exists between the acoustic wavelength and the deflection angle (spatial positioning) of the diffracted order. The deflection angle (Bragg angle) is given by

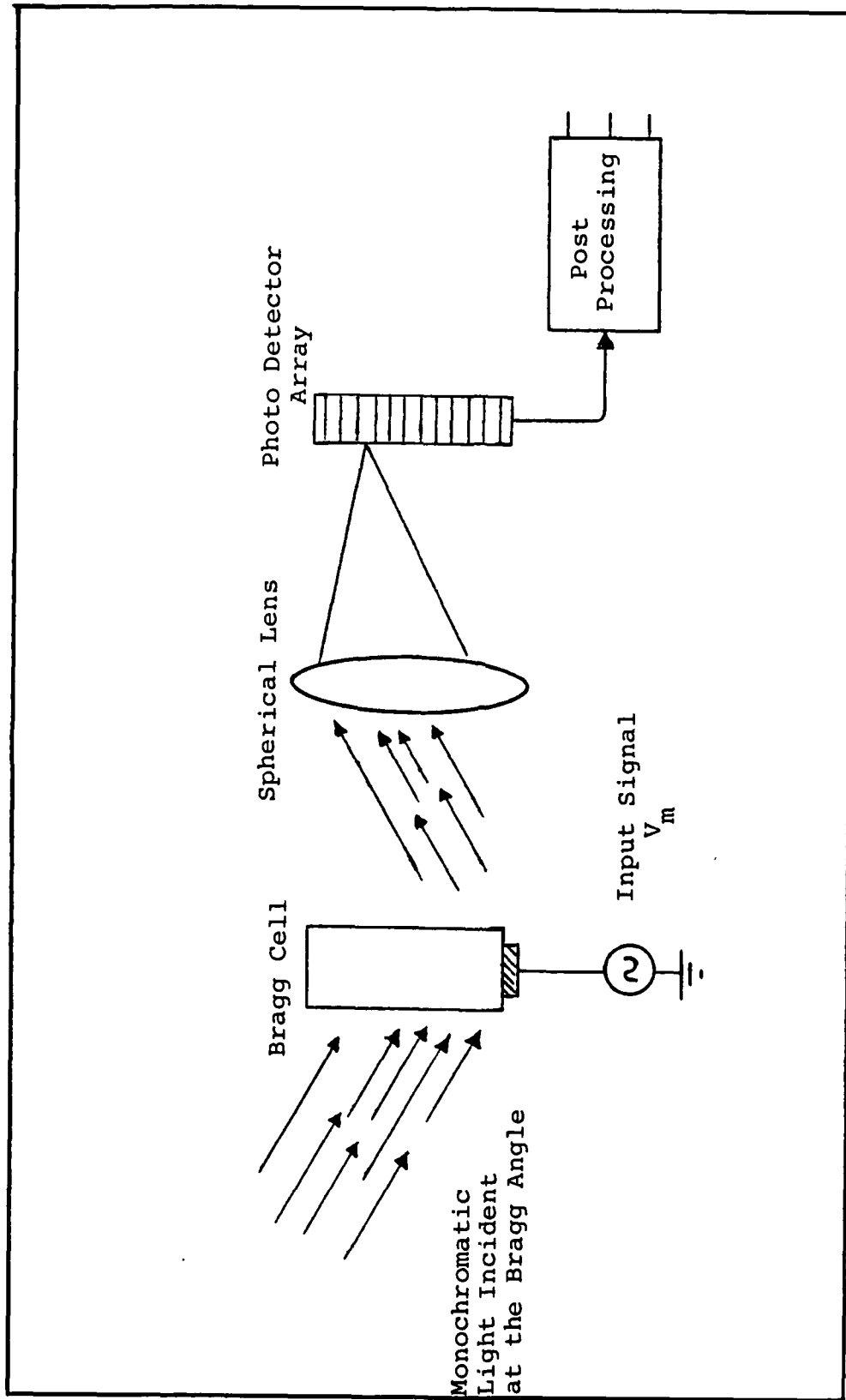


Fig. VII-1. Optical Processing System

$$\sin \theta_B = \frac{\lambda}{2\Lambda} \quad (1)$$

where

λ = free space light wavelength, and

Λ = acoustic wavelength in the medium.

Since the Bragg angle is usually very small ($\theta_B \ll 1$) the approximation $\sin \theta_B \cong \theta_B$ will be used. Thus

$$\theta_B \cong \frac{\lambda}{2\Lambda} \quad (2)$$

$$\alpha = \frac{\lambda}{\Lambda} \quad (3)$$

where $\alpha = 2\theta_B$ is the angle between the zeroth and first diffracted order component in the Bragg regime (Figure VII-2). The acoustic wavelength is related to the input RF frequency (f_{RF}) by the speed of sound in the acoustic medium. Thus if the acoustic velocity is "V," then

$$\alpha = \frac{\lambda}{V} f_{RF} \quad (4)$$

The optical wavelength and the acoustic velocity are usually constant for a given Bragg cell. Therefore, a linear relationship exists between the angle deflection and the RF frequency (4). Thus for a small change in RF frequency, say $\Delta f_{RF} = f_{RF} + \Delta f$, the deflection angle will change by some small amount $\Delta\alpha$ given by

$$\Delta\alpha = \frac{\lambda}{V} \Delta f_{RF} \quad (5)$$

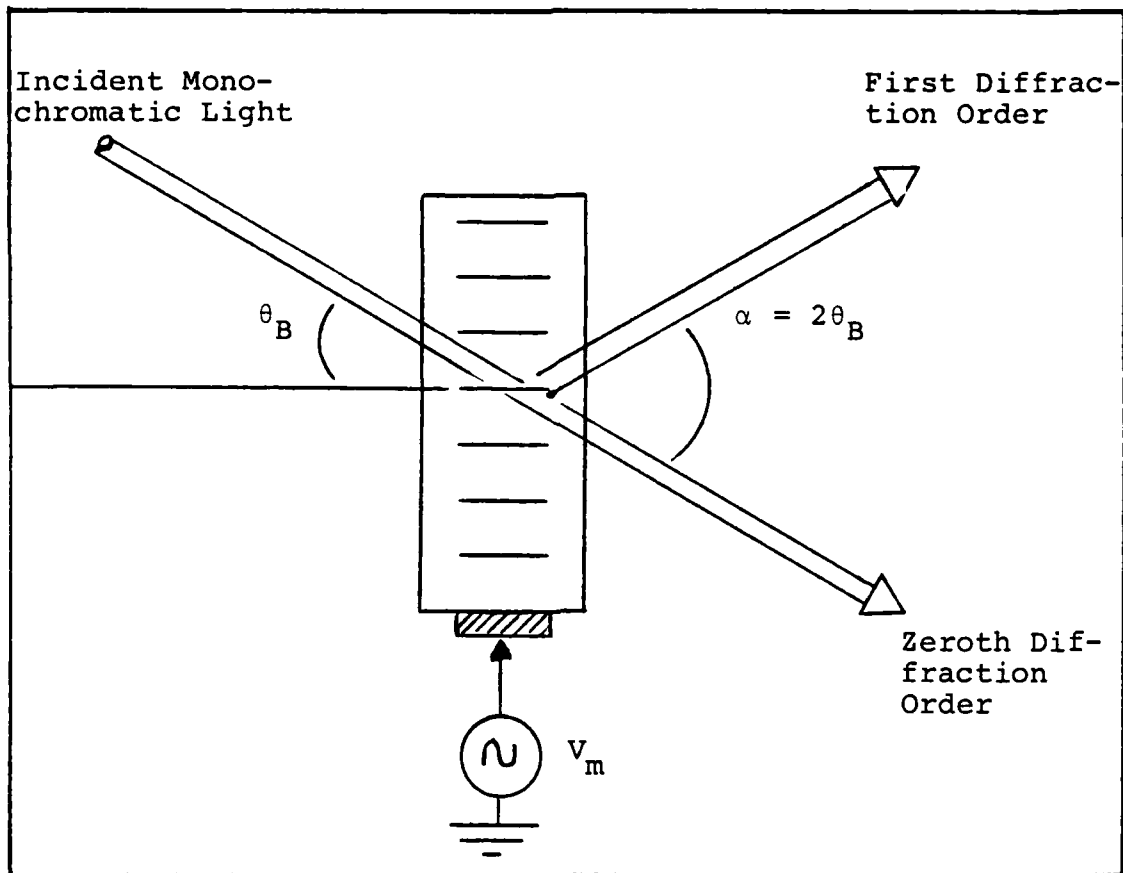


Fig. VII-2. Acousto-Optic Interaction in the Bragg Regime

From Eq (5), we see that a Bragg cell can be used as a spectrum analyzer in which input signals of different frequencies will correspond to unique spatial frequencies in the Fourier Transform domain (i.e., the back focal plane of a convex lens). Figure VII-3 illustrates the use of the Bragg cell as a spectrum analyzer (4).

A critical factor in using the Bragg cell as a spectrum analyzer is the number of diffracted orders that can be clearly resolved from one another. The criterion

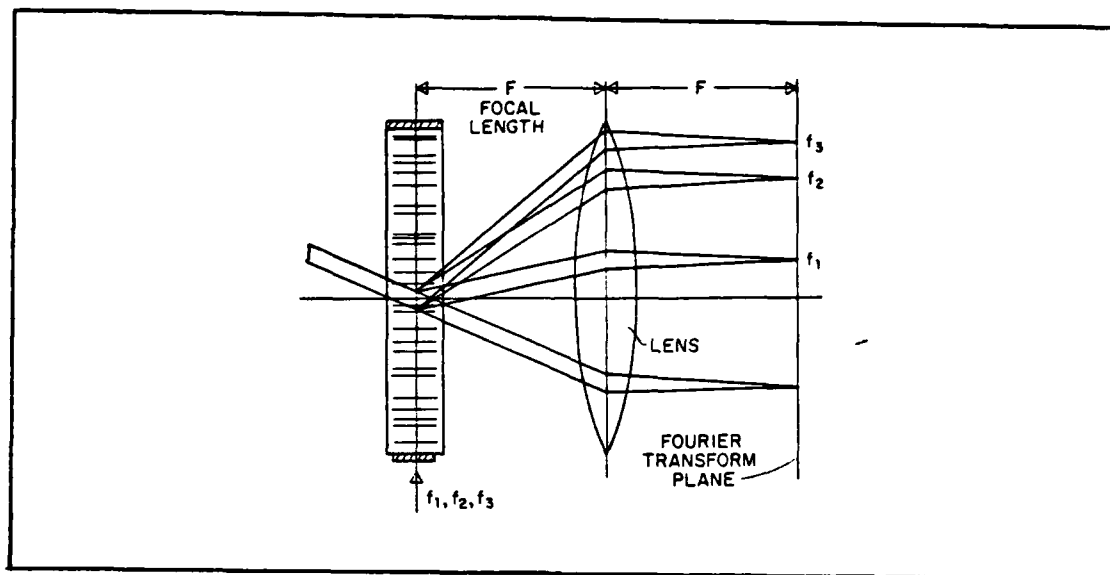


Fig. VII-3. Bragg Diffraction Sound Cell Used as Spectrum Analyzer (4:51)

used for resolving two adjacent diffraction orders is the Rayleigh criterion outlined in (3). The number "N" of resolvable spots is determined by dividing the total angular displacement $\Delta\alpha$ by the unavoidable diffraction spread of the laser beam. The unavoidable diffraction spread is given by

$$\alpha_{\min} = \frac{\lambda}{h} \quad (6)$$

where

h = the optical beam height in the Bragg cell.

Thus dividing Eq (5) by Eq (6) results in

$$\begin{aligned}
N &= \frac{\Delta\alpha}{\alpha_{\min}} \\
&= \frac{\frac{\lambda}{V}\Delta f}{\frac{\lambda}{h}} \\
&= \frac{h}{V}\Delta f \\
&= \tau\Delta f \tag{7}
\end{aligned}$$

where τ is the transit time of the Bragg cell (rise time) and Δf is the peak to peak frequency change of the acoustic wave in the Bragg cell (i.e., the bandwidth of the Bragg cell). The number "N" is known as the time-bandwidth product of the Bragg cell. This product is an indication of the number of angular positions a Bragg cell can clearly resolve.

This characteristic of the Bragg cell is very useful in that it can process N spectral coefficients of a signal in parallel in real time. "N" is also known as the processing gain of the Bragg cell. The Bragg cell has found practical applications in radar signal processing and adaptive linear prediction signal processing (6).

In this experiment, the student will perform some calculations of spatial positions (i.e., Bragg angles) for various input RF frequencies to the Bragg cell. The student will then measure these spatial positions and compare

them to predicted values. The student will actually view the beam deflection of the first diffracted order by varying the input RF frequency to the Bragg cell. Finally, the student will input two different RF frequency signals to the Bragg cell and view the resolution quality of the Bragg cell. Note: Due to the lack of an appropriate photo-sensitive array for this experiment, the output of the spectrum analyzer will be viewed on a white screen and limited to the human visual perception instead of electronic sensors.

Theoretical Calculations. Before conducting this experiment, perform the following computations for the beam deflection of various input RF frequencies and calculate the time-bandwidth product for this particular type of Bragg cell.

Given Data:

Acoustic velocity	4.26 x 10 m/s
Center RF frequency	80 MHz
Light wavelength	633 nm
Bandwidth of Bragg cell	30 MHz
Optical beam height is cell	1 mm

1. From the given data, determine the Bragg angle of the Bragg cell using the center RF frequency (see Chapter VI).

2. Determine the change in angle deflection ($\Delta\alpha$) for 70 MHz and 90 MHz using Eq (5).

3. Determine the Time-Bandwidth product of the Bragg cell.

Beam Deflection and Spectrum Analysis Measurement Procedures

Performing this experiment will be very similar to that of Chapter VI. The difference with this chapter is that the RF generator that will be used (Hewlett Packard 8640B) can sweep the RF spectrum bandwidth of interest (namely, from 70 to 90 MHz). This will allow the student to vary the RF frequency input and observe the angle deflection (Eq (5)) on a white screen. Again, due to the lack of proper optical sensing equipment (Photodetector Array), observation will be limited to human visual perception.

The Bragg cell being used in this experiment is the same model as that from Chapter VI. Therefore, the same precautionary steps should be taken as not to overload the Bragg cell. Refer to Chapter VI (Experimental Procedures) for safety tips on protection to the equipment.

The following steps should help the student through successful implementation of this experiment. The experimental setup used is in Figure VII-4. The picture of the optical system (Figure VII-5) should help to illustrate the equipment setup.

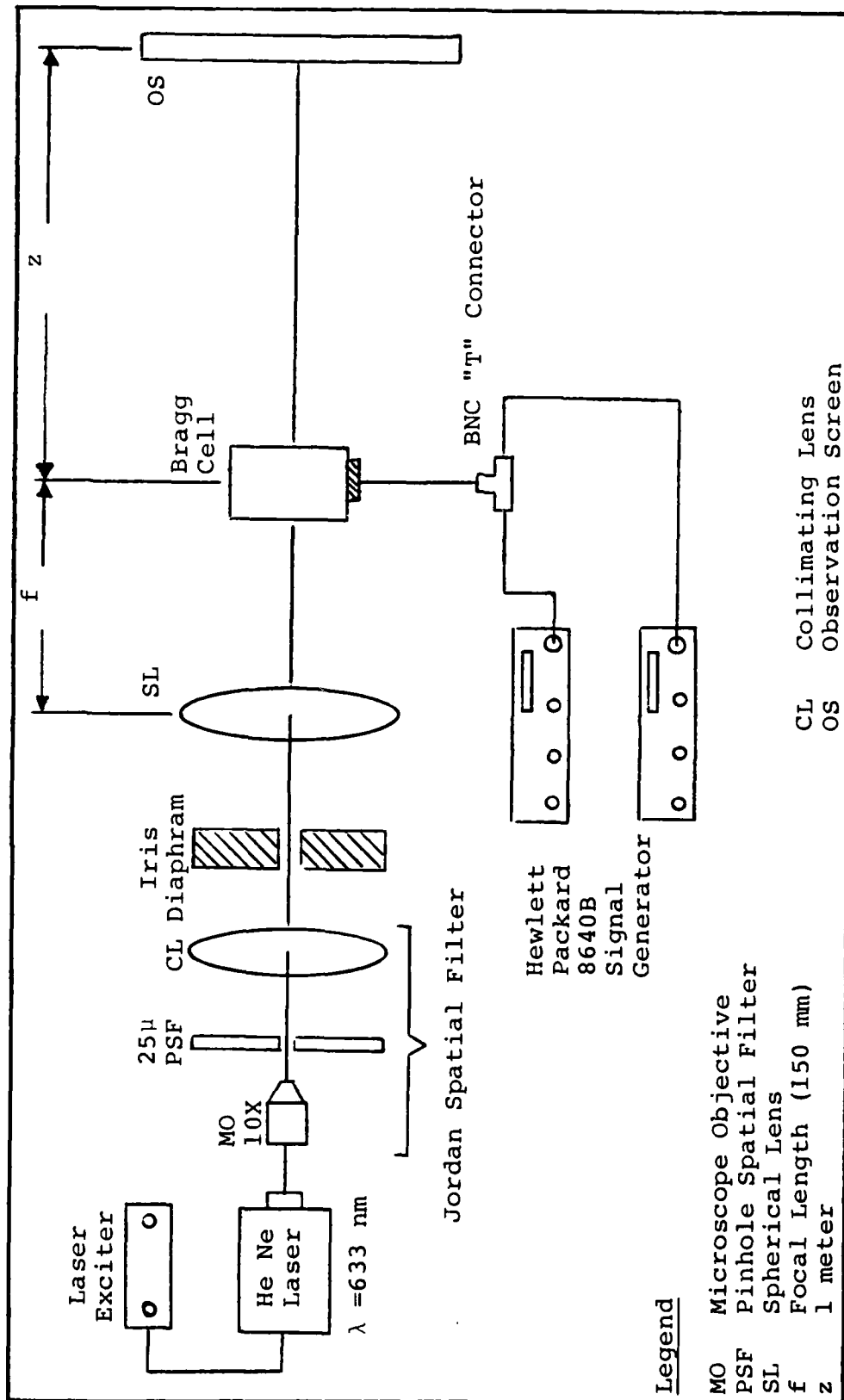


Fig. VII-4. Beam Deflection and Spectrum Analysis Experimental Setup

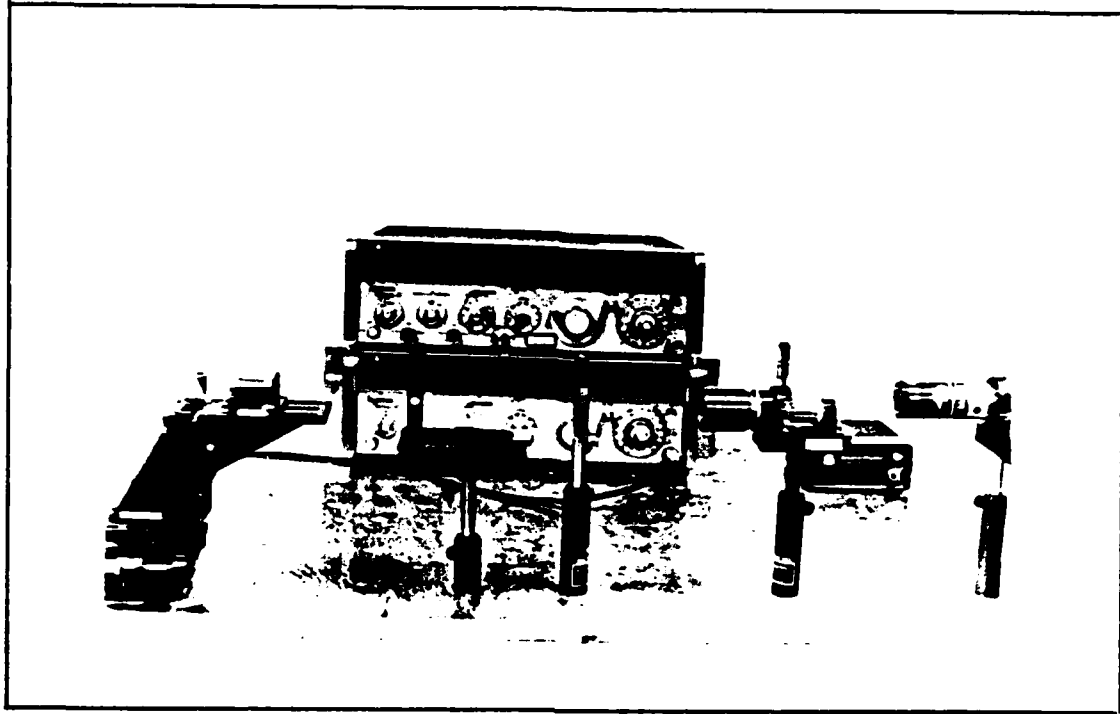


Fig. VII-5. Photograph of the Optical System

STEPS

INSTRUCTIONS

1. Assembling the Laser Source--assemble Spectra Physics laser into laser mount and attach to support post and post holder. Fasten the post holder to the optical table. Connect the He-Ne laser to the laser exciter.
2. Jordan Spatial Filter (JSF)--fasten a post holder, approximately four inches in front of the laser post holder, to the optical table. Attach a support post to the JSF and secure it in the post holder.
3. Collimating the laser beam--turn on the laser exciter and allow a few minutes for the laser to

laze. Remove the spherical collimating lens from the JSF. Adjust both the laser mount and the 25 micron pinhole filter for a good airy disk pattern out of the pinhole. (The airy disk pattern can be observed on a screen placed approximately one meter away from the JSF.) Note: This step may take a few moments to align properly. Next, replace the spherical collimating lens back on the JSF and adjust until a good collimated beam is observed.

4. Connect an Iris diaphragm to a support post and secure it in a post holder. Fasten the post holder approximately two inches in front of the JSF. Next, close the diaphragm down until the laser beam diameter is approximately three to four mm in diameter. Note: This should allow only the central portion of the airy disk through and block all the other rings.
5. Focusing Lens--fasten a support post to a translation stage and secure the post in a post holder placed in front (one to two inches) of the iris diaphragm. The stage should move in a parallel line with the laser beam. Next, fasten a spherical lens with holder to the translation stage and adjust the height of the support post so the laser beam strikes the center portion of the lens.

6. Bragg Cell and Mount--build an X-Y-Z translational stage using three translational stages and two 90-degree angle mounts. See Figure VII-5. Fasten the Bragg cell to the stage and place the stage one focal length (i.e., 150 mm) in front of the focusing lens. Ensure that the Bragg cell aperture is perpendicular to the laser beam.
7. Alignment--adjust both the X-Y-Z translational stage and the focusing lens to center the laser beam on the Bragg cell aperture.

```

*****
*                                     *
*                               CAUTION *
*                                     *
* Exercise extreme care to avoid focusing the *
* laser beam on the gold bond wires of the *
* acoustic transducer. This may cause the *
* wires to vaporize and severely damage the *
* operation of the Bragg cell. *
*****

```

8. Setting up the Hewlett Packard (HP) 8640B--connect the HP 8640B Signal Generator RF out to the Bragg cell. Before turning on the power to the HP 8640B signal generator, set the following configuration:
 - AM Modulation: OFF
 - FM Modulation: OFF
 - Counter Mode: INT/EXT Depressed

Range (MHz): 64-128

Output Level: +10 dBm

RF: OFF

9. Turn on the power to the HP 8640B signal generator and adjust the frequency to 80 MHz. Next, switch the "RF" switch to "ON."
10. Adjust the angle the Bragg cell makes with the laser beam until the first order diffraction component is visible on the white screen placed approximately two meters away from the Bragg cell. To ensure that the diffraction pattern observed is the zeroth and first diffracted orders, on the HP 8640B signal generator, switch the "RF" switch to "OFF" and observe that the first diffracted order will disappear.
11. Switch the "RF" switch back to "ON" and ensure that only one of the first order diffraction components is strongly illuminated (i.e., adjust for the Bragg angle).
12. Measure the distance from the Bragg cell to the screen and record it. Next, measure the distance from center to center of the zeroth and first order diffraction components. The Bragg angle can be computed by the formula:

$$(\theta_B) = \sin^{-1}[\text{CCD}/Z] \quad (8)$$

where

CCD = the center-center distance between the
zeroth and first order component, and

Z = distance from the Bragg Cell to the
screen.

Note: Much of the steps up to this part are exactly as in Chapter VI. The results of the Bragg angle should be the same as that found in the previous experiment. The Bragg angle measured here will be the reference angle used for this experiment.

13. Slowly change the RF frequency to 70 MHz and notice the beam deflection of the first diffracted order moves towards the zeroth order. Measure the change in deflection angle and record it.
14. Repeat STEP 13 for 90 MHz. Compare the measured values of the beam deflection with that calculated earlier. How do the measured values compare with the theoretical values?
15. Resolution Quality of the Time-Bandwidth Product-- adjust the RF frequency on the HP 8640B signal generator back to 80 MHz. Use a BNC "T" connector and connect a second HP 8640B signal generator to the Bragg cell. Before turning on the power to the second signal generator, set it up for the configuration from STEP 8.

16. Turn on the power to the second HP 8640B signal generator and switch the "RF" switch to "ON." Sweep the RF frequency until the resolution of two distinct diffraction orders are observed. Note the difference in frequency on the two signal generators. This is the resolution of the Time-Bandwidth product of the Bragg cell as interpreted by the human visual perception. Is this a good indication of the resolution quality of the Bragg cell? How well does the difference in frequencies compare to the resolution quality calculated earlier? Is this a good Bragg cell to use in applications where a large time-bandwidth product is needed? Why or why not?

Special Problems

Since this experiment is very similar to Chapter VI, the special problems discovered in Chapter VI apply to this experiment. It is recommended for the student to review the special problems section of Chapter VI before conducting this experiment.

As pointed out in the results section of Chapter VI, the illumination of the laser intensity on the screen was very low and difficult to see. The JSF was the primary cause for blocking much of the laser light propagating through the Bragg cell. Thus, for a brighter illumination

of the diffraction pattern on the white screen, the JSF was removed from the equipment setup and the experiment conducted as such. Caution must be exercised as not to focus the laser beam on the transducer wires of the Bragg cell (see STEP 7).

As mentioned earlier, an important item that was missing from this experiment is the use of a good photodetector array. Depending on the time-bandwidth product of the Bragg cell, spatial distribution of the diffracted orders caused by various input frequencies is on the order of a few micrometers. Therefore, it is usually very impractical for an observer to try and view the resolved spots on a screen. Thus, the use of a photodetector array becomes an essential element in determining the actual resolution quality of the Bragg cell. In many instances, the resolution quality of the optical processor is dependent on the specific architecture of the system along with the spatial distributions of the photodetector elements in an array (2).

Results

The beam deflection aspect of the Bragg cell demonstrates how a Bragg cell can be used as a spatial Fourier Transform device. The remarkable thing about the Bragg cell, as demonstrated in this experiment, is that it performs the Fourier Transform of an RF input signal

instantaneously. This aspect of the Bragg cell allows a user to perform a "real-time" analysis on the spectrum of a signal.

Comparisons of the theoretical results with the measured results are as follows:

Theoretical Calculations.

RF Frequency (MHz)	*Angle deflection
80	11.8 milliradians
70	10.4 milliradians
90	13.37 milliradians

*The angle measured from the zeroth order diffraction component to the first order diffraction component (Eq (8)).

Measured Values.

RF Frequency (MHz)	Angle deflection
80	12.7 milliradians
70	11.5 milliradians
90	14.1 milliradians

All measured values were taken with a Bragg cell to screen distance of one meter. All measurements were made with a meter stick and/or a small 30 cm ruler. Thus, the measurements are subject to round-off errors and subjective interpretation.

As seen from these results, the measured values agree with the theoretical values with a little error

round-off. This indicates that there does exist a linear relationship between the input RF frequency and beam deflection. With the use of a good photodetector array, and the proper architecture for an optical system, the Bragg cell can be used as a spectrum analyzer. The amount of light diffracted by an input frequency is an indication of the amplitude of the signal at that particular frequency. This was evident from Chapter VI.

The resolution quality of the time-bandwidth product of this Bragg cell is as follows:

Time-Bandwidth Product = 7.04

Resolution Quality = 4.26 MHz

Observed Resolution Quality = 15 MHz

From these results, it is evident that this type of Bragg cell is not a good device to use in optical applications where a large time-bandwidth product is needed. The reason for such a small time-bandwidth product is the physical limitation of the Bragg cell. The Bragg cell requires a very narrow beam of light for the input. Thus, the rise time of the Bragg cell is very fast. For a large time-bandwidth product, a slower rise time is needed (rise times in a Bragg cell can be anywhere from 5 to 60 microseconds depending on the time window of the cell). This would constitute a Bragg cell with a larger effective optical aperture.

As discussed earlier, the use of observing the resolution quality of the Bragg cell on a white screen is not a good indication of discriminating the diffracted orders. Again, the use of a good photodetector array is essential in these types of applications. Although this type of Bragg cell is not a good example to illustrate the time-bandwidth product or resolution quality of Acousto-optics, it will suffice to portray a simple example of the physical effects of resolving two signals from a Bragg cell. The procedures written for this experiment are general enough such that the use of a Bragg cell with a larger time-bandwidth product can be easily implemented.

Bibliography

1. Alder, Robert. "Interaction between Light and Sound," IEEE Spectrum, 4: 42-53 (May 1967).
2. Borsuk, Gerald M. "Photodetectors for Acousto-Optic Signal Processors," Proceedings of the IEEE, 69(1): 100-118 (January 1981).
3. Class Lectures or Lecture Materials. Syed, Vagar lecture notes distributed in EE 672 "Optical Communications," School of Engineering, Air Force Institute of Technology (AU), Wright-Patterson AFB OH, January 1984.
4. Korpel, Adrianus. "Acousto-Optics--A Review of Fundamentals," Proceedings of the IEEE, 69(1): 48-53 (January 1981).
5. Peebles, Peyton Z., Jr. Communication System Principles. Reading MA: Addison-Wesley Publishing Co., 1976.
6. Rhodes, William T. "Acousto-Optic Signal Processing: Convolution and Correlation," Proceedings of the IEEE, 69(1): 68-79 (January 1981).
7. Turpin, Terry M. "Spectrum Analysis Using Optical Processing," Proceedings of the IEEE, 69(1): 79-92 (January 1981).
8. Young, E. H., Jr. and S. K. Yao. "Design Considerations for Acousto-Optic Devices," Proceedings of the IEEE, 69(1): 54-64 (January 1981).

VIII. Laser Communications Using Acousto-Optic Cells

Assignment

The student will implement a laser communications system using an Acousto-Optic Cell and a black box photo-detector circuit. The type of modulation used will be AM modulation.

Objectives

1. To acquaint the student with using the Bragg Cell as a laser communications device.
2. To relate classroom theory of the Bragg Cell transmittance function with a practical application.
3. To acquaint the student with the use of photo-detectors and their application to optical communication systems.

Equipment Needed

Laser Source: Spectra Physics Helium-Neon Class IIIb
4 mw (Model 102-1)

Newport Laser Mount (Model 806), 1 each

Newport Support Post (Model VPH-4), 1 each

Newport Post Holder (Model SP-4), 1 each

Focusing
Lens:

- a. Spherical Convex Lens with Holder
(150 mm) or equivalent, 3 each
- b. Translational Stage Newport Model 430,
3 each
Newport Support Post (Model VPH-4), 3 each
Newport Post Holder (Model SP-4), 3 each

Bragg Cell
and Mount:

- a. Newport EOS Acousto-Optic Modulator
Model N230
- b. Newport Translational Stage Model 430,
3 each
- c. Newport 90 degree Angle Mount, 2 each

Photodetector
Box:

Metrologic Instruments, Inc.
143 Harding Avenue, P.O. Box 307
Bellmawr, New Jersey 08031

45-720 Laser Video Kit Contents:

Black circuitry control box (W-5 1/4" x
L-6 7/8" x H-2 3/8"): Part No. 00129,
1 each
Control Box lid: Part No. 30855, 1 each
Slide Switches (ON/OFF): Part No. 00317,
2 each
Red binding posts: Part No. 00143, 4 each
Black binding posts: Part No. 00144, 4 each
8 ohm speaker: Part No. 00119, 1 each
Printed Circuit Board: Part No. 35115,
1 each

Battery clamp: Part No. 00006, 1 each

Battery connector: Part No. 00008, 1 each

Support Stand for
Photodetector

Box: Newport Rod and Platform Assembly (Model 300)

Photodetector Mounting Platform

Microphone with Amplifier

Small AM/FM Radio

Audio Amplifier with Speaker

RF Driver: Hewlett Packard 8640B Signal Generator

Theory/Background

From Chapters VI and VII the use of an Acousto-Optic Cell was used as a light modulator and a beam deflection device (1; 3; 5). In this chapter we will model the Bragg Cell as a spatial light modulator and try to relate the electrical drive signal to the resultant modulation of light both spatially and temporally. In order to facilitate a better understanding of the system, we must first review the basic characteristics of Acousto-Optic Cells as spatial light modulators.

Analytical Modeling. The Acousto-Optic Cell, when used as a spatial light modulator, is illuminated by a beam of light (usually collimated) in which the wave field is modified by the sound wave in the cell via diffraction processes. For our analysis, we will only work with the one-dimensional case.

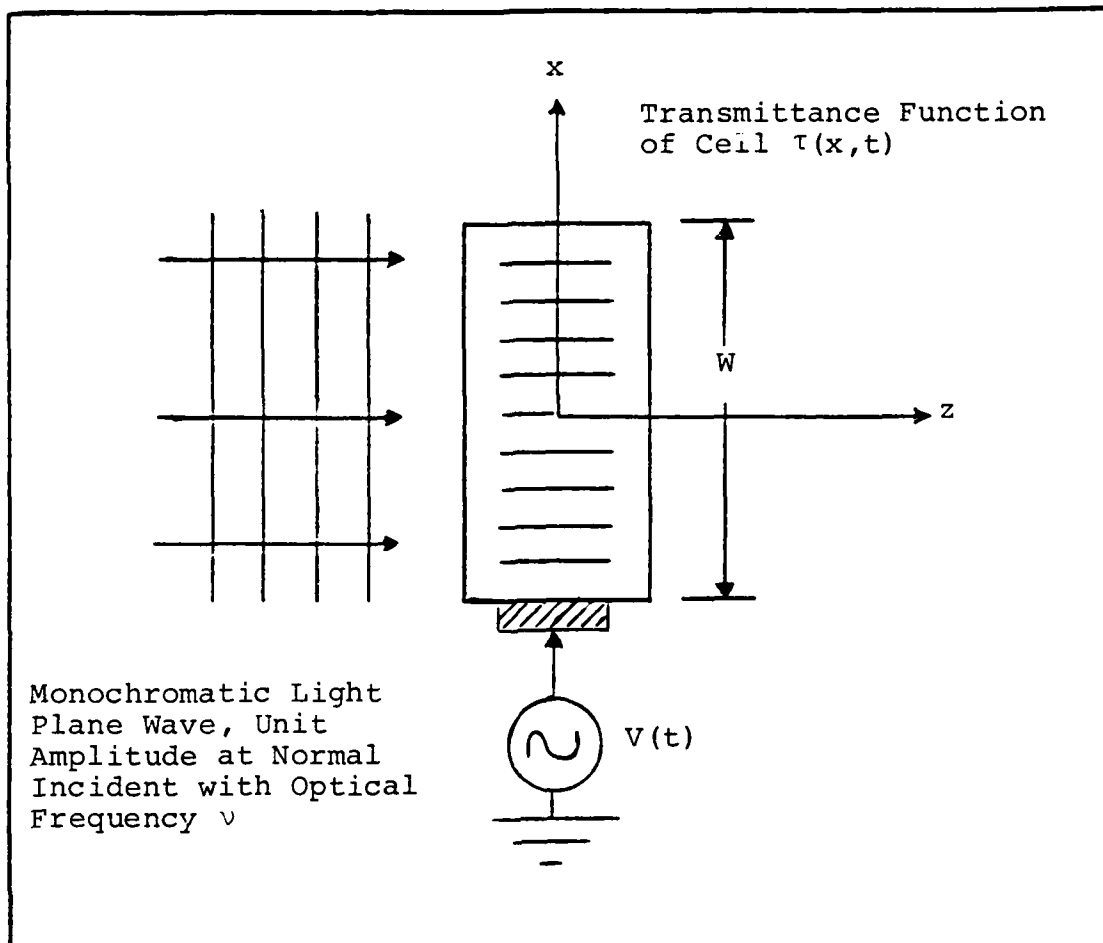


Fig. VIII-1. Bragg Cell with Plane Wave Illumination

With reference to Figure VIII-1, the Acousto-Optic Cell is characterized by the complex wave amplitude transmittance function $\tau(x,t)$, where x is the spatial coordinate along the length of the cell. Let $s(x)$ represent the transducer-strain field in the Acousto-Optic medium at time $t=0$. Then the amplitude transmittance function becomes (6)

$$\tau(x,t) = \exp[js(x-Vt)]\text{rect}(x/W) \quad (1)$$

where V is the acoustic velocity and W is the finite aperture window of the cell. Placing the origin of the x -axis in the middle of the cell (Figure VIII-1), the strain field at the transducer end $s(-W/2-Vt)$ is proportional to the input signal voltage $V(t)$ by

$$s[-W/2-Vt] = mV(t) \quad (2)$$

where m is a proportionality constant.

As determined from Chapter VI, the signal $V(t)$ that is launched into the Acousto-Optic Cell is an RF modulated signal. Thus, by Eq (2), if $s(\cdot)$ and $mV(\cdot)$ are plotted as functions of the same variable, they would only differ by a horizontal scale factor (the sound velocity) and a delay. Therefore, we can write the strain field $s(x)$ as an RF carrier that is modulated in magnitude and phase at $t=0$ as:

$$s(x) = a(x) \cos[2\pi f_0 x + \alpha(x)] \quad (3)$$

From Reference (3) the transmittance function $\tau(x,t)$ can be expressed in a power series as:

$$\tau(x,t) = \{1 + js(x-Vt) - \frac{1}{2}s^2(x-Vt) + \dots\} \text{rec}(x/W) \quad (4)$$

If the modulation amplitude $a(x)$ is assumed to be small, the higher order terms (i.e., $s^2(x-Vt)$) can be neglected, thus substituting Eq (3) into Eq (4), we get:

$$\tau(x,t) = \{1 + ja(x-Vt) \cos[2\pi f_0(x-Vt) + \alpha(x-Vt)]\} \cdot \text{rect}(x/W) \quad (5)$$

Expanding the cosine term into its exponential form we obtain

$$\begin{aligned} \tau(x,t) = \{1 + \frac{j}{2} a(x-Vt) \exp[j2\pi f_0(x-Vt)] \exp[j\alpha(x-Vt)] \\ + \frac{j}{2} a(x-Vt) \exp[-j2\pi f_0(x-Vt)] \exp[-j\alpha(x-Vt)]\} \cdot \\ \text{rect}(x/W) \quad (6) \end{aligned}$$

Simplifying Eq (6) we get:

$$\begin{aligned} \tau(x,t) = \{1 + \frac{j}{2} \tilde{A}(x-Vt) \exp[j2\pi f_0 x] \exp[-j2\pi v_0 t] \\ + \frac{j}{2} \tilde{A}^*(x-Vt) \exp[-j2\pi f_0 x] \exp[j2\pi v_0 t]\} \cdot \\ \text{rect}(x/W) \quad (7) \end{aligned}$$

where v_0 is the temporal frequency of the driving RF signal related to spatial frequency f_0 by $v_0 = Vf_0$ and $a(x) = |\tilde{A}(x)|$, $\alpha(x) = \arg[\tilde{A}(x)]$ and (*) indicates the complex conjugate of the function. The transmittance function can be expressed in terms of the analytic signal ($\tilde{S}(x)$) by

$$s(x) = \text{Re}[\tilde{S}(x)] \quad (8)$$

where

$$\tilde{S}(x) = \tilde{A}(x) \exp[j2\pi f_0 x] \quad (9)$$

Thus the transmittance function becomes,

$$\tau(x,t) = \{1 + j\frac{1}{2} \tilde{S}(x-Vt) + j\frac{1}{2} \tilde{S}^*(x-Vt)\} \text{rect}(x/W) \quad (10)$$

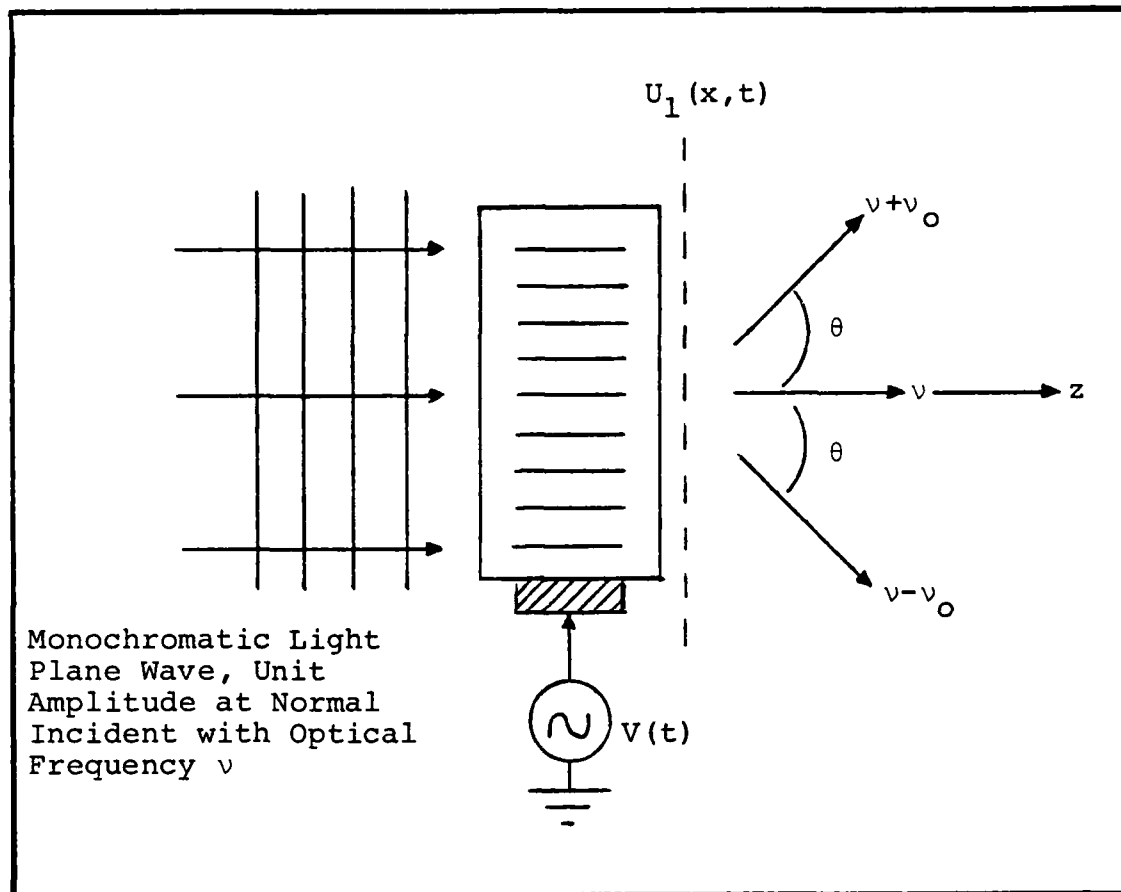


Fig. VIII-2. Bragg Diffraction of an Acousto-Optic Cell

Now let an Acousto-Optic Cell be illuminated with a monochromatic plane wave of light with unit amplitude impinging at normal incidence (Figure VIII-2). The complex wave amplitude $U_1(x,t)$ at the output of the Acousto-Optic Cell is just the complex amplitude transmittance function of the cell; i.e.,

$$U_1(x,t) = \tau(x,t) \tag{11}$$

For simplicity of analysis, let's consider the special case of $\tilde{A}=1$ (i.e., the signal $V(t)$ is an unmodulated carrier). From this, the complex wave field $U_1(x,t)$ after substituting Eq (7) into Eq (11), becomes

$$U_1(x,t) = \frac{1}{2} \{ 2 + j \exp[j2\pi f_o x] \exp[-j2\pi v_o t] + j \exp[-j2\pi f_o x] \exp[j2\pi v_o t] \} \text{rect}(x/W) \quad (12)$$

If v is the optical frequency of the incident light and the effects of the window (i.e., $\text{rect}(x/W)$) is ignored, then the interpretation of Eq (12) is as follows: the first term is the undiffracted component with optical frequency v , traveling in the $+z$ -direction. The second term is a diffracted plane wave component with optical frequency $(v-v_o)$ traveling at an angle $\theta = -\sin^{-1}(f_o \lambda)$. The third term is a diffracted plane wave component with optical frequency $(v+v_o)$ traveling at an angle $\theta = \sin^{-1}(f_o \lambda)$ (see Figure VIII-1).

From these results, we see that the diffraction process of the Acousto-Optic Cell agrees with that of Chapter VI. The shift in frequency of the diffracted wave can be determined in three different ways (1; 4):

1. Conservation of photon and phonon momentum
2. Doppler shift of frequency
3. Diffraction process of light

From Chapter VI (Bragg Angle) the Acousto-Optic Cell must be tilted at an angle

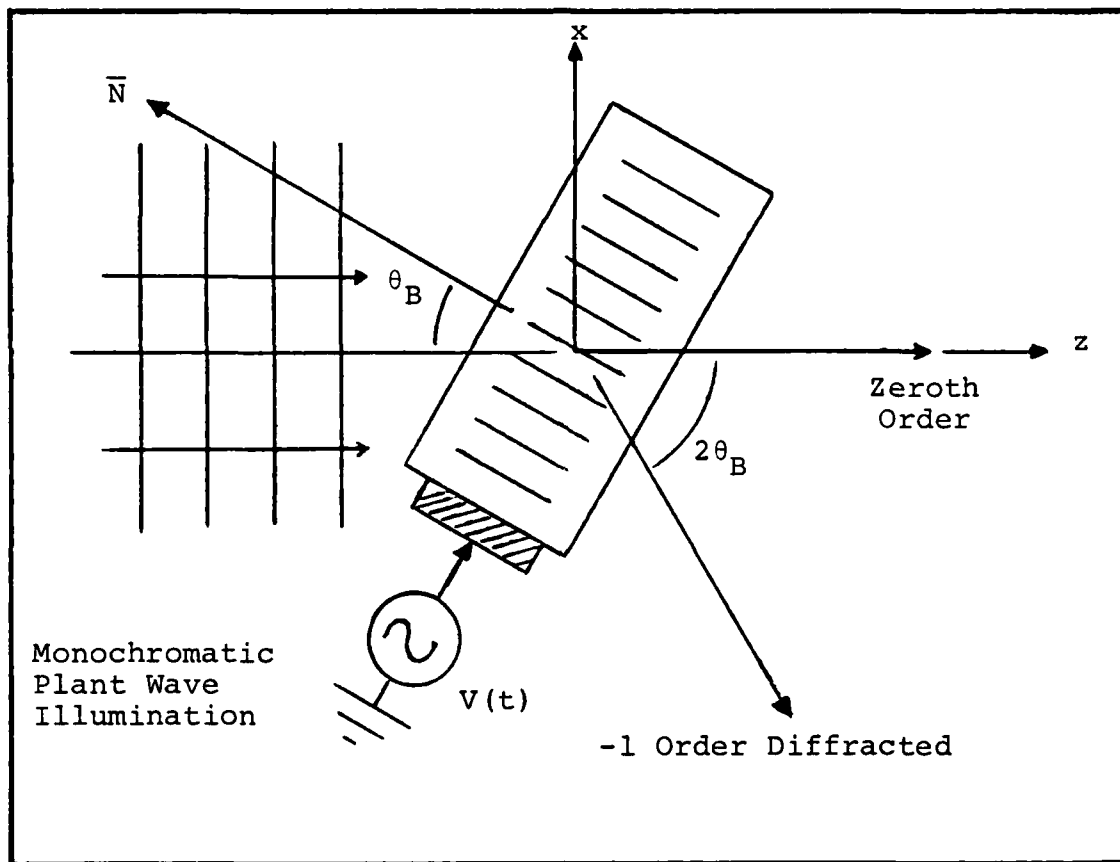


Fig. VIII-3. Illustration of an Acousto-Optic Cell Tilted at the Bragg Angle

$$\theta_B = \sin^{-1}(\lambda/2\Lambda) \quad (13)$$

where Λ = acoustic wavelength
 known as the Bragg angle to achieve maximum diffraction efficiency. Thus, tilting the Acousto-Optic Cell as shown in Figure VIII-3 (i.e., eliminating the +1 diffraction order), the transmittance function of Eq (7) can be written as

$$\begin{aligned}
\tau(x,t) &= \frac{1}{2} \{ 2 + j\tilde{A}(x-Vt) \exp[j2\pi f_0 x] \exp[-j2\pi v_0 t] \} \cdot \\
&\qquad\qquad\qquad \text{rect}(x/W) \\
&= \frac{1}{2} \{ 2 + j\tilde{S}(x-Vt) \} \cdot \text{rect}(x/W) \qquad\qquad\qquad (14)
\end{aligned}$$

An important aspect of Acousto-Optic is the means of converting the information signal from a light format back to an electrical signal. Figure VIII-4 illustrates a way of converting the temporal and spatial phase modulation of the light field to a temporal and spatial intensity modulation. Note that in the back focal plane of L1, spatial filtering may be performed to block the zeroth and either +1 or -1 diffraction order. However, operating in the Bragg regime, one of the orders is already suppressed. Thus, neglecting the effects of the window [rect(x/W)], the field in the image plane is

$$U_i(x,t) = 1 + j\frac{1}{2}\tilde{S}(x-Vt) \qquad\qquad\qquad (15)$$

The corresponding intensity is

$$\begin{aligned}
I(x,t) &= |U_i(t)|^2 \\
&= [1 + j\frac{1}{2}\tilde{S}(x-Vt)]^2 \\
&= 1 + \frac{1}{4}a^2(x-Vt) + 2s(t) \qquad\qquad\qquad (16)
\end{aligned}$$

From this we see that we can use a bandpass filter followed by an image plane detector to capture the modulation waveform since the second term is low-pass in nature. Note that a(x) represents a real baseband signal and will be

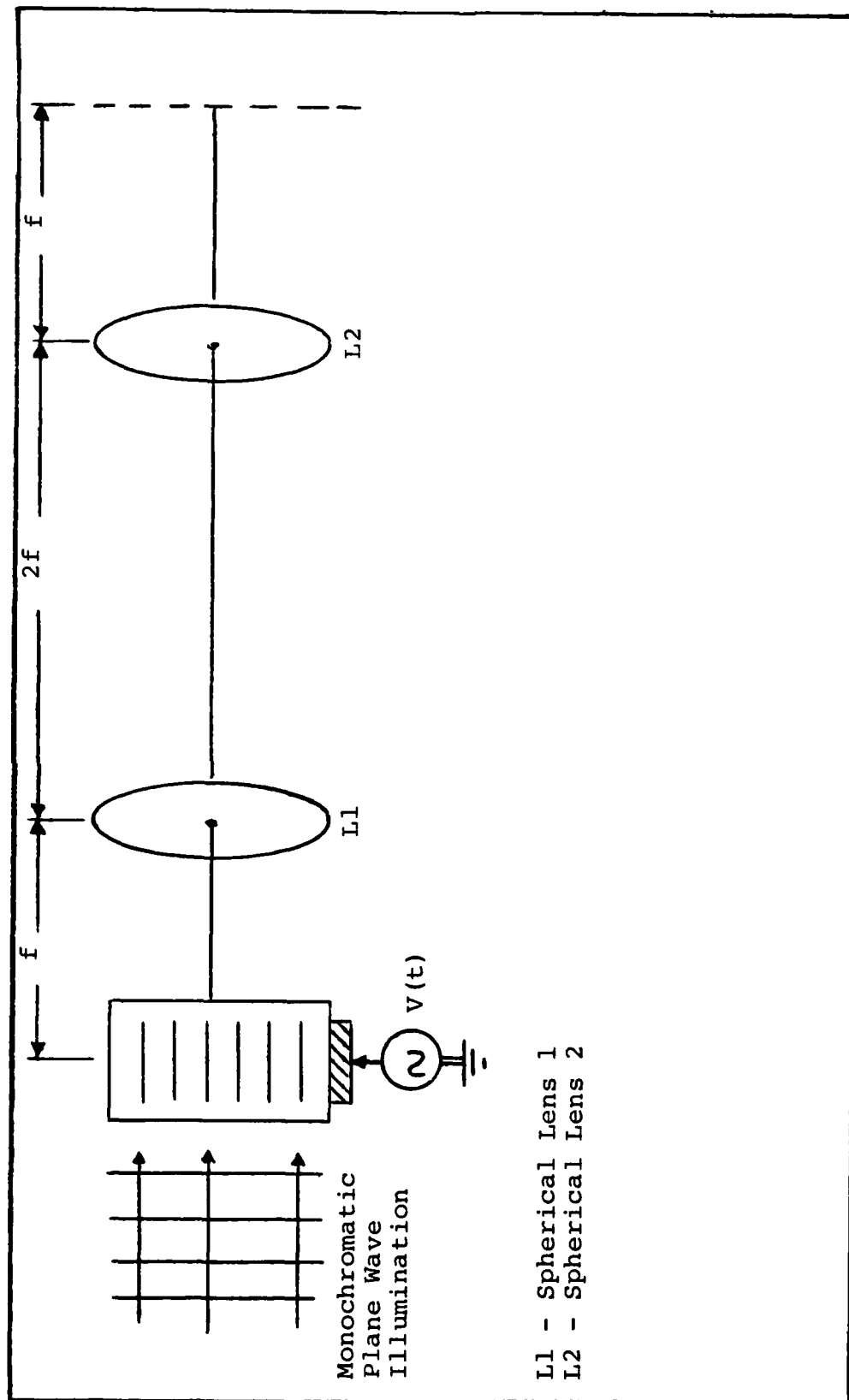


Fig. VIII-4. Acousto-Optic System Converting Phase Modulation to Amplitude Modulation

filtered with the bandpass filter. If $\alpha(x)$ in Eq (3) is zero, then $s(x)$ is a pure amplitude modulated carrier with the amplitude conveying the information of the baseband signal. Therefore, since the current out of the photodetector is proportional to the intensity, the information signal can be recovered.

In this experiment, the student will implement a laser communications system using Acousto-Optics with amplitude modulation. Later the implementation of frequency modulation will be discussed. This scheme of FM laser communications was not performed due to the lack of proper equipment.

Experimental Procedures

The experimental setup shown in Figure VIII-5 will be used to perform the laser communications experiment. The Newport N230 Bragg Cell is used for this experiment. As light propagates through the Bragg Cell the cell is adjusted for the Bragg angle. A spatial filter is used to block the zeroth order component. A focusing lens (SL2) is used to keep the first diffracted order from diverging too much and SL3 is used to concentrate the light energy onto the photodetector. The current out of the photodetector is proportional to the intensity of the light. The intensity of the diffracted beam is given by:

$$I_{DB} = I_{IN} \{ \sin^2 Kv(t) \} \quad (17)$$

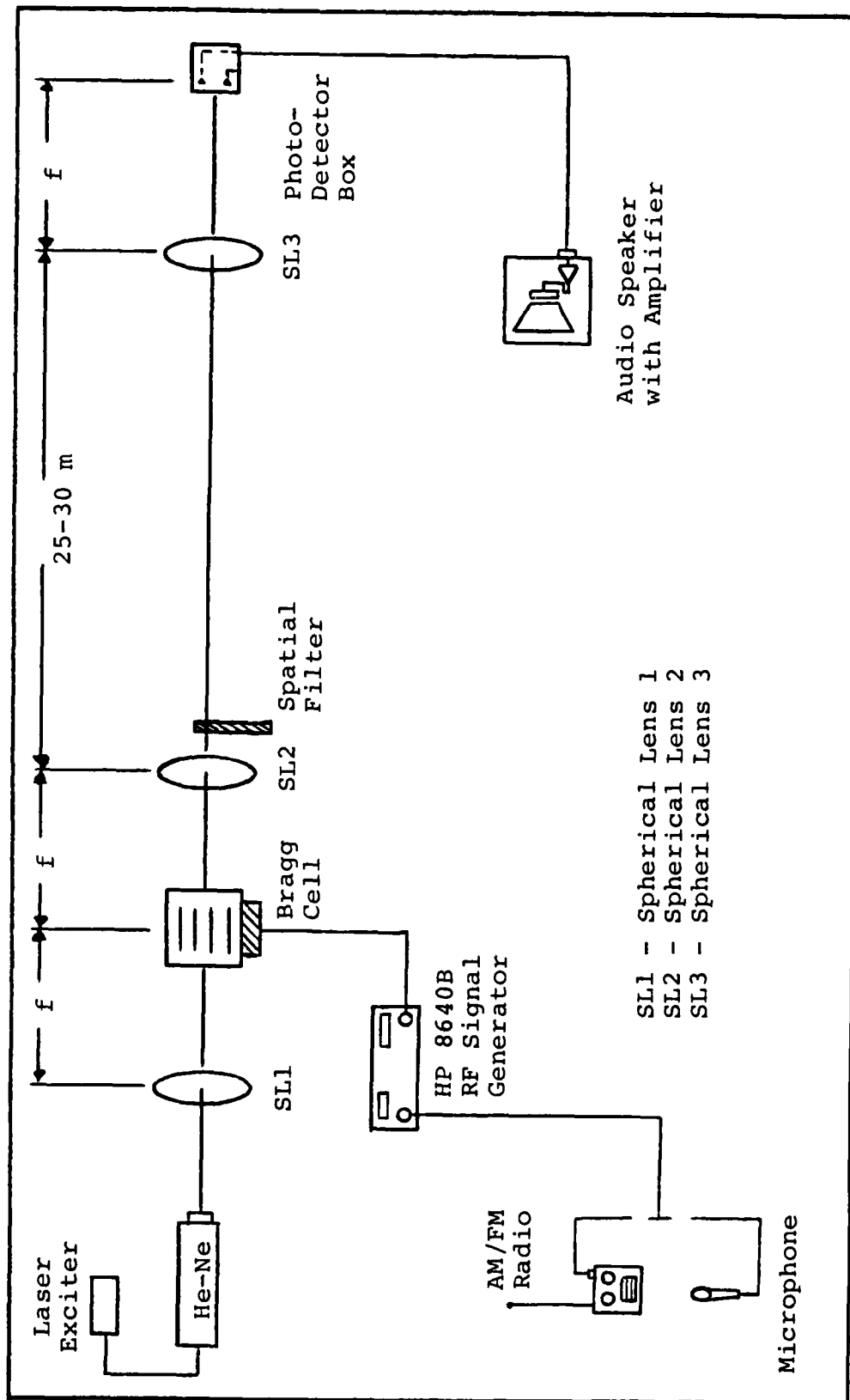


Fig. VIII-5. Amplitude Modulated Laser Communications System Implemented with an Acousto-Optic Modulator (Bragg Cell) Experimental Setup

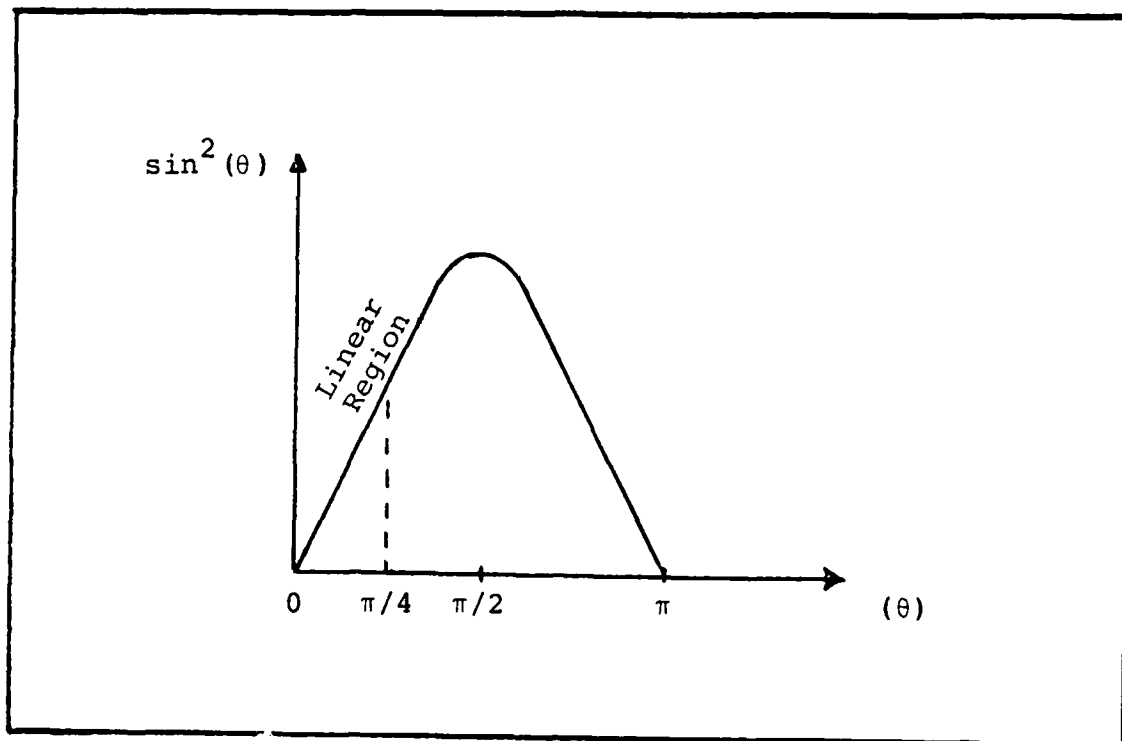


Fig. VIII-6. $\sin^2(\theta)$ Curve

where

I_{DB} = intensity of diffracted beam,

I_{IN} = intensity of incident light,

K = constant,

$v(t) = V_0 + v_1(t)$, and

$Kv(t) \ll 1$.

Thus,

$$I_{DB} = I_N \sin^2(KV_0 + K_1(t)) \quad (18)$$

The $\sin^2(\cdot)$ and its argument are shown in Figure VIII-6.

Notice that the curve is almost linear in the region about

$\pi/4$. Thus, if $KV_0 = \pi/4$ then the Bragg Cell will operate in the linear in intensity region. Thus, Eq (18) becomes

$$I_{DB} = I_{IN} \sin^2(\pi/4 + Kv_1(t)) \quad (19)$$

After some work the diffracted beam intensity is:

$$I_{DB} = I_{IN}(1/2 + Kv_1(t)) \quad (20)$$

The current out of the photodetector is proportional to I_{DB} ; thus,

$$\begin{aligned} I_D(t) &\propto I_{DB} \\ &\propto I_{IN}(1/2 + Kv_1(t)) \end{aligned} \quad (21)$$

Notice the first term is just a bias and can be filtered while the second term is the recovered signal.

Laser Communications with Acousto-Optic Cell Procedures

It is recommended that two students work together to set up this experiment since aligning the laser with the photodetector may take some meticulous alignment. Refer to Figure VIII-5 when performing these procedures.

STEPS

INSTRUCTIONS

1. Assembling the Laser Source--assemble Spectra Physics laser into laser mount and attach to Support post and post holder. Fasten the post holder to the optical table. Connect the He-Ne laser to the laser exciter. Turn on the laser exciter and allow a few minutes for the laser to warm up.

5. Connect the Hewlett Packard (HP) 8640B Signal Generator RF out to the Bragg Cell. Before turning on the power to the HP signal generator, set the following configuration on the front panel:
AM Modulation: OFF
AM Modulation 0-100%: Fully CCW
Audio Output Level: Fully CCW
Scale: AM(x10%) Depressed
Modulation Frequency: 1000 Hz
FM Modulation: OFF
Counter Mode: INT/EXT Depressed
Range (MHz): 64-128
Output Level: +10 dBm
RF: OFF
6. Turn "ON" the power to the HP 8640B and adjust the frequency output to 80 MHz. Next switch the "RF" switch to "ON." Note: The power setting of +10 dBm on the output level is below the recommended RF power to the Bragg Cell. This is a safe power setting and may be used to perform this experiment; however, for a better diffraction efficiency of the Bragg Cell, the output level may be increased to +20 dBm. When doing this, ensure that the "REDUCE PEAK POWER" light on the HP 8640B is NOT illuminated. Although the Bragg Cell is designed to handle the peak power out of the HP 8640B signal

generator, the signal generator is not designed to operate at its peak power.

7. Adjust the angle the Bragg Cell makes with the laser beam until the first order diffraction component is visible on a test screen. (A white card, placed approximately 50 centimeters behind the Bragg Cell, was used as a test screen.) To ensure that the diffraction pattern observed is the zeroth and first diffracted orders on the HP 8640B, switch the "RF" switch to "OFF" and observe that the first diffracted order will disappear.
8. Switch the "RF" switch back to "ON" and ensure that only one of the first order diffraction components is strongly illuminated (i.e., adjust for the Bragg angle).
9. Set up a lens on a translational stage (as in Step 2) and place the focusing lens (SL2) approximately one focal length (150 mm) behind the Bragg Cell. Use a small cardboard box to block the zeroth order component.
10. Approximately 20-30 feet away, place a third focusing lens (SL3) in the line of the laser (first diffraction order). Note: At this distance, the laser will have diverged and the circular pattern of the first diffracted order will be much larger than the zeroth order on the spatial filter at SL2.

11. Place the photodetector box one focal length behind SL3 and align it so the laser beam (first diffracted order) focuses on the detector's active area (either detector "1" or "2" may be used).
12. Connect a small Audio Amplifier with a speaker to the output of the photodetector and ensure the power switch of the photodetector circuitry is "ON."
13. The laser communications system should now be ready for demonstration. On the HP 8640B, switch the "AM" switch from OFF to INT (internal modulation). This will modulate the RF carrier with a 1000 Hz signal. The output of the photodetector and the speaker should be a 1 KHz tone. If this does not happen, recheck the alignment and ensure the laser is striking the active area of the detector.
14. To process a voice signal over the laser, simply connect a microphone with the proper biasing voltage (i.e., use a small amplifier for amplifying the voice signal to approximately 1-2 volts peak-peak) to the AM modulation "input." Switch the "AM" switch to "AC" to allow an external signal to modulate the RF carrier. Ensure the modulation index is not over 100 percent (i.e., do not over-modulate!!!). This may cause distortion of the baseband (voice) signal.

15. As a Gee Wiz demonstration, use a small AM/FM radio and connect the "Earphone" output of a small radio to the HP 8640B AM modulation "input." Adjust both the percent modulation of the AM signal generator and the volume of the radio to ensure a good fidelity of the audio signal out of the speaker. The volume of the speaker may also be controlled by adjusting the amount of RF power delivered to the Bragg Cell.

Special Problems

Refer to Chapter VI for special problems with adjusting the laser beam in the Bragg Cell. For this experiment the Jordan Spatial Filter and the Iris Diaphragm were not used because they would have severely reduced the amount of laser energy delivered to the photodetector. Since the current of the photodetector output is proportional to the intensity of the light striking it, the objective was to deliver as much laser energy to the detector as possible.

Spherical Lens 2 is used to keep the laser beam (first diffracted order) from diverging out too much before reaching the photodetector. The SL2 lens was adjusted to propagate the laser beam as near collimated as possible. Because the laser beam exiting the Bragg Cell was not perfectly spherical, the effects of SL2 were limited and could not perfectly collimate the light. As noticed

during this experiment, the beam still diverged over the propagation distance.

SL3 is very important during the detection process. This lens will collect as much energy from the laser as possible and focus it onto the detector. Without it, the amount of laser energy that actually strikes the photodetector is so small that the information signal would be lost below the detection threshold of the photodetector and therefore no output would be detected.

The photodetector box came in a kit by Metrologic Instruments, Inc. and was already assembled prior to use. Thus no major problems were encountered with the detector except the power source (9 volt battery) needed replacing.

In performing this experiment, an oscilloscope was used to monitor the RF signal out of the HP 8640B signal generator. The AM waveform was monitored while adjusting the percent modulation out of the signal generator. This helped to ensure a good RF modulated signal was being delivered to the Bragg Cell. The oscilloscope was also used to monitor the output of the photodetector which made aligning the photodetector with the laser beam (first diffracted order) quite simple. The signal out of the photodetector circuit box was compared to the signal out of the HP 8640B signal generator and it was noticed that the photodetector signal was simply the envelope of the RF signal (as expected from AM modulation). Thus, the

output of the photodetector circuit box is the input baseband (voice/radio) signal.

Results

The results of this experiment proved to be quite favorable. Laser communications using an Acousto-Optic Cell was successfully implemented with little trouble. The next step after successfully completing the AM modulation technique was to try the FM modulation technique.

Several articles have been written by others describing the FM modulation technique using Acousto-Optic interaction as the means of modulating the light (2; 7). The idea of FM laser communications with Acousto-Optic Cells is to combine two spatially separated beams of light, namely that of the zeroth order component and the first diffracted order, by interference principles to produce an ultrasonic frequency for processing by some suitable detector (photo-multiplier tube, photodiode array). The article by Thaler (7) describes a technique for modulating a He-Ne laser by Standing Ultrasonic Waves. Today, the same idea can be implemented using Acousto-Optic Cells as the ultrasonic wave medium.

The experimental setup of Figure VIII-7 was used to demonstrate the use of FM laser communications using Acousto-Optic cells. The major problem with this setup was the lack of proper equipment to successfully implement

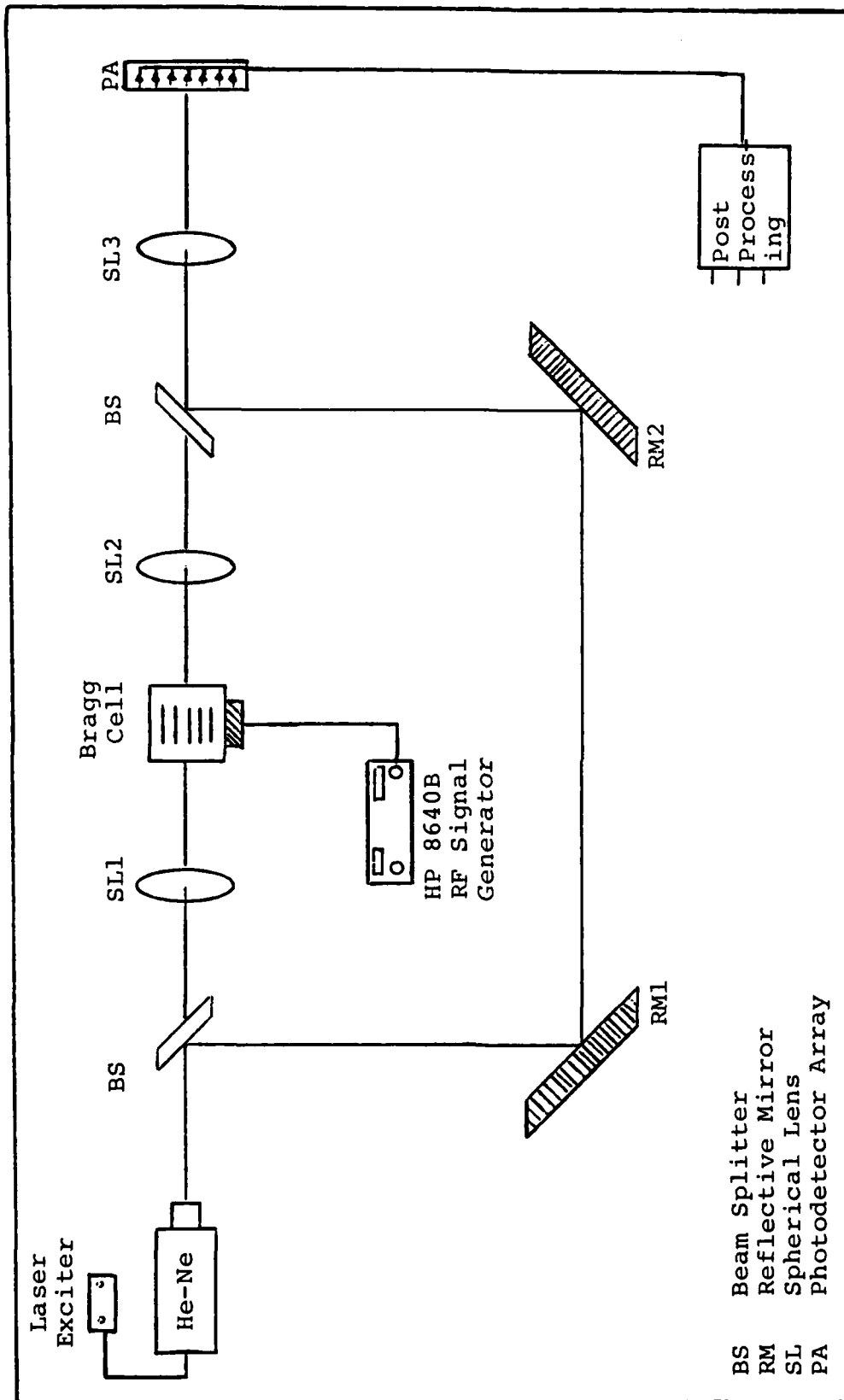


Fig. VIII-7. Frequency Modulated Laser Communication System Implemented with a Bragg Cell

the system. The equipments (optical components) that were needed are

1. Two beam splitters
2. Newport mirror holder (Model 600A-4R), 2 each
3. Photodetector array
4. FM demodulation circuitry

It is recommended that with the equipment list from this chapter and the equipment just mentioned, a student would be able to successfully implement a full FM laser communication system.

Bibliography

1. Alder, Robert. "Interaction Between Light and Sound," IEEE Spectrum, 4: 42-53 (May 1967).
2. Borsuk, Gerald M. and William J. Thaler. "Frequency Modulated Laser Communications System," IEEE Transaction on Sonics and Ultrasonics SU-17(4): 207-209 (October 1970).
3. Class Lectures or Lecture Materials. Syed, Vaqar lecture notes distributed in EE 672 "Optical Communications," School of Engineering, Air Force Institute of Technology (AU), Wright-Patterson AFB OH, January 1984.
4. Dixon, R. W. and E. I. Gordon. "Acoustic Light Modulators Using Optical Hetrodyne Mixing," Bell System Technical Journal, 46: 367-389 (1967).
5. Korpel, Adrianus. "Acousto-Optics--A Review of Fundamentals," Proceedings of the IEEE, 69(1): 48-53 (January 1981).
6. Rhodes, William T. "Acousto-Optic Signal Processing: Convolution and Correlation," Proceedings of the IEEE, 69(1): 68-79 (January 1981).
7. Thaler, William J. "Frequency Modulation of an He-Ne Laser Beam via Ultrasonic Waves in Quartz," Applied Physics Letter, 5(2): 29-31 (July 1964).

IX. Correlation Using Acousto-Optic Cells

Introduction

Acousto-Optic Cells are known for their fundamental simplicity in optical signal processing systems and their wide bandwidth. For real-time signal processing, these types of cells become a very good candidate.

The basic principle involved in correlating two signals via optical signal processing using acousto-optic cells, is to launch a signal into a Bragg Cell so that a time window format of the signal, containing many signal cycles, is present to the optical system. The signal, displayed spatially, is illuminated by a collimated beam of light and imaged, using geometric optic techniques, onto a second Bragg Cell. The second Bragg Cell contains a time window with many signal cycles of a second signal. The field exciting the second Bragg Cell is proportional to the product of the two signals. Again by geometrical optics, the light is further processed and imaged onto a photodetector array. The photodetector array will integrate the light distribution over all the surface of the detector and the time varying output of the detector array will be the desired correlation function.

Signal correlation, by spatial integration, is performed by spatially integrating light collected from

all parts of a signal which is simultaneously present in an acousto-optic device or pair of devices. This type of correlation is limited by the time-bandwidth product (number of signal cycles that are correlated) of the acousto-optic device. In working with the equipment available at the AFIT communications electronic laboratory, this type of scheme was not considered due to the lack of sufficient equipment available. Thus a different approach to signal correlation was attempted using a time integrating correlation structure and will be the topic of this chapter. Due to the lack of proper equipment available, this particular experiment was not fully performed; however, the means for realizing the full implementation of this experiment will be discussed in this chapter.

Theory Description

The basic structure of time integrating correlation using acousto-optic cells is depicted in Figure IX-1. The signals to be correlated are $S_1(t)$ and $S_2(t)$. The signal $S_1(t)$ is used to modulate the intensity of a small Bragg Cell (BC1). The zeroth order beam is spatially filtered and the first diffracted order light from BC1 is expanded and imaged onto Bragg Cell 2 (BC2). $S_2(t)$ is used to modulate an rf carrier that drives BC2. The Bragg Cell BC2 creates a time window of $S_2(t)$ and displays it in space along the length of the Bragg Cell. The spatial distribution

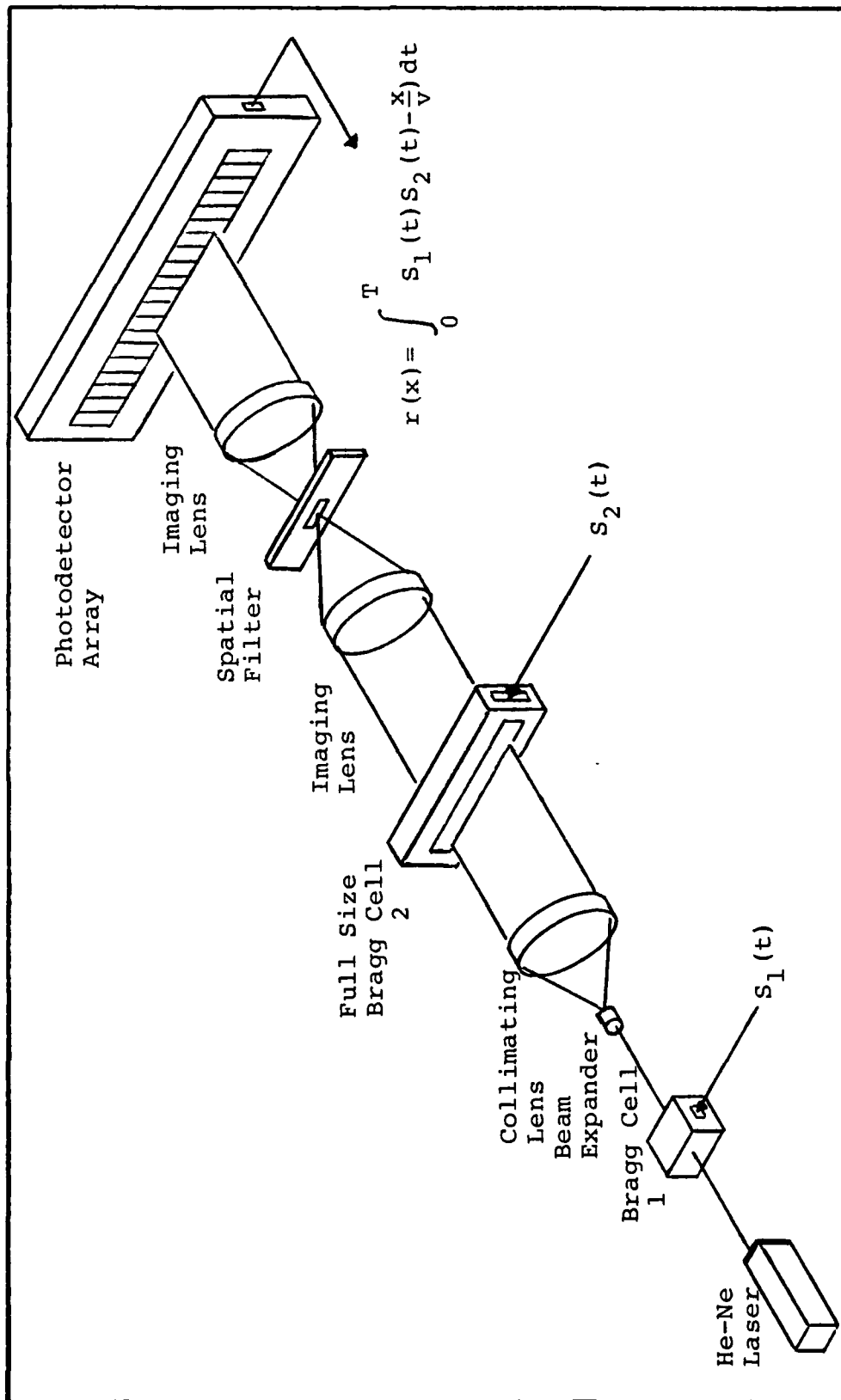


Fig. IX-1. Time Integrating Correlator

of the signal becomes $S_2(t-x/V)$ where x is the position along the length of the Bragg Cell and V is the acoustic velocity in the cell.

The acoustic signal emerging from BC2 is Fourier transformed, using an imaging lens, and spatially filtered in the Fourier plane where only the first order diffracted component and its sidebands are allowed to pass through the system.

A second lens is used to inverse Fourier Transform the acoustic signal and image it onto an array of photo-diodes which integrate the light intensity. The output of the diode at position x is given by Eq (1) where T is the detector integration time (i.e., detector time constant) (5).

$$r(x) = \int_0^T S_1(t) S_2\left(t - \frac{x}{V}\right) dt \quad (1)$$

As noticed by Eq (1), the time integrating correlator integrates with respect to time instead of space. The time bandwidth product of the correlator, which is the total number of signal cycles involved in the correlation, is limited in practice by two constraints: (1) the detector integration time, which is limited by its dark current; and (2) the usable portion of the time window in the cell. In general, large time bandwidth products enable recovery of a signal whose voltage level is very near the noise level (5).

The bandwidth of the correlator is determined by the bandwidth of the Bragg Cell and the bandwidth of the modulator driver to the cell. Typically, state of the art acousto-optic cells have bandwidths of hundreds of megahertz (MHz) (1; 5). The limiting factor is the modulating speed of the modulator. Using light emitting diodes as a source for modulation one could achieve up to 200 MHz of bandwidth. However, light level illumination is very low. A continuous wave (cw) laser can be used with an electro-optic modulator which can achieve up to 500 MHz of bandwidth (3). Acousto-optic modulators normally have bandwidths of tens of megahertz (e.g., 20 MHz). Usually above 20 MHz the diffraction efficiency will go down and the low contrast of modulation will reduce the dynamic range of the correlator. However, the usable bandwidth of these types of modulators can be extended by using a Schlieren readout slit (5).

The time difference acceptable by the correlator is determined by the time window of the cell. Normally, Bragg Cells have a time delay of 5 to 60 microseconds depending on the bandwidth of the cell. This time delay can be extended by use of a stacked array of transducers in conjunction with delay lines. To utilize the maximum extent of the time window, a sufficient number of detectors must be available to sample the correlation function at the proper intervals.

Experimental Procedures

The experimental setup shown in Figure IX-2 is designed to illustrate the operation of the time integrating acousto-optic correlator. A Newport (Model N230) acousto-optic modulator (bandwidth = 30 MHz), driven by $S_1(t)$, was used to modulate a cw He-Ne laser. The modulated light (first diffracted order) was expanded and collimated to illuminate a second acousto-optic cell (IntraAction AOD-70). The phase variations within the Bragg Cell, caused by the electrical input signal ($S_2(t)$) were Fourier transformed by a spherical lens behind the cell. In the focal plane of the lens, the zeroth order component was filtered so only the first diffracted order was imaged onto a photodetector array. The phase variations of the Bragg Cell were imaged as intensity variations onto the image plane. Linearity was achieved in the two Bragg Cells by operating in the linear in intensity region of the Bragg Cell (see Chapter VIII--Experimental Procedures). The intensity variations on the photodetector array are integrated and the time varying output of the array is the desired correlation function.

The procedures just described are the procedures used to implement the time integrating correlator using acousto-optic cells. However, this implementation was not fully carried out due to the lack of proper optical equipment. The following is a list of the equipment needed to

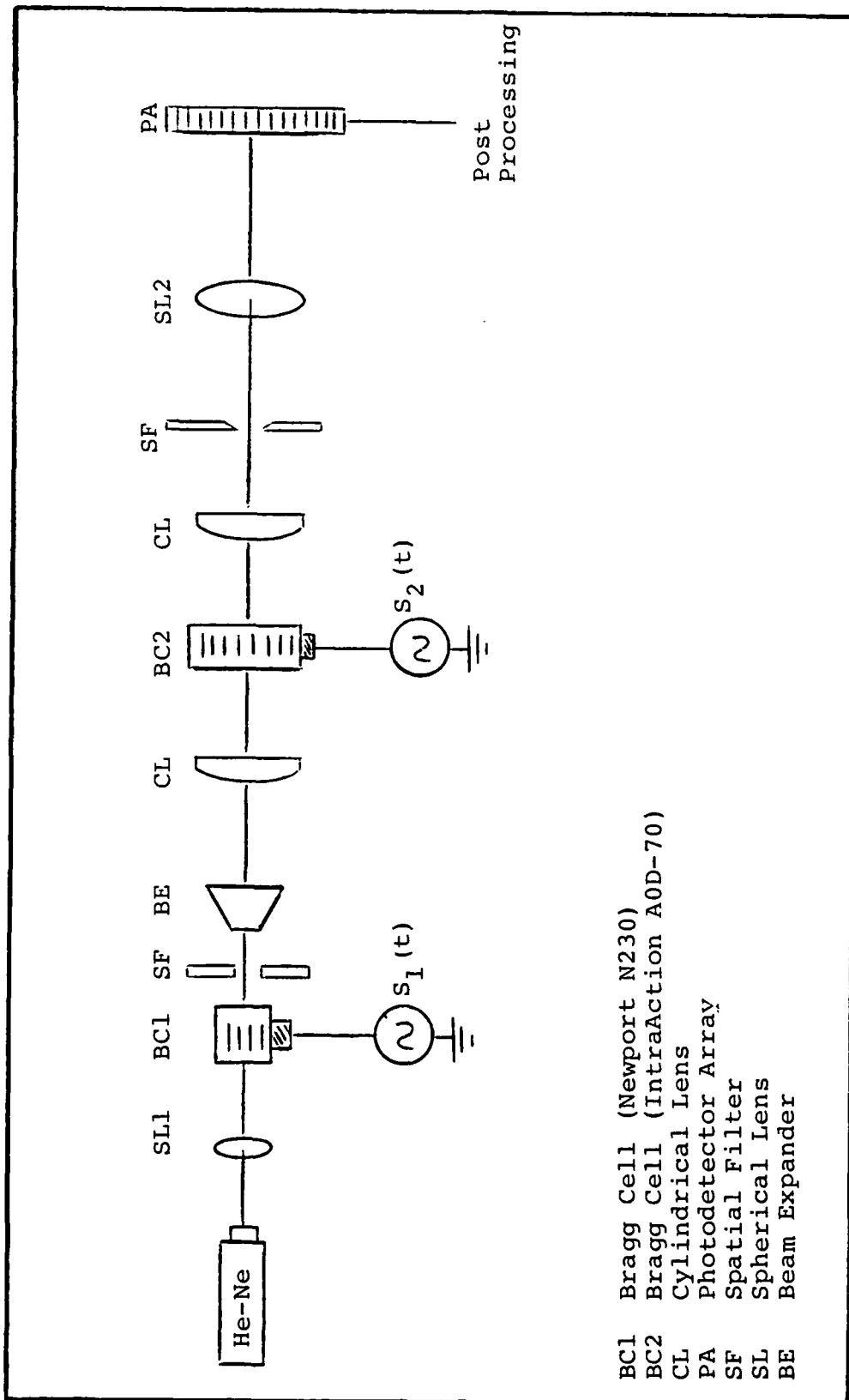


Fig. IX-2. Time Integrating Correlator Experimental Setup

carry out this experiment and the problems encountered in performing this experiment.

1. Cylindrical lens: In performing this experiment, the AOD-70 Bragg Cell was used to spatially distribute $S_2(t)$. This type of Bragg Cell is a one-dimensional cell and requires longitudinal waves as an input to the cell. The spherical lens used, generated spherical waves from the collimated laser beam. In using this type of waves to illuminate the Bragg Cell, much of the energy was lost due to the windowing effect of the Bragg Cell. Cylindrical lens will provide the proper phase transformation on a collimated beam of light (generating longitudinal waves) for illuminating the Bragg Cell.

2. Photodetector array: As pointed out earlier, the use of a photodetector array is essential in capturing the sampled values of the correlation function. The photodetector available (Metrologic photodetector box) did not sample and integrate the light distribution since this type of detector is not designed to do so. A photodetector array is needed to integrate each section of the image waveform and produce a spatial distribution of the correlation function as a function of "x" (distance along the Bragg Cell or detector array). With a photodetector array, the correlation function can be observed on an oscilloscope connected to the output of the detector array.

3. Schlieren readout slit: This type of slit is basically a spatial filter which filters the zeroth order and other unwanted diffracted order components. The physical size of the slit depends on the architecture or geometry of the system.

This experiment was taken from the article by Sprague (5). Several other time integrating correlator architectures were investigated (2; 4; 6) and the architecture by Sprague was the simplest to implement with the equipment available.

The laser source (Spectra Physics Model 102) available, although sufficient for aligning the system, did not provide a good illumination level to the second Bragg Cell. Consequently, the illumination to the image plane (detector plane) was even lower. It is recommended that for any student wishing to perform this experiment, he/she may want to get another laser source with an output power higher than 2 milliwatts.

Conclusion

Although this experiment was not performed, the means for its full implementation are almost there. As discussed above, the additional equipments needed for implementing this experiment are few yet necessary. The IntraAction AOD-70 Bragg Cell used in this experiment was on loan from National Security Agency, Ft. Mead MD.

The AFIT EE Communications department does not have a full size Bragg Cell. Thus, it would be to the department's advantage to order one for further development of the optical communications program.

Bibliography

1. Class Lectures or Lecture Materials. Syed, Vaqar lecture notes distributed in EE 672 "Optical Communications," School of Engineering, Air Force Institute of Technology (AU), Wright-Patterson AFB OH (January 1984).
2. Kellman P. "Time Integrating Optical Signal Processing," SPIE, 214 (Acousto-Optic Bulk Wave Devices): 63-73 (1979).
3. Rhodes, J. R. and D. E. Brown. "Adaptive Filtering with Correlation Cancellation Loops," SPIE, 314 (Real Time Signal Processing V): 140-147. (1982).
4. Rhodes, William T. "Acousto-Optic Signal Processing: Convolution and Correlation," Proceedings of the IEEE, 69(1): 68-79 (January 1981).
5. Sprague, Robert A. and Chris L. Koliopoulos. "Time Integrating Acousto-optic Correlator," Applied Optics, 15(1): 89-92 (January 1976).
6. Turpin, Terry M. "Time Integrating Optical Processors," SPIE, 154 (Real-Time Signal Processing): 196-203 (1978).

X. Conclusion

A number of experiments in optical communications/signal processing were designed, implemented and demonstrated. These experiments were developed to give the student a stronger understanding of the principles and practices of Optical Communications. Each experiment developed portrays a different aspect of either optical principles or Acousto-Optical principles. With the addition of more equipment into the laboratory, the student should be able to expand on the theoretical background of optics and communications and create some different experiments which would enhance various aspects of the Optical Communications field.

In pursuing this thesis effort of organizing the existing laboratory equipment and developing some simple experiments to aid the learning process of understanding classroom theory, many thoughts came to the author's mind as to improving the existing conditions of the laboratory. The following is a list of the possible recommendations which could help future students in the field to be better prepared for pursuing either research or basic understanding of the Optical Communications science.

Recommendations

1. An important piece of equipment for working with optical equipment is a good optical table. The table

used to conduct all the experiments in this thesis was a sturdy 3'x8' wooden work bench. The bench was secured against a wall so it would not shake while conducting the experiments. Two aluminum slabs (3'x4') were used on top of the table which had screw holes drilled approximately four inches apart all throughout the slab. The optical components were screwed to the aluminum slabs to keep them from vibrating. Although this worked satisfactorily for the time being, it is recommended that a good sturdy optical table be purchased for the use of future optical communications projects. A recommended source is the Newport Research series Honeycomb table top (5'x16'). See the Newport Catalog (1984 Series).

2. During the process of this thesis effort, many different types of optical components were borrowed from various departments within the AFIT department. This created many problems with support, time, and quality. The major items that were not available within AFIT are: lenses, beam splitters, mirrors, and a photodetector array. Instead of listing all the various equipment that is needed, refer to the equipment list of each experiment. The equipment listed is what is necessary for conducting the experiment with one group (two persons) of people. To implement a full laboratory with many people, it is recommended that the AFIT EE Department purchase the required equipment.

needed for conducting each experiment. A recommended source is the Newport Corporation of Melbourn, Florida.

3. The Acousto-Optic Modulator (Bragg Cell) used throughout this thesis is the Newport Corporation Model N230. Although this was instrumental in learning the simple principles and practices of Acousto-Optic interaction, this type of modulator was not designed to perform correlation processes and techniques. The time-bandwidth product of this device is much too small. Therefore, it is recommended that a full size Bragg Cell be purchased for implementing light and sound interaction experiments. A recommended source is the IntraAction Corporation with the AOD/70 model. This particular model was loaned to the AFIT EE department by the National Security Agency for the purpose of experimenting and research efforts.

4. Frequency Modulated Laser Communications: The reality of this type of system using acousto-optics is not far from reach. As pointed out in Chapter VIII, only a few pieces of equipment are all that is necessary for conducting this experiment. It is recommended that after the department acquires the necessary equipment needed for this experiment, that several schemes for performing FM laser communications be implemented by utilizing both a video and an audio signal to be transmitted simultaneously on a single laser beam (i.e., transmit the video signal via FM communications and transmit the audio signal via

AM communications. Two Bragg Cells will have to be used to properly implement this scheme.) See article by Borsuk and Thaler, Chapter VIII, reference 2.

5. Holography: The laboratory has a holography kit by the Metrologic Company and comes with a booklet which describes the basic principles for setting up a holography experiment. Any student interested in setting up a holography demonstration may do so since all of the equipment necessary is available in either the Communications laboratory or the Physics laboratory. Since a booklet along with the holographic kit was available, procedures were not written up for this type of experiment. It is left up to the initiative of the student to pursue this exciting field of endeavor.

6. Cross-correlation and Ambiguity Functions using Acousto-Optic Cells: The references at the end of Chapters VIII and IX have several references to acousto-optic architectures which perform either a cross-correlation or an ambiguity function. To implement these architectures, two or three full size Bragg Cells are needed. Much research and development is being done in the area of radar signal processing in which these techniques are used. Implementing a cross-correlation on a radar signal using acousto-optic techniques can be performed in real time. Since this is a very open area of research, it is recommended that upon acquiring several

full size Bragg Cells for the AFIT Communications laboratory, students develop experiments and conduct research for this area of Acousto-Optic signal processing.

7. Since much research and development in communications is in the area of fiber optic technology, it is also recommended that some good sources of both laser diodes and semiconductor lasers be acquired for the use of developing experiments in the area of fiber optic communications. Also an important item not to be forgotten is the detector. Since detectors are just as important as the transmitters (laser sources), it is recommended that several quality detectors be acquired for this same purpose of fiber optic communications.

VITA

Captain William K. Aiu was born on 25 June 1958 in Los Angeles, California. He graduated from high school in Kapaa, Hawaii in 1976 and attended the University of Portland from which he received the degree of Bachelor of Science in Electrical Engineering in May 1980. Upon graduation, he received a commission in the USAF through the ROTC program. He was employed as a Hydro-Electric Design Engineer at the Army Corps of Engineers in Portland, Oregon until being called to active duty in August 1980. He graduated from the Communications-Electronics Engineer Course at Keesler AFB, Mississippi in January 1981. He served as a Systems Evaluation Team Chief with the 1815 Test and Evaluation Squadron, Wright-Patterson AFB, Ohio until entering the School of Engineering, Air Force Institute of Technology. Upon graduation from AFIT in December 1984, he is scheduled for assignment to the Air Force Communications Command Headquarters at Scott AFB, Illinois.

Permanent address: 4855-C Nonou Rd
Kapaa, Hawaii 96746

UNCLASSIFIED

SECURITY CLASSIFICATION OF THIS PAGE

REPORT DOCUMENTATION PAGE				
1a. REPORT SECURITY CLASSIFICATION UNCLASSIFIED		1b. RESTRICTIVE MARKINGS		
2a. SECURITY CLASSIFICATION AUTHORITY		3. DISTRIBUTION/AVAILABILITY OF REPORT Approved for public release; distribution unlimited.		
2b. DECLASSIFICATION/DOWNGRADING SCHEDULE				
4. PERFORMING ORGANIZATION REPORT NUMBER(S) AFIT/GE/EE/84D-12		5. MONITORING ORGANIZATION REPORT NUMBER(S)		
6a. NAME OF PERFORMING ORGANIZATION School of Engineering	6b. OFFICE SYMBOL (If applicable)	7a. NAME OF MONITORING ORGANIZATION		
6c. ADDRESS (City, State and ZIP Code) Air Force Institute of Technology Wright-Patterson AFB, Ohio 45433		7b. ADDRESS (City, State and ZIP Code)		
8a. NAME OF FUNDING/SPONSORING ORGANIZATION	8b. OFFICE SYMBOL (If applicable)	9. PROCUREMENT INSTRUMENT IDENTIFICATION NUMBER		
8c. ADDRESS (City, State and ZIP Code)		10. SOURCE OF FUNDING NOS.		
		PROGRAM ELEMENT NO.	PROJECT NO.	TASK NO.
				WORK UNIT NO.
11. TITLE (Include Security Classification) See Box 19				
12. PERSONAL AUTHOR(S) William K. Aiu, B.S.E.E., Capt, USAF				
13a. TYPE OF REPORT MS Thesis	13b. TIME COVERED FROM _____ TO _____	14. DATE OF REPORT (Yr., Mo., Day) 1984 December	15. PAGE COUNT 176	
16. SUPPLEMENTARY NOTATION				
17. COSATI CODES		18. SUBJECT TERMS (Continue on reverse if necessary and identify by block number)		
FIELD	GROUP	SUB. GR.		
17	02	Acousto-Optics, Optics, Optical Communications, Telecommunications		
19. ABSTRACT (Continue on reverse if necessary and identify by block number)				
Title: THE DEVELOPMENT AND IMPLEMENTATION OF AN OPTICAL COMMUNICATIONS LABORATORY				
Thesis Chairman: Dr. Vaqar H. Syed				
<div style="text-align: right;"> Approved for public release: 1AW AFR 190-17. LYNN E. WOLKOFF Dean for Research and Development Air Force Institute of Technology (AFIT) Wright-Patterson AFB, Ohio 45433 </div>				
20. DISTRIBUTION/AVAILABILITY OF ABSTRACT UNCLASSIFIED/UNLIMITED <input checked="" type="checkbox"/> SAME AS RPT. <input type="checkbox"/> DTIC USERS <input type="checkbox"/>		21. ABSTRACT SECURITY CLASSIFICATION UNCLASSIFIED		
22a. NAME OF RESPONSIBLE INDIVIDUAL Kenneth Castor, Major	22b. TELEPHONE NUMBER (Include Area Code) (513) 255-3576	22c. OFFICE SYMBOL ENG/AFIT		

DD FORM 1473, 83 APR

EDITION OF 1 JAN 73 IS OBSOLETE.

UNCLASSIFIED
SECURITY CLASSIFICATION OF THIS PAGE

This report is an accumulation of seven optical laboratory experiments developed for the Optical Communications Program at the Air Force Institute of Technology. The projects include measurement of pertinent parameters of Fourier Optics (diffraction patterns and lenses) and Acousto-Optics (Bragg angle and beam deflection using an acousto-optic modulator), image construction and spatial filtering, laser communications with an acousto-optic modulator and a scheme for implementing a time integrating correlator using two full size acousto-optic modulators.

Each experiment is self-contained with subsections on project assignments, objectives, theory/background, special problems, and experimental results.

The results of this report recommend that the Optical Communications Program at AFIT further develop their experimental laboratory and acquire some state-of-the-art acousto-optic modulators for students to pursue research and future studies.

END

FILMED

5-85

DTIC